Physics of Life Reviews 57 (2026) 4–60

Contents lists available at ScienceDirect

Physics of Life Reviews

journal homepage: www.elsevier.com/locate/plrev

Review

Networked collective dynamics in animal ecology and cell biology

Yongzheng Sun [a,b,c,*], Huimin Wang [a], Xiaoting Liu [a,d], Guanghui Wen [e,*], Wei Lin [f,*], Philip K. Maini [c,*]

[a] School of Mathematics, China University of Mining and Technology, 221116, Xuzhou, China
[b] Shenzhen Research Institute, China University of Mining and Technology, 518000, Shenzhen, China
[c] Mathematical Institute, University of Oxford, OX2 6GG, Oxford, UK
[d] Department of Mathematics and Statistics, The University of Western Australia, Crawley, 6009, Australia
[e] School of Mathematics, Southeast University, 210096, Nanjing, China
[f] School of Mathematical Sciences, Fudan University, 200433, Shanghai, China

ARTICLE INFO

Communicated by J. Fontanari

Keywords:
Collective behavior
Network science
Information transmission
Swarm intelligence
Animal ecology
Cell biology

ABSTRACT

Collective behavior, emerging from interactions among individuals, is a ubiquitous phenomenon observed across a wide range of biological systems—from cellular dynamics to animal ecology. Network science offers powerful tools for understanding the structure and functional properties underlying such systems. Despite significant progress in modeling, data-driven analysis, and interdisciplinary approaches, several critical challenges persist. How do complex social interactions among individuals influence the emergence of collective behavior? Moreover, in what ways do individual information and social interactions jointly shape collective decision-making? To address these challenges, this review synthesizes recent advances in network science, statistical physics, and artificial intelligence as applied to the study of collective phenomena. We focus on collective patterns in animals and cells, highlighting the interplay between structure and dynamics. The review begins with an overview of basic forms of collective behavior, followed by discussions of microscopic and macroscopic modeling approaches, structural and functional features of social interaction networks, mechanisms of information transmission, decision-making processes, and emergent collective intelligence. We also explore cutting-edge applications, including bio-inspired robotic swarms and coordination systems for unmanned aerial vehicles. We conclude by outlining open questions and potential research directions, aiming to provide insights into the design, control, and understanding of complex collective systems across biology, physics, and artificial intelligence.

1. Introduction

1.1. Background and motivation

Complex systems consist of many interacting components whose collective behavior cannot be understood solely by examining the behavior of individual parts [1]. This phenomenon is widely observed in animal groups, such as large flocks of starlings that gather and rotate above their resting grounds [2,3], schools of fish that swirl like a violently stirred fluid [4], and ants that systematically

* Corresponding authors.
E-mail addresses: yzsun@cumt.edu.cn (Y. Sun), ghwen@seu.edu.cn (G. Wen), wlin@fudan.edu.cn (W. Lin), Philip.Maini@maths.ox.ac.uk (P.K. Maini).

https://doi.org/10.1016/j.plrev.2026.02.003
Received 28 August 2025; Received in revised form 26 February 2026; Accepted 26 February 2026
Available online 2 March 2026

form trails [5]. Examples of collective motion are also found on the microscopic scale, such as cell migration during tissue repair [6], cancer invasion [7,8], bacterial colony formation [9,10], and cellular oscillations [11]. In many cases, such organized collective motion emerges through a phase transition from disordered motion.

Investigating collective behavior provides critical insights into the mechanisms driving animal behavior, group dynamics, and the evolutionary processes that shape biological systems in nature. It has wide-ranging applications in the social sciences [12–14] and engineering technologies [15–18]. For example, in social networks, individuals' decisions are influenced not only by their own preferences and judgments but also by the opinions of other members, leading to collective decision-making [14]. The theory of collective behavior can also be applied to optimize and control emerging technologies such as multi-agent systems and drone swarms [15]. Therefore, the study of collective behavior is not only fundamental to understanding natural and social phenomena, but also provides essential theoretical support for the innovation and advancement of related technologies and systems.

From collective migration and foraging of animal groups to phenomena such as information dissemination and public opinion formation in human society, all of these can be viewed as global patterns emerging from local interactions between individuals within a group [19]. From a network science perspective, the structural connections between individuals within a moving group significantly influence collective behavior [19,20]. Furthermore, the network structure provides a foundation for communication, information processing, and coordinated responses among group members. The impact of social interactions on collective behavior has only recently gained attention, driven by advances in network science. Therefore, investigating collective behavior through the lens of network science is essential.

In recent years, a wealth of significant discoveries in collective behavior have provided new approaches to analyzing complex systems and uncovering the underlying mechanisms of collective dynamics. Several highly cited and noteworthy review articles have addressed recent developments from various perspectives, but have yet to fully consider the critical role of social interactions, information transmission, and decision-making in shaping collective behavior [1,21–23]. Thus, a comprehensive review that integrates these cutting-edge methodologies within the framework of network science is timely and essential.

1.2. Understanding collective behavior via network science

Network science has become one of the core components of the knowledge framework used to describe, analyze and understand complex systems. It plays a pivotal role, particularly in deepening our understanding of the dynamics and emergent properties of large-scale systems [24]. Networks effectively capture the essence of complex systems, with their structure significantly shaping both function and dynamic behavior [25–27]. By analyzing networks, we can uncover how interactions between individuals and information transmission impact the overall performance and evolution of a system.

Information transmission among individuals plays a crucial role in shaping collective behavior across microscopic, animal, and robotic systems. However, noise from both external and internal sources often leads to imprecise information being received [28,29]. Additionally, time delays arise due to the finite speed of information propagation and the time that individuals require to process information and adjust their states [30,31]. Notably, noise and time delays in information transmission can influence the collective dynamics of a group, inducing phenomena such as the emergence of collective order, shifts in motion patterns, and directional switching [31–34]. Moreover, network attacks—widely present in the real world—can disrupt or tamper with individual level information, thereby exerting significant influence on collective dynamics. Therefore, accounting for the effects of information transmission is essential for understanding collective motion.

The structure and dynamics of social interactions play a pivotal role in shaping decision-making processes, influencing how information flows within a group and how consensus is reached. Studies have shown that social connectivity, individual influence, and interaction rules determine the efficiency and accuracy of collective decisions [35–39]. Mechanisms range from dominance by a single leader to influence hierarchies and democratic processes, where each member contributes to a group decision. The presence of a well-connected or knowledgeable leader can significantly enhance decision-making efficiency, yet in some systems, distributed influence among peers leads to more robust outcomes [35,37,40]. Understanding the interplay between social interactions and decision-making is essential for insights into group foraging, migration, and navigation strategies.

This review offers a comprehensive examination of collective behavior through the lens of network science, covering a broad spectrum of topics within animal ecology and cell biology. First, it explores the diverse manifestations of collective motion in biological systems, exemplified by the frequent vortex formations employed by food-deprived tadpole groups to optimize nutrient acquisition [41]. Second, it surveys recent advancements in dynamic modeling of collective behavior, encompassing both microscopic and macroscopic animal systems. Third, it investigates the role of social interactions in shaping collective dynamics, illustrating, for instance, how higher-order interactions can precipitate abrupt transitions from asynchronous states to phase waves and synchronized patterns [42]. Subsequently, it examines the mechanisms of information transmission, highlighting various phenomena, including how noise and time delays can induce directional reversals between clockwise and counterclockwise movements in locust swarms [31,43,44]. Moreover, the review addresses collective decision-making processes and the emergence of collective intelligence, including the phenomenon whereby a minority of informed individuals can steer uninformed group members toward optimal outcomes [35]. Finally, it discusses technological applications inspired by biology, focusing on bio-inspired robotic systems such as distributed control frameworks derived from the hierarchical navigation strategies of homing pigeons, designed to enhance flocking behavior in unmanned aerial vehicles [15]. Throughout, we emphasize that understanding the interplay between network structure and dynamics is fundamental to uncovering the mechanisms driving coordinated phenomena in animal ecology and cell biology.

Table 1
Key concepts and representative models in animal and cellular collective motion.

Term	Definition	Representative models
Flocking	The coordinated behavior exhibited by birds flying in a group, demonstrating collective movement.	Reynolds' Boids model [48]; Couzin's self-organizing model [49]; Cucker-Smale model [50]; Vision-based model [51,52]
Schooling	A basic feature of aquatic species in which individuals arrange themselves in an orderly formation according to certain rules (such as position and velocity).	Couzin's self-organizing model [49]; Self-propelled particle (SPP) model [53]
Swarming	Collective behavior of insects and other organisms on the ground or in the air.	Vicsek model [54]; SPP model [32,55]; Kuramoto model [42]
Collective cell migration	A phenomenon where a group of cells moves collectively within a tissue while maintaining interactions, observed in embryonic morphogenesis, wound repair, and cancer invasion.	Reaction–diffusion model [56]; Individual-based model (IBM) [57]; Data-driven model [58]
Collective cellular oscillation	A phenomenon in which a group of cells generates periodic oscillations in a coordinated manner.	SPP model [11]; Fluid dynamics-coupled model [59]
Bacterial colony	Bacteria forming complex spatial distributions through interactions.	Fluid dynamics model [60]; Reaction–diffusion model [61]

2. Forms of collective motion

Collective animal motion, such as flocking birds, schooling fish, and swarming ants, has long attracted considerable attention [1,19,21,45]. These group behaviors in animals are not only common in nature but also exhibit highly complex and diverse movement patterns. Collective behavior extends beyond animal groups; indeed, the diversity of systems and patterns exhibiting collective motion is far broader and more intricate than previously recognized. For example, cells can display collective behaviors, such as dense clusters of bacterial cells generating large-scale vortex motion [46,47]. From animal ecology to cellular biology, investigations into group dynamics across these domains provide profound insights and diverse perspectives that are essential for a comprehensive understanding of collective behavior. Prior to this, we present the definitions of several terms related to collective behavior, as shown in Table 1.

2.1. Collective motion in animal ecology

2.1.1. Flocking

Organized flight in birds is one of the most easily observed phenomena in animal ecology. Flocks of birds often exhibit complex and coordinated formations in the sky, particularly during migration seasons, when thousands of birds are able to fly with astonishing synchronicity, demonstrating highly organized behavior. Flocking birds typically fly in one of two patterns: line formation and cluster formation, see Fig. 1. The former is typical of larger bird species, such as waterfowl, which fly in a single file, usually closely aligned. Cluster formation, on the other hand, is typically seen in large groups of smaller birds, such as pigeons or starlings, which fly in more irregular arrangements [62].

In the 1980s, Potts conducted a frame-by-frame analysis of high-speed footage of a flock of sandpipers to explore how bird flock movement begins and coordinates [65]. He proposed that any individual could initiate collective motion, and then the group would propagate outward in a wave-like manner from the point of initiation. Hierarchical organization is a common phenomenon in animal groups. Nagy et al. used high-resolution, lightweight GPS devices to track the flight paths of up to 10 homing pigeons during group flights and conducted a detailed analysis [66]. Their study found that birds often assume different roles within the group, occupying relatively fixed positions, revealing a clear hierarchical structure. Throughout this process, the relationship between leaders and followers remained consistently apparent. Although the social structure and leadership dynamics in collective motion are crucial, accurately identifying them can be challenging. Nagy et al. further developed an automated method to assess social dominance and applied it to compare the dominance and leadership abilities of homing pigeons [67].

The distinct social relationships that characterize many animal societies can significantly influence collective dynamics. Individuals in various species, including birds [68], mammals [69], and humans [70], are often observed to maintain close relationships and engage in activities with individuals with whom they share strong social bonds. Understanding how different social relationships influence the dynamics of collective motion or information transmission is crucial. Collective movement models based on social network structures [71] suggest that social relationships can alter the spatial positions of individuals within a group [72] and affect the cohesion of the entire group [73]. Ling et al. tracked the three-dimensional trajectories of individuals in a group of jackdaws, a species known for forming lifelong pair bonds [74]. They found that paired birds interacted with fewer neighbors and flapped their wings more slowly than unpaired birds, likely to conserve energy, see Fig. 2. Flocks with a higher proportion of paired birds exhibited shorter correlation lengths, which could inhibit the effective transmission of information through the flock. These findings underscore the impact of social relationships on collective behavior.

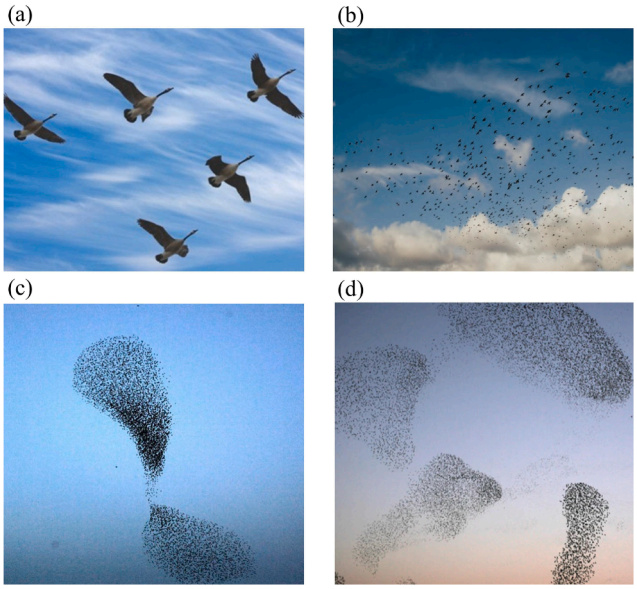

Fig. 1. Two patterns of flocking. (a) Line formation. (b)-(d) Cluster formation. *Source:* The figure is from [63,64].

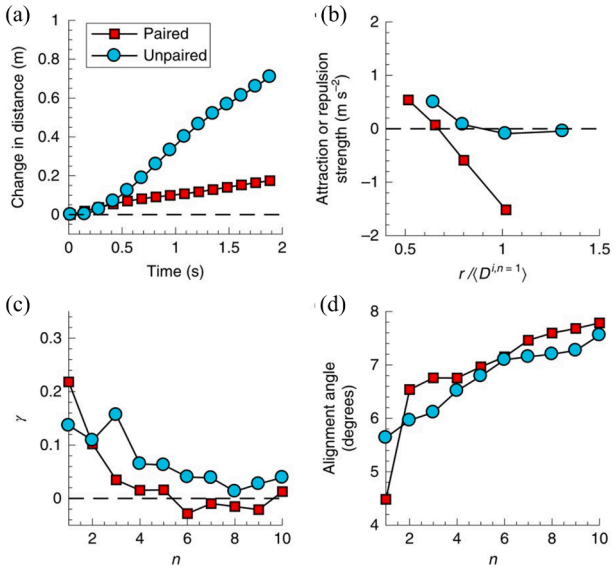

Fig. 2. Pairing causes variations in local interaction. (a) Change in distance between a bird and its nearest neighbour. (b) Acceleration in the direction away from the nearest neighbour; positive values are repulsive and negative values are attractive. Here, r represents the distance between a focal bird and its neighboring bird, and $\langle D^{i,n=1}\rangle$ denotes the mean nearest-neighbour distance. (c) Anisotropy factor γ of the spatial distribution of the n-th neighbour. $\gamma > 0$ indicates a higher probability of finding a neighbour next to, rather than in front of or behind, the focal bird. (d) Alignment angle between a focal bird and its n-th neighbour. *Source:* The figure is from [74].

Animal groups may transition from one type of collective behavior to another in response to internal or external stimuli. Couzin et al. demonstrated that even small changes in interactions between individuals in bird flocks could lead to a shift in collective behavior [49]. When a moving group is attacked by a predator, the group typically rapidly changes its shape and internal structure [75,76]. These collective motion patterns often confuse the predator, increasing the survival rate of the prey [77]. To explore the coordination of group members and collective escape patterns when under attack, Papadopoulou et al. introduced an aggressive robotic falcon [78,79]. By analyzing the GPS trajectories of the group, they found that pigeons flying in a group exhibited early splits and collective turns when confronted with an attack by the robotic falcon, as shown in Fig. 3.

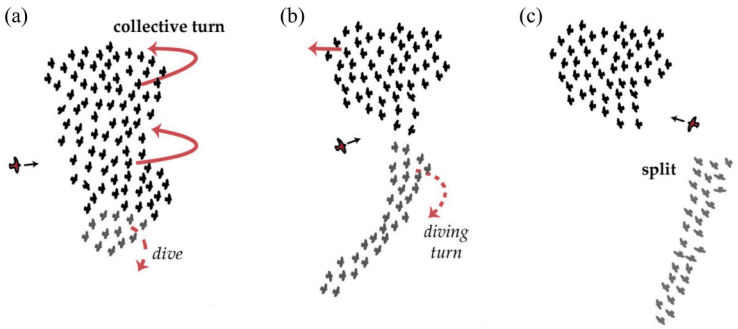

Fig. 3. Patterns of collective escape. (a) The initial position of the flock. (b) Collective turn. (c) Split. The black bird figures represent the prey, while the larger red figure (near the origin of the black arrow) represents the predator. *Source:* The figure is from [79].

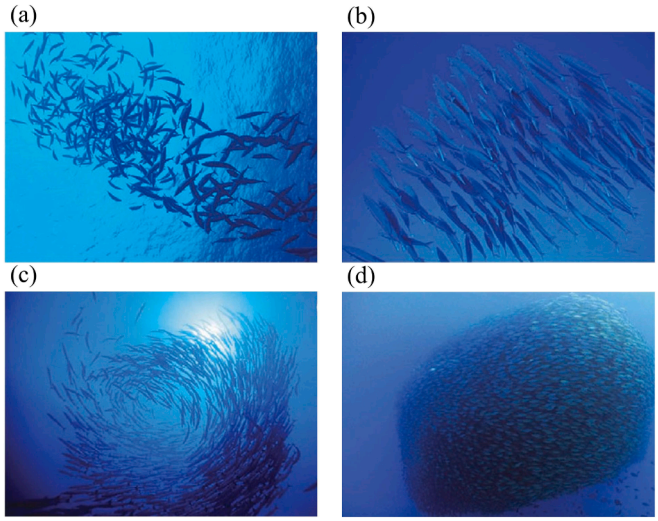

Fig. 4. Patterns in fish schools. Individuals' interactions give rise to a variety of dynamical structures that can be (a) poorly or (b) highly polarized. Other configurations of fish schooling include (c) milling and (d) bait ball structures. *Source:* The figure is from [81].

2.1.2. Schooling

Schooling in fish is a ubiquitous and prototypical example of collective behavior, see Fig. 4. Most fish species are likely to form cohesive social groups at some stage of their life. In schools, fish collectively exhibit behaviors that are distinct from those of individuals. The movement response of schools is characterized by highly synchronized coordination, with the behavior of individuals being strongly correlated and mutually coordinated. The biological significance of this behavior is crucial, directly influencing the fish's ability to perform various life functions [80].

Fish form schools to gain several benefits, including reducing predation risk, improving foraging efficiency, and enhancing environmental perception. Individuals in a fish school can share foraging information and coordinate their actions, thereby improving foraging efficiency [82]. When faced with danger, fish typically gather in groups, enhancing the group's vigilance and responsiveness to threats [83,84]. Fish schools are also thought to confuse predators by providing disorienting visual signals. The movement of a large number of fish can make it difficult for predators to target a single individual. Consequently, larger schools are considered safer, as their size and coordinated movement provide better protection and reduce the risk of predation [85].

Another benefit of swimming in a coordinated school is that fish can gain energy from the vortices created by their neighbors, reducing the cost of movement [86]. However, testing this hypothesis in real fish schools is challenging. To address this, Li et al. developed biomimetic fish-like robots to directly measure energy consumption associated with swimming together in pairs [87]. By comparing the speed and power consumption of the robots swimming alone versus swimming side by side, they found that, regardless of the relative phase of their body undulations, swimming side by side significantly improved both speed and efficiency [88]. Furthermore, the studies of the swimming mechanisms of biomimetic fish have provided significant insights and guidance for the accurate understanding of fish swimming mechanisms [89,90].

Schooling behavior is shaped by both internal group dynamics and external environmental factors. In 2006, Becco et al. recorded the movement trajectories of juvenile fish in schools [91]. They studied the effect of fish density on individual and collective behavior, observing a transition from disordered to correlated motion. Animal groups are often predicted to exhibit "multistability", where

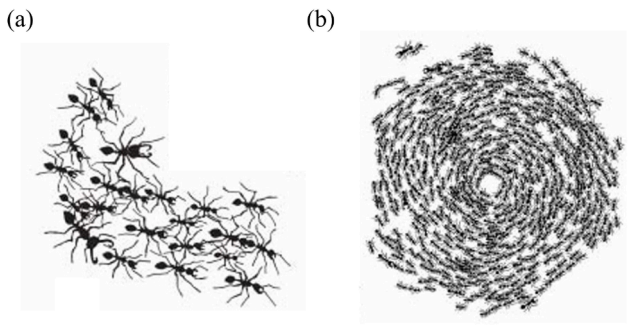

Fig. 5. A pattern in insect swarming. (a) Close-up view and (b) wide view of the collective behavior. *Source:* The figure is from [1].

multiple collective states coexist in individual behaviors, and the group rapidly transitions between alternating structural configurations. Couzin et al. proposed a model in which the milling and polarized states coexist within a specific region of the parameter space [49]. In this context, if the group starts in a relatively disordered state, then it tends to form a milling-type formation, whereas with sufficient alignment, it tends to maintain a polarized configuration. Tunstrøm et al. demonstrated that the stability of discrete collective behaviors in fish schools depends on the number of group members, with transitions between states influenced by both external (boundary-driven) and internal (changes in group member motion) factors [92]. Noise has been found to induce schooling behavior in small- to medium-sized fish groups, driven by the intrinsic stochasticity arising from the limited number of interacting individuals. Notably, the smaller the group, the greater the influence of noise, and consequently, the higher the probability of alignment [93].

2.1.3. Swarming

Insects are among the most diverse animal groups, and some are social, known for their large and well-organized colonies [21]. Coordinated movement occurs when individuals move cohesively towards a common direction or location, either by aligning with each other or clustering around a position, see Fig. 5. The underlying mechanisms of collective behavior often operate on a local scale, involving interactions between individuals in close proximity. The interactions that support collective behavior in social insects are diverse. For example, ants can effectively create paths between their nests and food sources by utilizing pheromone trails [94]. The bee waggle dance is another key example, a specific form of interaction where information is directly shared with many others [95].

Ants provide a classic example of how self-organization and collective motion emerge in social systems. Couzin and Franks' model shows how individual movement rules along foraging paths enable the group to select specific directions, forming traffic routes that minimize congestion [5]. A central question in understanding collective behavior is how many individuals are required for self-organization to emerge. Beekman et al. addressed this by studying Pharaoh's ants, showing that small colonies forage in a disordered, uncoordinated manner, whereas larger colonies adopt organized, pheromone-mediated strategies [96]. Biancalani et al. further explored collective decision-making, quantifying the mean switching time between two food sources and illustrating how local interactions drive group-level choices [34]. Together, these studies highlight general principles of self-organization, scaling, and decision-making in social collectives, providing a conceptual framework relevant to collective behavior across biological systems.

Similar dynamics have been observed in locust swarms, where Buhl et al. confirmed that a critical density exists at which locusts transition from disordered to ordered movement [55]. Escudero et al. further explored the role of intrinsic noise, showing that it can enhance directional switching within the swarm [43]. Additionally, time-delayed interactions also influence the collective movement of locust swarms [31]. Specifically, for sufficiently small response delays, increasing transmission delay prolongs the average switching time. For larger response delays, however, increasing transmission delay may disrupt the swarm's orderly direction switching. The findings reported by Sayin et al. challenge the long-held belief regarding how order emerges from disorder in animal collectives [97]. Specifically, the authors argue that locusts do not conform to the "self-propelled" particle model; instead, they demonstrated that sensory and cognitive mechanisms modulate such interactions.

2.1.4. Human collective behavior

Collective phenomena are not limited to animals or cells; they are also pervasive in various forms of human behavior. For instance, after a spectacular performance, the audience expresses their appreciation and joy through applause, which often leads to collective acoustic synchronization [98]. Néda et al applied the Kuramoto model to transform the synchronization of applause into a phase synchronization problem, see Fig. 6. From the perspective of nonlinear dynamics, they elucidated the mechanism behind the synchronization of applause and provided the critical coupling strength required for synchronization [99]. Sun et al. investigated the synchronization of applause with a leading applauder [100]. They proposed that rhythmic applause is more likely to occur in theaters with high occupancy rates. Additionally, even in very large theaters, a single leading applauder can guide the entire audience to clap in synchrony.

In addition to the emergence of applause from the audience, music performances also illustrate the transition from individual behaviors to multi-agent interactions. Proksch et al. analyzed a musical performance that achieved a carefully orchestrated (non-urgent) transition from non-coordinated to coordinated interactions, simulated physically [101]. Playing music together is an

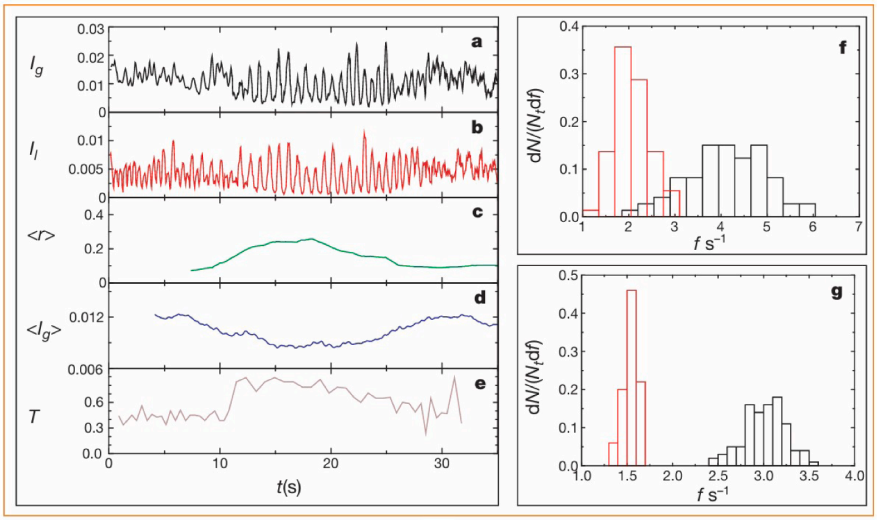

Fig. 6. Emergence of synchronization in clapping. (a) Global noise intensity as a function of time. (b) Local noise intensity measured by a hidden microphone in the vicinity of a spectator. (c) Order parameter, r, defined as the maximum of the normalized correlation between the signal and a harmonic function, and $\langle r \rangle$ represents the average value. (d) Average noise intensity. (e) The clapping period, T, defined as the intervals between the clearly distinguishable maxima. (f) The normalized histogram of clapping frequencies measured for 73 high-school students for mode I (black) and mode II (red) clapping. Individual students, isolated in a room, were instructed to clap as they would immediately after a good performance (mode I clapping) or during the rhythmic applause (mode II clapping). (g) Normalized histogram for mode I and II clapping obtained for a single student, sampled 100 times over a one-week period. *Source:* The figure is from [98].

illustrative example of the interplay between emergent and planned coordination expressed in entrained behavior. To investigate the role of interbrain synchronization in interpersonal motor coordination, Lender et al. simultaneously recorded electroencephalogram (EEG) data from 13 pairs of pianists performing a duet [102]. The study demonstrates that interbrain synchronization is grounded in the interpersonal temporal alignment of different brain mechanisms and cannot be simply reduced to similar sensory or motor responses [102].

Human crowds also exhibit a wide range of self-organizing behaviors [12,103,104]. One of the most catastrophic forms of collective behavior is crowd stampedes caused by panic, and several studies have modeled crowd dynamics [70,104,105]. Moussaï et al. proposed a cognitive science approach to address situations where pedestrians are hidden or out of sight, successfully predicting the occurrence of self-organizing phenomena [104]. Gu et al. analyzed trajectory data from over 5000 people gradually gathering in a 1,000-square-meter square during the San Fermín festival in Spain [106]. The researchers found that in confined spaces, as crowd density increased, a phase transition occurred, shifting from basic stillness to self-driven, large-scale, synchronized chiral oscillations involving hundreds of people, which posed a risk of individuals being pressed against walls and suffocating. Understanding crowd dynamics is crucial for improving safety at group events.

2.2. Collective dynamics in cellular biology

In cell biology, examples of collective behavior are abundant, such as biofilm expansion driven by extracellular polymeric matrices [10,107], the aggregation and migration of cell populations that promote wound healing [6,108–110], and cell oscillations generated in high-density bacterial suspensions [11], as shown in Fig. 7. These collective behaviors result from interactions between cells, changes in the local environment, and the combined effects of external stimuli. Next, we will discuss the different types of cellular collective behaviors.

2.2.1. Collective cell migration and invasion

Collective cell migration is a hallmark of tissue remodeling events, which form the basis for processes such as embryonic morphogenesis, wound repair, and cancer invasion [111,112]. A classic example of this is observed in the zebrafish lateral line primordium, where a group of over 100 cells migrates collectively along the embryo's flank to form interconnected mechanosensory organs essential for organ development [113]. Similarly, the migration of neural crest cells is fundamental to embryonic development, and recent mathematical models using partial differential equations have provided insights into the mechanisms driving this collective behavior [56,114,115].

In tissue repair, such as skin or corneal epithelial repair, keratinocytes collectively migrate toward the wound site, forming a cohesive barrier to promote tissue closure [6]. This process is tightly regulated by various signals, including growth factors, extracellular matrix components, and cell-cell interactions, which guide the speed and direction of movement to restore tissue integrity. Recent studies have also explored the therapeutic potential of natural compounds to enhance these migratory processes, offering promising

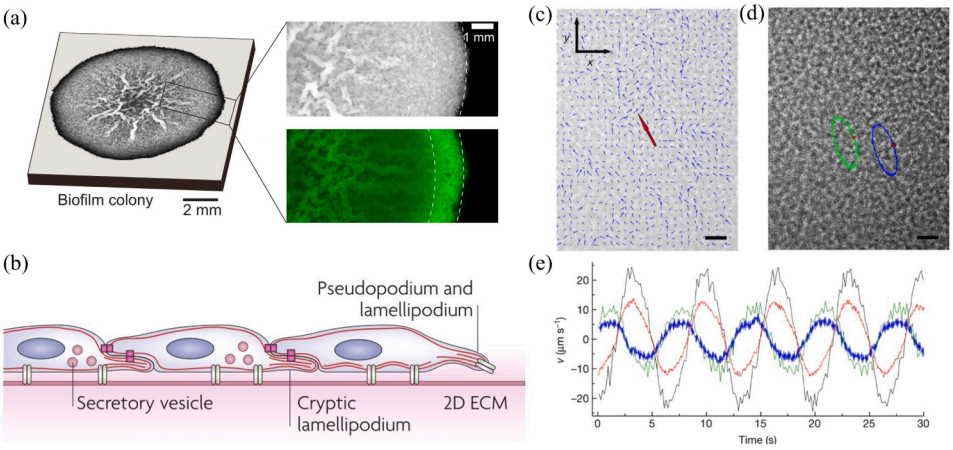

Fig. 7. Examples of cellular collective behaviors. (a) A *Bacillus subtilis* biofilm colony. (b) A coherent epidermal monolayer moving across a two-dimensional ECM substrate. (c) Representative velocity field of cells' collective motion obtained by PIV analysis. (d) In the same field of view as (c), two silicone oil tracers (red dots) displayed synchronized oscillation in elliptical trajectories. (e) The collective velocity of the cells in (c) (blue for the x-axis component; red for the y-axis component) and the velocity of the tracers in (d) (green for the x-axis component; black for the y-axis component). *Source:* The figures are from [6,11,107].

avenues for improving wound healing. For example, Luparello et al. investigated how compounds extracted from invertebrates can influence collective migration in skin tissue, suggesting new strategies for tissue reconstruction and repair [116].

Collective invasion is a key mode of cell migration, particularly in the context of cancer metastasis [8,117,118]. Experimental studies show that clusters of cancer cells can survive in the bloodstream and efficiently seed metastatic sites, underscoring the functional importance of collective motion. Collective invasion dynamics are shaped by a combination of cellular interactions and microenvironmental cues, which together regulate coordination, persistence, and invasion efficiency [7,8,119]. Interactions between cells and the extracellular matrix (ECM) play a central role in this process, influencing migration pathways and collective organization, with important implications for cancer progression, tissue engineering, and regenerative medicine [120]. From a modeling perspective, these findings also highlight a broader trade-off: while simplified models can capture essential collective behaviors, increasing model complexity often amplifies sensitivity to experimental variability and parameter uncertainty, emphasizing the need for balanced, mechanism-informed modeling approaches [121,122].

2.2.2. *Collective cellular oscillation*

Collective cellular oscillations play an important role in a wide range of biological systems [123]. In the pancreas, for example, oscillations regulate insulin secretion, and similar oscillatory behaviors are observed in yeast populations, both glycolytic and non-glycolytic [124]. Hubaud et al. identified the conditions necessary for stable oscillations at the cellular level, highlighting the molecular signals that initiate and stabilize these rhythms [125]. In addition, cellular metabolism can trigger oscillations during biofilm formation [126], where biofilms use oscillatory behavior to balance cooperation (protection) with competition (hunger), as illustrated in Fig. 8. Furthermore, collective oscillatory behavior can also manifest in the movement trajectories of cells [11,59]. Chen et al. demonstrated that cells in dense bacterial suspensions can self-organize into highly robust collective oscillatory motion, whereas individual cells move in an irregular manner [11]. As shown in Fig. 7(c–e), the average speed of the cells oscillates, and the average position of the cells can describe a regular elliptical trajectory. Japaridze et al. showed that in micro-pores, *Escherichia coli* can produce periodic oscillations and developed a method using a fluid dynamics-coupled system to detect the movement of *E. coli* [59].

2.2.3. *Bacterial colony*

Bacterial colonies provide a compelling example of collective behavior, often forming structures like biofilms or chains. Recent studies have advanced our understanding of these systems by applying agent-based modeling to simulate bacterial behavior at the population level, including processes such as colony expansion and biofilm growth [9,10]. Agent-based models (ABMs) and individual-based models (IBMs) both represent systems as collections of discrete, autonomous individuals governed by local interaction rules. Although the two terms are often used interchangeably, IBMs are more commonly adopted in ecological and biological modeling, whereas ABMs are widely used across broader complex systems research. These approaches are particularly well suited for capturing heterogeneity among individuals and for examining how simple local rules can generate nonlinear, emergent group-level dynamics. In such frameworks, network structure provides the interaction scaffold through which local interactions propagate, shaping information flow and collective outcomes. In contrast, some models focus primarily on macroscopic, population-level properties, such as coarse-grained or aggregate models, which describe averaged system behavior but cannot explicitly resolve individual heterogeneity or interaction-level mechanisms [127]. Moreover, multi-agent systems typically originate from control theory and robotics, with a stronger emphasis on communication protocols, distributed coordination, and system-level consensus or control objectives. Lega

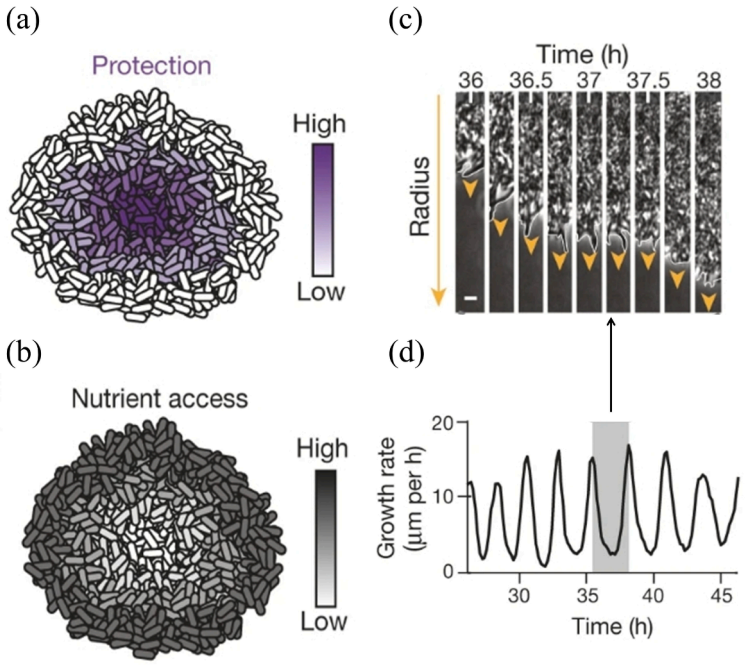

Fig. 8. Biofilms show oscillations in colony expansion. Biofilms must reconcile opposing demands for protection from external challenges (a) and access to nutrients (b). (c) A film strip of the biofilm radius over time shows a pause in colony expansion. This film strip represents one cycle of biofilm oscillations, indicated by the shaded region in (d). Scale bar, $5\mu m$. The arrowheads indicate direction of biofilm growth. (d) Growth rate over time shows persistent oscillations in colony expansion. *Source:* The figure is from [126].

et al. proposed a fluid dynamics model suitable for describing the growth of dense bacterial colonies on agar plates [60]. In the context of the gut, bacterial clustering has been shown to play a role in healing intestinal inflammation, with intestinal pressure promoting the formation of bacterial groups [128]. To explore this process, Cremer et al. introduced a reaction-diffusion model, capturing how gut contractions affect the organization of bacterial communities [61].

2.3. Swarm robotic and UAVs

The study of collective behavior in animals and cells has significantly influenced the development of swarm robotics and the control of collective motion in systems like unmanned aerial vehicles (UAVs). In both biological systems and robotics, collective motion arises from extensive interactions between individual agents, enabling them to work together cohesively. This concept has led to the creation of swarm robotics, where multiple robots coordinate their movements to accomplish complex tasks, such as navigating from one location to another. A prime example is drone light shows, where drones equipped with LEDs hover in precise formations to create dynamic patterns, as shown in Fig. 9(a).

Inspired by natural systems, researchers have increasingly focused on the collective motion of robots, with the goal of achieving coordinated and cooperative task execution. In swarm robotics, this includes methods for guiding self-organizing robot swarms, as explored by Celikkanat et al., who demonstrated how to control a subset of robots to direct a swarm in a desired direction [129]. Zhao et al. further advanced this by developing leaderless algorithms that enable robots to travel along pre-determined paths in a coordinated manner [130]. However, just as in biological systems, various challenges arise in swarm robotics, such as environmental noise, communication delays, and heterogeneous robot capabilities. These factors can disrupt the coordination between robots and affect the overall performance of the swarm [131–133]. Notably, when robots with heterogeneous capabilities work together to achieve a common goal, system heterogeneity naturally emerges [134]. Addressing this, Szwaykowska et al. conducted a systematic investigation of collective motion in agent systems with heterogeneous delayed coupling, highlighting the pronounced effects of heterogeneity on emergent motion patterns [135].

Collective motion of robots holds significant importance in various practical applications. For instance, in search-and-rescue operations, a group of robots can move collaboratively along a predefined path while simultaneously collecting data and searching for targets across large areas [137,138]. In the film industry, swarm drones can work together to capture or record events from multiple angles, offering diverse perspectives and enhancing the content's richness [139]. Zhou et al. developed miniature but fully autonomous drones, enabling efficient swarm navigation [136]. They tackled the fundamental challenge of autonomous navigation for aerial swarms operating in chaotic outdoor environments, as illustrated in Fig. 9(b), thereby improving the swarm's applicability to real-world tasks such as disaster relief, collaborative transportation, and exploration of confined spaces.

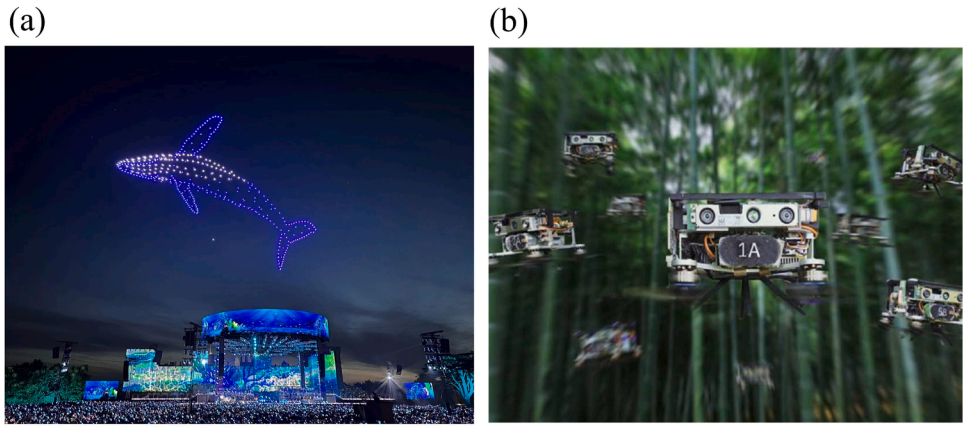

Fig. 9. Examples of swarm behaviours. (a) Drone display at the coronation concert of the King of the United Kingdom, 7 May 2023. (b) A swarm of drones flying over a dense forest. *Source:* Figure (a) is from https://www.iotworldtoday.com/robotics/drones-light-up-coronation-of-king, and Figure (b) is from [136].

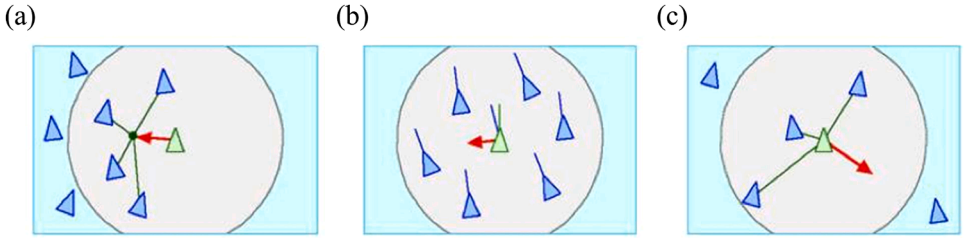

Fig. 10. The three basic steering behaviors determining the motion of the objects in the Reynolds model. (a) Separation. (b) Alignment. (c) Cohesion. *Source:* The figure is from http://www.red3d.com/cwr/boids/.

3. Dynamic modeling of collective behavior

3.1. Microscopic and macroscopic models

There is a rich array of models that elucidate the fundamental principles underlying the emergence of collective behavior through self-organizing processes [49,50,54,140]. Self-organization phenomena are not only ubiquitous in nature but also exhibit a broad range of adaptability, covering synchronization from macroscopic animal groups to microscopic cell populations. However, when attempting to model the behavior of real animal or cell populations, more detail and precision are often required, as the interaction dynamics in real systems are much more complex and diverse. In this section, we introduce several models developed to investigate collective behavior in animal ecology and cell biology, and discuss their applications. Table 1 presents examples of models associated with different types of collective behavior.

In 1987, Reynolds introduced the first widely recognized particle-based simulation model of flocking behavior [48], in which each bird was represented as a particle and moved according to three key behavioral rules: alignment with neighbors, cohesion through proximity, and separation to avoid collisions (see Fig. 10). Building on the idea that large-scale order can emerge from local interactions under uncertainty, Vicsek et al. introduced a minimal self-propelled particle model in 1995 [54]. In this model, N particles move with a constant speed v and update their positions according to

$$x_i(t+1) = x_i(t) + v_i(t)\Delta t. \tag{1}$$

The velocity $v_i(t+1)$ is constructed to have a magnitude v and a direction given by the angle $\theta(t+1)$. The expression for the angle is

$$\theta(t+1) = \langle\theta(t)\rangle_r + \Delta\theta, \tag{2}$$

where $\langle\theta(t)\rangle_r$ represents the average velocity direction of the particles (including particle i) within a radius r around the given particle. In Eq. (2), $\Delta\theta$ is a random number selected with uniform probability from the interval $[-\eta/2, \eta/2]$, and thus $\Delta\theta$ represents noise. The Vicsek model exhibits a phase transition from a disordered to an ordered state as group density increases and the noise strength is low.

As interest in capturing richer biological phenomena grew, numerous extensions of the Vicsek framework were developed to incorporate more structured interactions. A particularly influential advance was introduced by Couzin et al., who proposed a spatially explicit model that emphasizes how individuals respond differently to neighbors at varying distances [49]. Instead of using a single

interaction radius, their approach divides the surrounding space into three behavioral zones— the “zone of repulsion" (zor), the “zone of orientation" (zoo), and the “zone of attraction" (zoa)—reflecting the graded local tendencies observed in natural animal groups (Fig. 11).

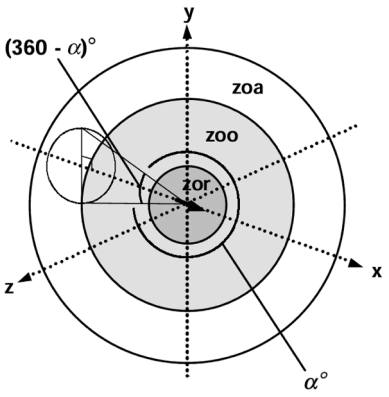

Fig. 11. Schematic diagram of the non-overlapping behavioral zones: repulsion, orientation, and attraction. *Source:* The figure is from [49].

Variants of the Vicsek model can effectively describe specific types of animal collective behavior. For example, Lukeman et al. demonstrated that a Vicsek-like model, incorporating alignment, attraction, repulsion, and additional surface interactions, could accurately capture the behavior of surf scoters floating on the water’s surface [141]. Even during fluctuations and instances of instantaneous group collapse, the model remained effective in capturing the behavioral characteristics of surf scoters [142]. Similar social forces have also been shown to describe the local interactions within various fish schools [53,143]. Another Vicsek-like model incorporating additional behavioral states, such as intermittent stillness, has been demonstrated to effectively capture the dynamics of sheep herding behavior [144].

To account for the influence of global information on individual behavior, Cucker and Smale proposed a model, formulated in both continuous and discrete time, to describe flocking dynamics [50]. This model assumes that each bird adjusts its velocity by incorporating a weighted average of the velocity differences relative to all other birds. Specifically, for bird i, the velocity update is given by

$$v_j(t+1) - v_i(t) = \sum_{i=1}^{k} a_{ij}\big(v_j(t) - v_i(t)\big). \tag{3}$$

The weight a_{ij} quantifies how birds influence one another and is assumed to depend on the distance between them. Hence, they proposed the adjacency matrix in the following form

$$a_{ij} = \eta\big(||x_i - x_j||^2\big), \tag{4}$$

where the non-increasing function $\eta : \mathbb{R}_+ \to \mathbb{R}_+$ has the specific form:

$$\eta(y) = \frac{K}{\big(\sigma^2 + y\big)^{\beta}}. \tag{5}$$

Here, $\sigma > 0$ and $\beta > 0$, with β characterizing the rate at which the influence between birds in the flock decays as a function of distance. Eq. (3) can be compactly expressed by introducing the adjacency matrix $A_x = (a_{ij})$, the diagonal matrix $D_x = \mathrm{diag}(d_i)$ with $d_i = \sum_j a_{ij}$, and the associated Laplacian $L_x = D_x - A_x$. The velocity update then becomes

$$v_i(t+1) - v_i(t) = -\big[L_x v(t)\big]_i. \tag{6}$$

Together with the position update, the discrete-time dynamics are

$$\begin{aligned} x(t+1) &= x(t) + \Delta t v(t) \\ v(t+1) &= \big(Id - L_x\big)v(t). \end{aligned} \tag{7}$$

The continuous-time counterpart is

$$\begin{aligned} \dot{x} &= v \\ \dot{v} &= -L_x v. \end{aligned} \tag{8}$$

One of the most important results from Cucker and Smale is that the emergence of flocking behavior depends on β [50]. Specifically, when $\beta < 1/2$, the convergence of the flock to a common velocity is guaranteed. For $\beta \geq 1/2$, convergence is guaranteed under certain conditions, depending on the initial positions and velocities of the birds.

Numerous extensions of the classical Cucker-Smale model have been extensively studied to capture a broader range of collective behaviors. For example, the case of singular communication rates, defined by $\psi(s) = 1/s^{\beta}$, was rigorously analyzed in [145]. Motsch

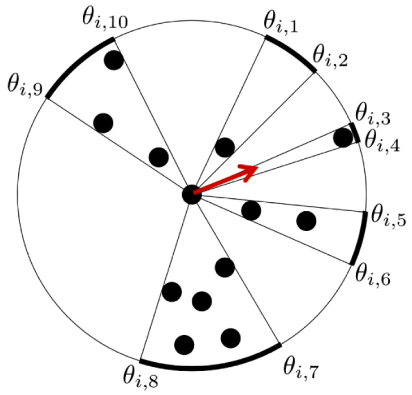

Fig. 12. The structure of the projection that the i-th individual observes, passing through the 2D swarm, where the individual is located at the center. The thick black regions surrounding the outer circle represent the angular regions where one or more other individuals obstruct the i-th individual's line of sight to infinity. The domain boundaries observed by the i-th individual define a set of angles θ_{ij}, where $j = 1, 2, \ldots, 10$. The sum of unit vectors pointing to each of these domain boundaries, at the given angles, results in the resolved vector $\underline{\delta}_i$, shown in red, where $\underline{\delta}_i = \frac{1}{10}\sum_{j=1}^{10}\begin{pmatrix}\cos\theta_{ij} & \sin\theta_{ij}\end{pmatrix}^T$. *Source:* The figure is from [51].

and Tadmor introduced a modification in which the communication rate between agents depends on their relative distances rather than explicitly on the total number of agents, thereby addressing limitations related to scalability [146]. Furthermore, stochastic variants of the Cucker-Smale system incorporating additive or multiplicative noise have been explored to account for environmental and internal uncertainties [147–149]. Erban et al. investigated the combined influence of multiplicative noise and response time delays on the system's asymptotic dynamics, revealing complex effects on flocking behavior [150].

In addition to distance-dependent communication rates, visual perception plays a significant role in shaping collective dynamics. In large flocks, an individual bird's visual perspective is often constrained, with many surrounding birds appearing only as silhouettes, either due to their rapid motion, large distance, or tracking difficulty. In such cases, individual birds may become indistinguishable from one another. To account for this phenomenon, Pearce et al. proposed a hybrid projection model, in which each bird responds to the visual projection of the group as perceived from its own point of view [51]. This model identifies dark angular regions where, from an individual's line of sight extending to infinity, their view intersects with one or more other flock members, as shown in Fig. 12. The presence of opaque edges in these projections significantly limits interactions between individuals within large flocks. It provides a mechanism for global interaction, allowing an individual to respond to the group it perceives. This approach facilitates faster information transfer, enabling rapid group dynamics, which offers a distinct advantage over models based solely on local interactions. However, the role of individual body size in visual projection or the influence of color patterns on visually mediated collective behavior had often been overlooked. To address this, a universal modeling approach has been proposed [52]. Bastien et al. developed a general mathematical framework for purely vision-based collective behavior, exploring the types of collective behaviors that can emerge under minimal conditions [52]. This work also provides new insights for the development of fully autonomous, visually-driven robotic swarm systems.

Network science provides a powerful framework for describing the intricate interactions among elements in complex systems that give rise to collective behavior. Consequently, many researchers have incorporated network concepts into the modeling of collective motion. In 2006, Olfati-Saber et al. proposed a framework to investigate the consensus problem in multi-agent networks with directed and switching topologies [151]. Each node in the weighted network is modeled as a dynamic agent governed by the following dynamics:

$$\dot{x}_i(t) = u_i(t), \tag{9}$$

where $x_i \in \mathbb{R}$ denotes the value associated with node v_i, $i = 1, \ldots, n$. For networks with fixed or switching topologies, the following linear consensus protocol is employed:

$$u_i = \sum_{v_j \in N_i} a_{ij}(x_j - x_i), \tag{10}$$

where N_i denotes the set of neighbors of node v_i. In networks with switching topology, N_i varies over time. The states of continuous-time agents evolve according to the linear system:

$$\dot{x}(t) = -Lx(t), \tag{11}$$

where L is the Laplacian matrix of the network. It has been shown that multi-agent systems with strongly connected topologies can achieve the average consensus, wherein all agents ultimately agree on a common state equal to the average of their initial states. From the perspective of network science, Reynolds' flocking model [48] can be interpreted as a mechanism that achieves velocity synchronization while regulating the relative distances between agents. Tanner et al. derived a decentralized controller

demonstrating that, regardless of network switching, as long as the network remains connected, convergence to a common velocity vector and stability of inter-agent distances are guaranteed [152].

The structure of interactions—cooperative and competitive relationships among individuals—has also been incorporated into the modeling of collective behavior. Chakraborty et al. investigated how the range of cooperative interactions within prey populations affects their survival under predator attacks [153]. Their results showed that prey survival peaked at intermediate interaction ranges. When the interaction range was too small, prey failed to coordinate their movement effectively, limiting their ability to escape as a group. Conversely, with large interaction ranges, each prey interacted with nearly every other individual, resulting in highly unified group motion that made it easier for predators to track and capture them.

Collective behavior in animals enables the achievement of specific functional outcomes, and similar phenomena are also observed in cell populations, where collective cell behavior serves to coordinate processes such as tissue morphogenesis, wound healing, and cancer invasion. Notably, most previous modeling efforts have focused on animal groups, yet some of these frameworks can also be applied to describe collective motion in cellular systems. Nevertheless, due to the inherent complexity of cellular behavior across both spatial and temporal scales, more refined mathematical models are required to capture specific phenomena such as collective cell migration, bacterial colony expansion, and cellular oscillations [11,61,114,115,154,155]. Recent advances in experimental techniques have further enriched our ability to analyze these systems. In particular, time-lapse imaging and fluorescence microscopy have become standard tools in life sciences research, enabling high-resolution, real-time observation of cellular dynamics.

Collective cell migration, which involves the simultaneous movement of multiple cells connected by intercellular adhesion, is commonly observed in processes such as development, tissue repair, tumor metastasis, and wound healing [6,117,156]. The ECM strongly influences migration dynamics through both biochemical signaling and biophysical interactions. Mathematical and computational models offer powerful means to dissect the complexity of collective cell migration by selectively incorporating ECM components and interactions. Three principal frameworks are widely used [157]: continuum models, which describe cell and ECM densities through ordinary or partial differential equations (ODEs or PDEs); individual-based models (IBMs), which represent single-cell behavior via rule-based interactions on or off lattices; and hybrid models, which couple cell-level dynamics with environmental evolution for a more integrated description.

In 2006, Szabó et al. used long-term videomicroscopy to track large populations of migrating corneal cells and revealed a density-driven transition from disordered to coherent collective motion [158]. Motivated by these experiments, Szabó et al. constructed a model for the collective motion of cells:

$$\frac{d\mathbf{r}_i(t)}{dt} = v_0\mathbf{n}_i(t) + \mu\sum_{j=1}^{N}\mathbf{F}(\mathbf{r}_i,\mathbf{r}_j), \tag{12}$$

where $\mathbf{r}_i$ represents the position of cell i ($i = 1, \cdots, N$). In this model, the N cells move at a constant speed v_0 in the direction of the unit vector $\mathbf{n}_i$. In addition to this active motion, cell pairs i and j also experience an intercellular force $\mathbf{F}(\mathbf{r}_i,\mathbf{r}_j)$ with migration rate μ, which moves the cell's position.

Arboleda-Estudillo et al. studied the formation of the zebrafish embryonic gastrula through numerical simulations [159]. In their simulations, the migration of cells is mediated by four distinct types of forces: (1) a short-range repulsive, mid-range attractive spring force (f_s) representing cell adhesion; (2) a chemotactic force (f_c) modeling polarized migration; (3) a Vicsek type force, f_v, modeling collective migration as each cell attempts to align its direction with its neighbors; (4) a noise force (f_n) modeling random migration. The system of N coupled Langevin equations are numerically integrated:

$$b^{-1}(\mathrm{d}r_i/\mathrm{d}t) = \sum_{j\neq i} f_\mathrm{s} + f_\mathrm{c} + f_\mathrm{v} + f_\mathrm{n}, \tag{13}$$

where b is the cell mobility. Arboleda-Estudillo et al. identified how the collective migration of mesodermal cells during zebrafish gastrulation establishes directional movement.

Based on the cellular and molecular mechanisms of neural crest cell migration, Carmona-Fontaine and colleagues developed an IBM [57]. The model incorporates three key factors: (1) short-range repulsive interactions corresponding to contact inhibition of locomotion, (2) long-range attractive interactions between cells, and (3) migration behavior driven by a chemotactic gradient. The simulation results indicate that these three interactions are sufficient to replicate the dynamics of Xenopus neural crest cell migration observed experimentally. Additionally, several studies have proposed PDE models to investigate the underlying mechanisms of neural crest cell migration and to simulate the migration process [114,115]. Cell-level IBMs, built from single-cell observations and key cell-specific parameters, explicitly capture biological details at the cellular scale, providing realistic descriptions of collective cell migration. In contrast, PDE models treat cell populations as continuous media, offering a mathematically consistent framework to examine how microscopic assumptions manifest at the tissue scale [56]. These mathematical models describe the temporal evolution of cell density alongside the dynamics of relevant biochemical signals or underlying substrates. The choice of terms in such models is often guided by the need to simplify the system. However, recent advances in experimental techniques have generated substantial quantitative data on collective cell migration. This progress now enables the use of statistical and machine learning tools to derive mathematical models directly from the data [58]. These approaches will be further discussed in the next section.

Inspired by fluid dynamics, particle image velocimetry (PIV) techniques have been widely employed to precisely map velocity fields and strain tensors within tissues. These imaging technologies not only facilitate detailed monitoring of collective cellular motion but also generate rich quantitative data that support the development and validation of theoretical models, thereby deepening our understanding of cellular collective behavior. Chen et al. employed the PIV method for measurement and observed that cells can self-organize into highly robust collective oscillations, while individual cells move irregularly [11]. As shown in Fig. 7(c–e), the

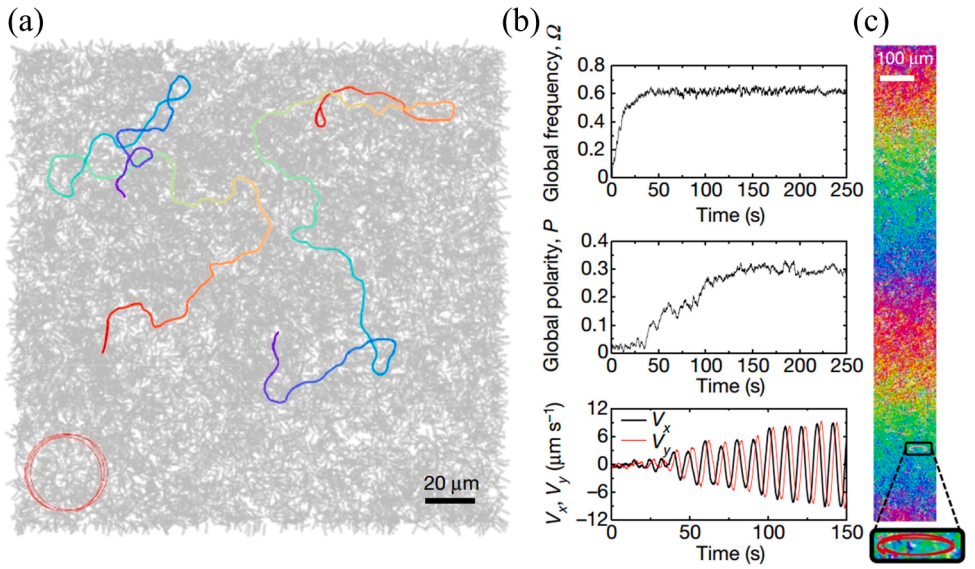

Fig. 13. Modelling results of collective oscillation. (a) Snapshot of the self-propelled particle model (Eq. (14)) without fluid, in a uniform counter-clockwise collective oscillation state. (b) Time series of global frequency Ω, global polarity P, and collective velocity components V_x (horizontal) and V_y (vertical) from random initial conditions (same parameters as in (a)). (c) Snapshot of the collective oscillation state in the wet model (Eq. (16)). *Source:* The figure is from [11].

average trajectory of the bacteria exhibited an elliptical shape. To explain the observed collective oscillatory behavior, Chen et al. proposed a self-propelling particle model with noise. First, they considered only the interactions between bacteria. The single-particle dynamics involve the evolution equation of the velocity direction θ, which allows for local alignment. It also incorporates angular velocity or instantaneous frequency $\omega = \dot{\theta}$ to account for the short-term memory effect introduced by local fluid vortices and enables the synchronization of local rotational motion. Within a distance of d_0 on the order of the bacterial body length, particles experience two types of interactions: diffusion coupling of angular velocities of strength k_ω and a polar alignment of strength k_θ:

$$\begin{aligned}\dot{\theta}_i &= \omega_i + \frac{k_\theta}{n_i}\sum_{j\sim i}\sin(\theta_j - \theta_i) + \xi_\theta,\\ \dot{\omega}_i &= -\frac{\omega_i}{\tau} + \frac{k_\omega}{n_i}\sum_{i\sim i}\left(\omega_j - \omega_i\right) + \xi_\omega + \xi_{\text{bias}},\end{aligned} \tag{14}$$

where the sums run over n_i neighboring particles j around particle i, and the delta-correlated noise terms ξ_θ and ξ_ω are drawn from symmetric uniform distributions over the intervals $[-\eta_\theta, \eta_\theta]$ and $[-\eta_\omega, \eta_\omega]$, respectively. Moreover, ξ_{bias} has the sign of ω and its amplitude decreases with $|\omega|$, with the following form:

$$\xi_{\text{bias}} = \text{sign}(\omega_i)\exp\left(-\left|\omega_i\right|/\omega_0\right)\xi, \tag{15}$$

where ξ is a uniform noise term in the range $[0, \eta_{\text{bias}}]$.

However, simulations of Eq. (14) produced average particle trajectories that were roughly circular (Fig. 13 (a) and (b)), in contrast to experimental observations, which show that the average trajectories are elliptical with the long axis perpendicular to the wave propagation direction. To address this, Chen et al. considered the surrounding viscous fluid. Cells interact with the agar gel surface, pushing themselves away from the gel while carrying some liquid. The incompressible damped fluid is governed by the Stokes equation, producing the convective fluid flow field $\mathbf{v}$ that advects particles:

$$\dot{\mathbf{r}}_i = \mathbf{v} + v_0\hat{\mathbf{u}}_i, \tag{16}$$

where $\hat{\mathbf{u}}_i$ is the unit vector in the direction θ_i. Simulations of this model demonstrate that the average trajectory of the bacteria is elliptical, with the major axis oriented perpendicular to the direction of wave propagation, as shown in Fig. 13 (c), consistent with experimental observations.

Despite the substantial differences in scale, organization, and complexity between animal groups and cellular populations, these systems exhibit remarkable similarities in the mechanisms that generate collective behavior. In animal groups, individuals typically adjust their actions through local information transfer when responding to environmental changes; for example, collective turning, aggregation, or escape behaviors may emerge under predation pressure or shifting resource availability. Likewise, when exposed to external stimuli such as wound healing or tumor expansion, cellular populations coordinate their collective responses through molecular signaling or mechanical cues. At the level of interaction rules, the repulsion, attraction, and alignment observed in animal groups have clear conceptual parallels in cellular systems, including volume filling, adhesion-mediated attraction, and directional

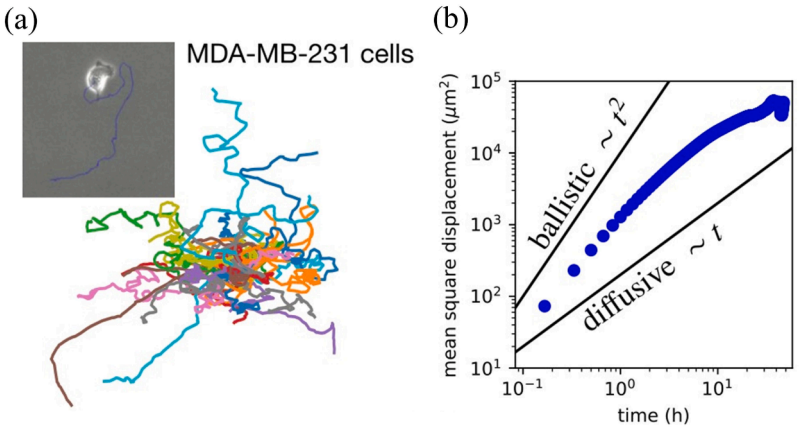

Fig. 14. Experimental images of cell migration. (a) Brightfield microscopy image of a migrating MDA-MB-231 cell. (b) Mean square displacement curves calculated from experiments. *Source:* The figure is from [167].

consistency. For example, volume filling generates repulsion during collective cell migration to prevent overcrowding, just as animals maintain minimum spacing to avoid collisions. The dynamic balance between cooperation and competition observed in animal groups—such as the synergistic benefits of collective foraging versus competition when resources are limited—is also evident in cellular systems. A representative example is the metabolic oscillations that arise during biofilm formation, where the population continually negotiates between cooperative construction of protective structures and competition for nutrients. These cross-scale commonalities uncover the universal principles underlying collective behavior and highlight the potential for conceptual exchange between animal ecology and cell biology.

3.2. Data-driven and machine learning models

We have discussed various models of collective dynamics [11,49,50,54], which can be studied qualitatively when the governing equations are known in advance. However, in situations where only short-term trajectories of the system are available and the underlying equations remain unknown, accurately predicting emergent behaviors becomes significantly more challenging. In such cases, uncovering hidden dynamical mechanisms from observational data is essential—a pursuit that has long played a central role in science and engineering. This tradition dates back to the 17th century, when Kepler deduced the laws of planetary motion from Tycho Brahe's astronomical observations. In recent years, the rapid expansion of data acquisition—driven by decreasing costs of sensors and measurement technologies—has greatly improved our ability to monitor large-scale complex systems [160,161]. Concurrently, there has been a surge of interest in model-agnostic inference techniques that are both scalable to high-dimensional systems and capable of handling large datasets. Among them, reservoir computing—a lightweight machine learning framework—and its variants have emerged as representative approaches, demonstrating remarkable success in modeling complex physical systems and predicting collective dynamics [162–166].

To investigate the mechanisms underlying cell migration, a variety of models have been proposed to describe cell motility [167]. A central challenge in developing these models is establishing a connection to experimental data in order to infer the dynamical rules governing cellular movement. A straightforward approach to quantifying the dynamics of migrating cells is to reduce the cell state to a single variable: its position as a function of time, typically represented by the trajectory of the cell nucleus or centroid, see Fig. 14. One of the simplest statistics derived from such trajectories is the mean-square displacement (MSD), which characterizes both the timescale of velocity correlation decay and the effective diffusion coefficient [168]. However, measuring MSD alone is insufficient to uniquely determine the underlying model of cell migration, as many distinct mechanisms can produce the same MSD. Consequently, additional statistical measures—such as acceleration—are necessary to more accurately distinguish between competing data-driven models [169].

In 2018, Zienkiewicz et al. conducted experiments on collective behavior in zebrafish, leading to the development of a data-driven model of zebrafish social interactions [170]. By analyzing empirical data collected during close-proximity swimming events, they were able to isolate the acceleration resulting from specific interaction responses among the fish. With sufficient data, they reconstructed the swimming kinematics, including position, velocity, angular velocity (turning rate), and corresponding accelerations as functions of time. In the experiment, pairs of swimming zebrafish were observed from above in a shallow (10 cm deep) circular tank. Trajectory data were then extracted to obtain a unique time series of the centroid position $x_i(t)$ for each zebrafish i at time t, see Fig. 15. Based on these findings, a novel bottom-up framework was developed directly from experimental data to characterize the spontaneous locomotion of zebrafish and the dynamics of their individual-level interactions.

In addition, a wide range of collective behaviors have been characterized through experimental data [171]. Despite significant interest, little is known about the detailed collective dynamics of fireflies, particularly their spatiotemporal patterns [172]. Using high-resolution stereoscopic video recordings, Sarfati et al. demonstrated the existence of chimera states, described their spatial distribution

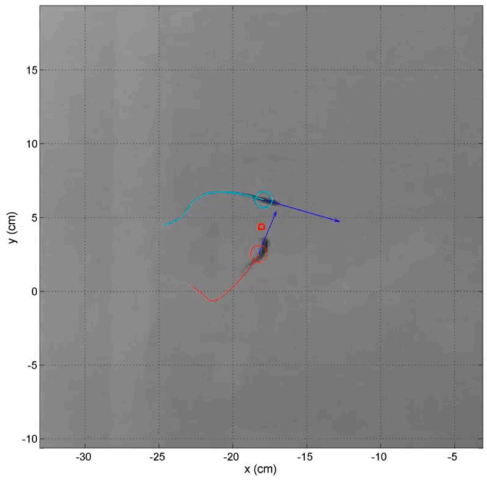

Fig. 15. Centroid trajectories of zebrafish observed in experiments. *Source:* The figure is from [170].

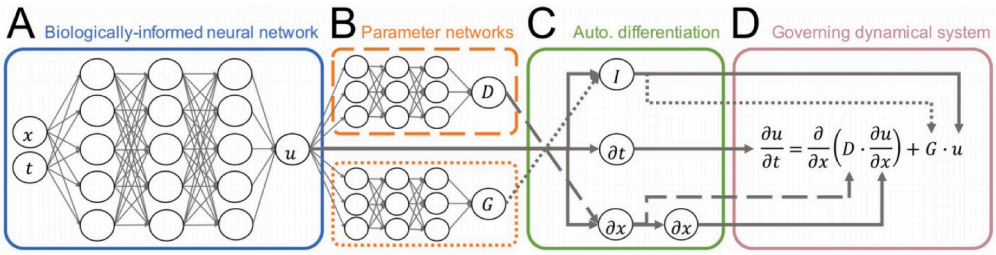

Fig. 16. Biologically-informed neural networks for reaction-diffusion models. (A) Biologically-informed neural networks (BINNs) are deep neural networks that approximate the solution of a governing dynamical system. (B) By allowing the terms of the dynamical system (e.g., diffusivity function D and growth function G) to be approximated by deep neural networks, the nonlinear forms of these terms can be learned without the need for a predefined mechanistic model or a library of candidate terms. (C) Automatic differentiation is applied to the compositions of different neural network models (e.g., u, D, and G) to construct the partial differential equation (PDE) that governs the dynamical system. (D) The governing system is incorporated into the neural network's objective function, enabling joint learning of the PDE while minimizing the error between the network outputs and noisy observations. *Source:* The figure is from [180].

and movement, and found that chimeras appeared to be spatially interwoven [171]. Although somewhat clustered, their displacements showed no enhanced correlations, and their phase distributions were typically stable. According to models proposed by Vicsek and Couzin, increasing the density of locusts in a circular arena leads to a transition from disordered to ordered motion [49,54]. However, while a positive correlation between density and order has been observed, establishing a causal relationship remains challenging. To address this, Sayin et al. conducted large-scale field experiments on juvenile locust swarms [97]. In order to disentangle the effects of density and order, the researchers employed virtual reality technology, allowing real locusts to interact with virtual conspecifics. They created a panoramic virtual environment in which real individuals could move freely and interact with these virtual agents. Simulation-based analyses of human crowds can help predict and prevent stampede risks. Gu et al., using trajectory data from over $5,000$ people gathering in a $1,000$-square-meter plaza during Spain's San Fermín festival, identified a phase transition in crowd behavior as density increased in a confined space [106]. When crowd density exceeded approximately four people per square meter, periodic oscillations began to emerge-posing risks of individuals being pressed against walls and suffocating. As the density continued to rise, the spatial extent of these coherent oscillations also increased.

Recently, numerous system identification methods based on observational data have been developed. These include techniques such as maximum likelihood estimation for learning parameterized systems via parameter inference [173,174], nonparametric estimation of drift in stochastic McKean–Vlasov equations [175], sparse identification of nonlinear dynamics (SINDy) [176], and its variant, weak SINDy, which employs the weak form of differential equations combined with sparse parametric regression [177]. Other approaches include physics-informed neural networks (PINNs) [178] and neural ordinary differential equations (NeuralODE) [179], among many others. Lagergren et al. trained biologically-informed neural networks (Fig. 16) within a supervised learning framework to approximate in vitro cell biology assay data, while simultaneously considering the general form of reaction-diffusion partial differential equations (PDEs) governing the system dynamics [180]. This approach was evaluated using sparse real-world data from wound healing assays, which varied in initial cell density.

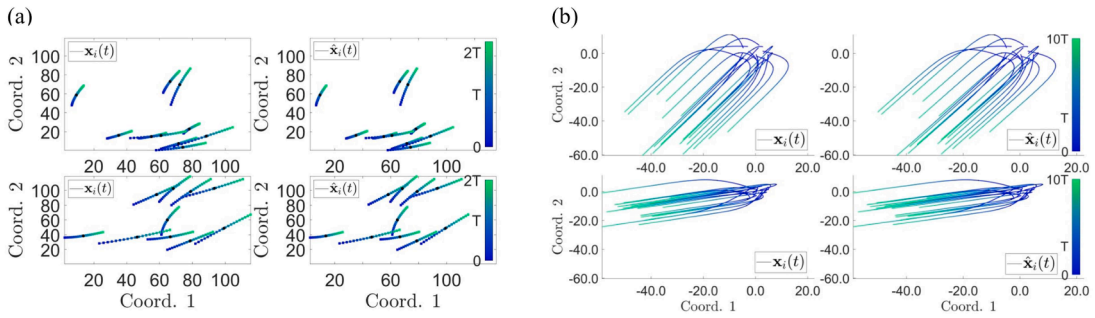

Fig. 17. Comparison of trajectories generated using the true and estimated interaction kernels (generated from Eq. (17)). (a) Trajectory prediction of the phototaxis system. (b) Trajectory prediction of the Cuker-Smale system. The first row of trajectories is generated based on initial conditions obtained from observational data, while the second row of trajectories is produced from another randomly selected set of initial conditions. $\mathbf{x}_i(t)$ represents the trajectories generated from the true interaction kernel, and $\hat{\mathbf{x}}_i(t)$ represents the trajectories generated from the estimated kernel with the same initial conditions, $i = 1, 2, \ldots, N$. The trajectories of the true system are well-approximated by those of the learned system, both in the "training" interval ($[0, T]$) and in the "prediction" interval ($[T, 2T]$ and $[T, 10T]$ respectively). Coord. stands for coordinate. The color of the trajectory indicates the flow of time, from deep blue at T_0 to light green at T_f. *Source:* The figure (a) is from [160], and (b) is from [161].

In high-dimensional settings, system identification becomes increasingly computationally intensive and time-consuming. To overcome the curse of dimensionality, Lu et al. employed a specialized and efficient dimensionality reduction technique [160]. Let $\mathbf{X} = (\mathbf{x}_i)_{i=1}^N \in \mathbb{R}^{dN}$ be the state vector for all of the agents. Assuming that the observed data follow an underlying dynamical system, the system is described by

$$\dot{\mathbf{X}}(t) = \mathbf{f}_\phi(\mathbf{X}(t)), \quad \mathbf{X}(0) = \mathbf{X}_0 \in \mathbb{R}^{dN}, \quad t \in [0, T], \tag{17}$$

where the right-hand side, $\mathbf{f}_\phi$, depends on the interaction kernel ϕ. The values of ϕ are not directly observable; instead, the available information consists of the system state $\mathbf{X}(t)$ over time and the pairwise distances between agents, which serve as the inputs to ϕ. The method aims to infer the interaction kernel ϕ in a nonparametric manner by constructing an estimator $\hat{\phi}$ from training data, such that the resulting system (17) reproduces the observed trajectories $\mathbf{X}(t)$ as closely as possible.

To validate the effectiveness of the proposed method, a specific example is considered to predict the trajectories of the system [160]. Agents interact within an environment, simulating the phototactic movement of bacteria toward a distant fixed light source. As shown in Fig. 17(a), the real trajectories $\mathbf{x}_i$ and the estimated trajectories $\hat{\mathbf{x}}_i$ closely align. The estimator performs exceptionally well, enabling accurate prediction of the trajectories in the phototaxis system. Further exploration was conducted on more complex dynamical systems to assess the performance of the estimator in predicting emergent behaviors of collective dynamics [161]. The comparison between the true trajectory $\mathbf{x}_i$ of the Cuker-Smale system and the learned trajectory $\hat{\mathbf{x}}_i$ is presented in Fig. 17(b). As shown, no discernible difference is observed between the real and learned trajectories, both for the training initial conditions and the randomly selected initial conditions.

4. Collective behavior with social interactions

Social interactions serve as a fundamental mechanism for the coordination and organization of collective behavior in biological systems. Whether in the context of cell migration, the formation of bacterial colonies, or animal groups such as bird flocks, fish schools, and insect swarms, individuals rarely act in isolation. Instead, they continuously respond to signals, cues, and movements from others in their local environment. These localized interactions give rise to structured global patterns that can naturally be represented as networks, in which nodes correspond to individuals and edges denote the transmission pathways of information, mechanical forces, or chemical signals. The emergence, stability, and adaptability of collective behavior depend not only on local interaction rules but, more fundamentally, on the structure of the underlying social interaction network. Different network topologies determine the pathways and efficiency of information transmission, the spatial extent of influence, and the effectiveness of coordination mechanisms. As a result, they play a decisive role in shaping diverse collective motion patterns. Therefore, understanding the dynamical evolution of collective behavior requires not only a focus on individual-level interaction rules but also a systematic investigation of the regulatory role played by network structures.

This section focuses on the central question: how does network structure influence collective behavior? It begins with an examination of collective dynamics on regular networks and progressively introduces small-world properties, heterogeneous connectivity, higher-order interactions, and temporal evolution. Through this layered approach, this section systematically analyzes how each structural feature contributes to the emergence and shaping of collective behavior. Classical lattice-based modeling approaches are first examined to illustrate how local interactions shape global dynamics. Following this, small-world networks are introduced, which combine local regularity with long-range connections to enhance synchronization and information flow. The discussion then moves to heterogeneous networks and emphasizes how variations in degree distribution and connectivity influence system robustness and the tendency toward desynchronization. Extending beyond pairwise interactions, higher-order network models, such as simplicial complexes and hypergraphs, are explored. These models represent simultaneous interactions among multiple nodes and give rise to

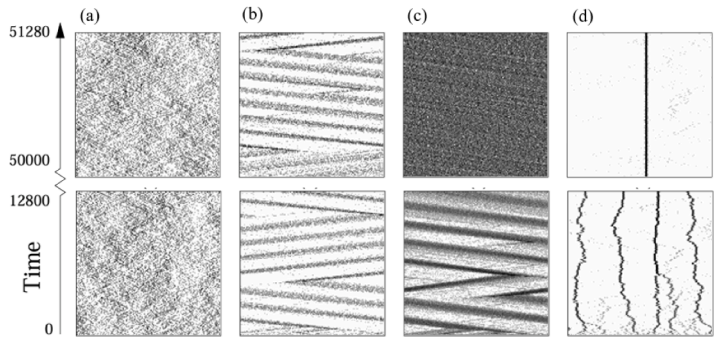

Fig. 18. Space–time plots from a one-dimensional lattice flocking model showing four distinct spatiotemporal states. A break in the vertical axis (12800–50000) indicates that only the final stages are shown in the top row. (a) Disordered state: homogeneous density, zero global velocity, no persistent spatiotemporal correlations. (b) Alternating flock: periodic reversals of collective motion, forming diagonal stripe patterns. (c) Homogeneous flock: constant non-zero global velocity and uniform density, often emerging from transient alternations. (d) Dipole state: dense localized dipoles separated by low-density regions; smaller dipoles are gradually absorbed by larger ones during coarsening. *Source:* The figure is from [182].

novel dynamical behaviors including explosive synchronization and chimera states. Finally, temporal networks are examined, focusing on how evolving interaction patterns, particularly switching frequency and timing, further influence the emergence and stability of collective dynamics.

4.1. Collective behavior on regular and complex networks

The lattice structure represents the most fundamental form of network used to study collective behavior. In these models, individuals are typically confined to move on one- or two-dimensional lattices and interact with others within their local neighborhood. This framework offers a tractable way to isolate the effects of local interaction rules on global pattern formation, especially in systems where spatial constraints dominate.

A seminal example is the one-dimensional lattice model proposed by O'Loan and Evans, which revealed a continuous nonequilibrium phase transition from a homogeneous to a condensed state [181]. Extending this framework, Raymond and Evans integrated Reynolds' three foundational rules—alignment, cohesion, and separation—into a simplified one-dimensional lattice model [182]. Their work demonstrated that the system could generate a variety of flocking regimes, including alternating flock, homogeneous flock, and dipole structures, depending on model parameters. These regimes, along with the disordered phase, are visually illustrated in Fig. 18, which highlights the pivotal role of local interactions in driving the emergence of self-organized collective patterns [182].

To model more biologically realistic collective motion, especially in cell and microbial systems, researchers have employed lattice-gas cellular automata (LGCA) models, where each agent updates its movement direction based on its local neighbors [183–185]. These models demonstrated that when key parameters, such as cell density or swarming sensitivity, exceed a critical threshold, the system undergoes a continuous transition, leading to the emergence of organized swarming behaviors [185]. However, due to their assumption of perpetual movement, early LGCA models failed to account for resting states or aggregation behaviors, which are prevalent in microbial populations. To address this limitation, Deutsch et al. proposed an extended LGCA model that captures the full behavioral spectrum of microbial systems, including random motion and eventual aggregation, while avoiding reliance on external chemical cues [186]. In this model, agents adjust their behavior based on local information, such as the density of nearby stationary agents and the directional alignment of neighboring agents. The model successfully reproduces large-scale aggregation phenomena observed in organisms like slime molds and myxobacteria. In addition, mean-field analysis reveals a self-organized instability mechanism that drives the aggregation process and provides a theoretical explanation for the spontaneous emergence of spatial clusters arising from local interactions.

Although the LGCA models have significantly contributed to understanding how local interactions give rise to collective motion, they suffer from limitations in synchronizability and information propagation efficiency. To address these limitations, Watts and Strogatz proposed the small-world network model, which bridges the gap between regular and random networks [187]. This transition is illustrated in Fig. 19, where a regular ring lattice is progressively randomized by increasing the rewiring probability, while preserving the total number of nodes and edges. They precisely characterized the structural features of small-world networks, where high clustering coefficients coexist with low average path lengths, and systematically analyzed the profound impacts of such structures on collective dynamics. They demonstrate that small-world topology can enhance system synchronizability, improve signal propagation efficiency, and increase computational capacity, thereby providing a theoretical foundation for research on synchronization and information spread in complex systems.

To advance the understanding of how small-world structures facilitate synchronization, researchers have systematically investigated the relationship between network topology and synchronizability. Barahona et al. were among the first to employ the master stability function to connect synchronizability with the Laplacian spectral properties of network topologies, demonstrating that small-world networks can achieve synchronization more readily even at the same link density [188]. Subsequently, Wang et al. extended

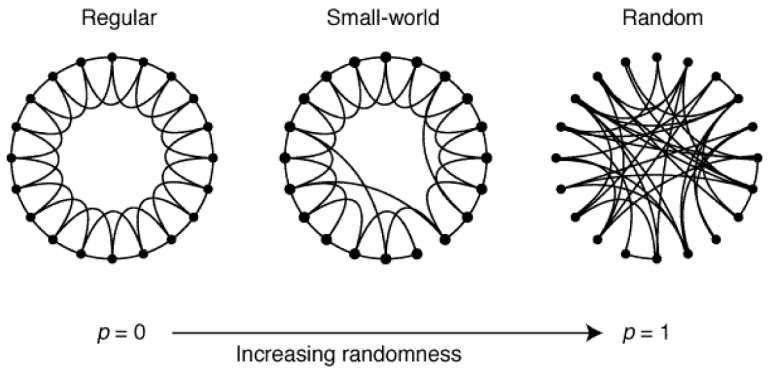

Fig. 19. Schematic illustration of the structural transition induced by random rewiring. As the rewiring probability p increases, the network evolves from a regular ring lattice ($p = 0$) to a completely random network ($p = 1$), while keeping the number of nodes and edges constant. At intermediate values of p, a small-world structure emerges, characterized by high local clustering and short average path lengths. *Source:* The figure is from [187].

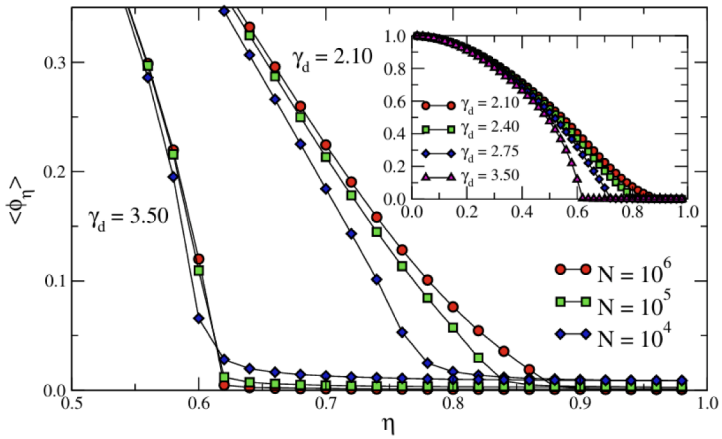

Fig. 20. Average order parameter as a function of the noise intensity η for different values of the degree exponent γ_d in scale-free networks of size $N = 10^4, 10^5, 10^6$. From this figure, it is apparent that for small γ_d the effective threshold depends strongly on N. For $\gamma_d \leq 2.50$, the order–disorder transition is suppressed and the system remains fully ordered for any $\eta < 1$ in large networks; for $\gamma_d > 2.50$, a true transition occurs, persisting even in the infinite-size limit. *Source:* The figure is from [20].

this analysis to continuous-time dynamical systems and showed that, for a given coupling strength, regular nearest-neighbor networks struggle to achieve synchronization, whereas small-world networks—formed by rewiring a small fraction of links at random—can attain global synchronization, provided the network size is sufficiently large and the rewiring probability is appropriately chosen [189]. These findings offer crucial theoretical support for designing cost-effective and highly synchronizable network structures in engineering systems.

The development of the small-world model sparked rapid growth in interest in networked dynamical systems. In this context, the scale-free network model, built on the principles of growth and preferential attachment, was introduced to capture the structural heterogeneity observed in many real-world systems [190]. Building on this foundation, Miguel et al. systematically investigated the collective dynamics of the Vicsek model on scale-free networks, focusing on how heterogeneity in the degree distribution of social networks affects order-disorder transitions and synchronization performance [20]. Large-scale simulations revealed that network heterogeneity, characterized by the power-law exponent of the degree distribution, critically determines synchronization robustness: highly heterogeneous networks can maintain synchronization under stronger noise, while less heterogeneous networks are more prone to desynchronization, as illustrated in Fig. 20. These findings enrich our understanding of the role of network structure in collective dynamics.

To further explore the role of heterogeneity, Ojer et al. proposed a weighted variant of the Vicsek model in which the alignment weight between any two individuals is proportional to the product of their node degrees, modulated by a power-law exponent α that systematically tunes the level of heterogeneity [191]. The authors identified three qualitatively distinct collective regimes and further showed that, in finite-size networks, the predicted external disturbance threshold reaches a maximum at a specific weight exponent. This suggests that the system's resilience to external perturbations can be optimized by choosing an appropriate weight structure. Building on classical alignment models, Bode et al. incorporated weighted social interactions into the agent-based framework and demonstrated that heterogeneity in network structure can either enhance or destabilize group cohesion, depending on how social

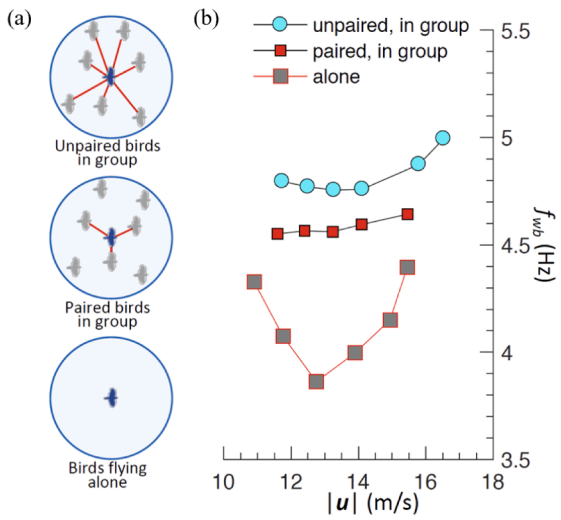

Fig. 21. Effect of pairing on the power consumption of individuals. (a) Illustrations of interaction networks of focal birds. (b) Wingbeat frequency f_{wb} as a function of flight speed $|u|$ during cruising flight mode. *Source:* The figure is from [74].

subgroups are distributed. Notably, individuals with higher connectivity tended to occupy more central spatial positions and exert disproportionate influence on group dynamics, even in the absence of predefined leadership roles [73].

Unlike models that assume individuals interact with neighbors based solely on fixed geometric or topological distances, empirical evidence suggests that social interactions are often shaped by individual-specific preferences, leading to structurally heterogeneous networks characterized by assortativity. For instance, guppies (*Poecilia reticulata*) exhibit a marked preference for familiar individuals during collective movement, forming stable pairwise associations that support reciprocal altruism [192,193]. Similarly, Croft et al. found that interactions in multiple fish species are driven by similarity in body size and shoaling tendencies, producing networks with positive degree correlations [194]. Similar preference-driven structuring has also been observed in mammalian societies. In mammalian societies such as Przewalski's horses, collective movement patterns reflect long-term social bonds, including kinship and familiarity, rather than being determined solely by instantaneous spatial proximity [195].

Most empirical and theoretical studies of collective motion have focused on conspecific groups, where individuals share similar interaction rules. Extending this framework to multispecies systems, mixed-species fish shoals provide an opportunity to examine how interspecific differences influence collective dynamics. Ward et al. compared single- and mixed-species groups of sticklebacks and roach and showed that mixed-species shoals generally exhibit reduced polarization, and in some species combinations, reduced cohesion relative to single-species groups [196]. Using transfer entropy to quantify information flow, they further demonstrated species-dependent asymmetries in information transmission. Such asymmetries likely arise because individuals of different species respond differently to the movements of conspecifics and heterospecifics, leading to uneven contributions to the predictability of collective motion. Together, these results indicate that interspecific differences in local interaction responses are reflected in group-level patterns of information flow and collective organization.

Selective interactions are not exclusive to vertebrate systems. At the microbial scale, it has been demonstrated that bacteria coordinate collective behavior through quorum sensing (QS)—a chemically mediated communication system involving the production and detection of autoinducers [197]. QS enables bacteria to regulate gene expression in response to local population density, such that gene activation only occurs when the concentration of signaling molecules exceeds a threshold. This ensures that coordinated behaviors—such as biofilm formation, virulence expression, and motility—are triggered only at the right time and in the presence of a sufficient number of suitable partners, reflecting a form of environmentally and socially contingent selective interaction. Moreover, QS mechanisms exhibit remarkable specificity: some signaling molecules function only within particular bacterial strains, while others enable cross-species communication. This molecular-level selectivity gives rise to interaction-specific communication channels, forming structurally organized information networks even in microbial communities. These findings suggest that the principles of selective interaction and structured information exchange are conserved across diverse levels of biological organization.

The structure and strength of social associations significantly influence individual efficiency and group adaptability in collective dynamics. Ling et al. observed that stable pairwise social bonds in jackdaws (*Corvus monedula*) enhance local coordination and reduce individual energy expenditure [74], as shown in Fig. 21. However, this tight coupling also constrains information flow within the group, thereby diminishing overall responsiveness. These findings reveal a fundamental trade-off between individual-level efficiency and group-level adaptability—a trade-off critically shaped by the structure and strength of social associations. In their subsequent study, they further found that birds tend to adjust their relative position to nearby neighbors by turning rather than changing speed during close-range interactions. The physical basis of this behavioral pattern lies in the fact that, compared to accelerating or decelerating, turning requires less energy consumption [198]. Similar mechanisms have also been observed in other species. For example, a study on ant colonies revealed a previously overlooked "reverse social contagion" mechanism, in which interactions between indi-

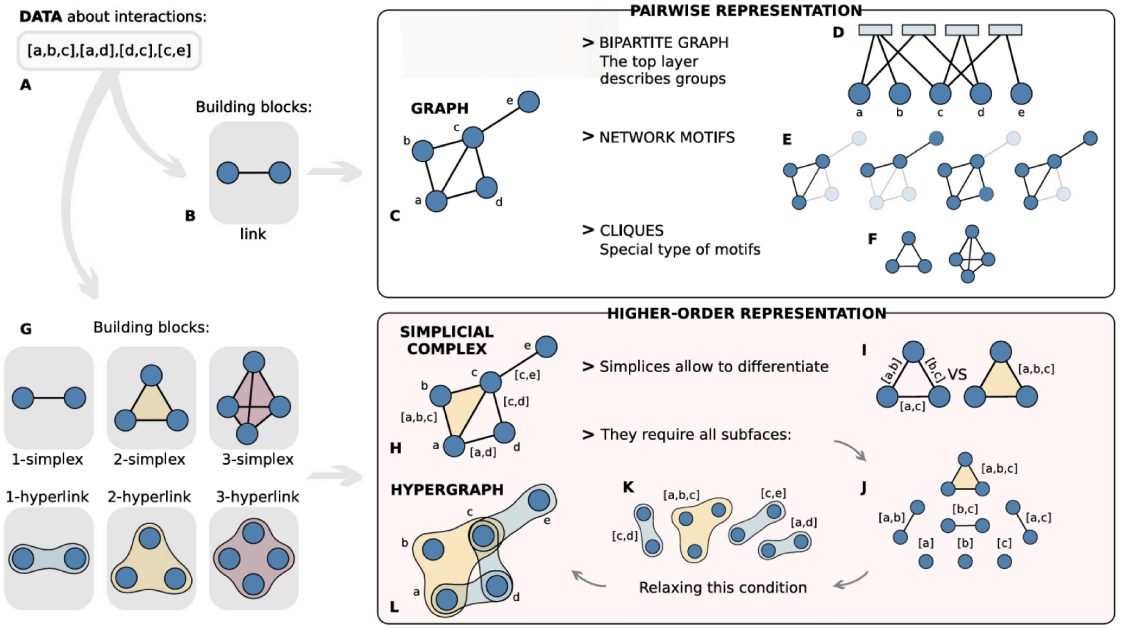

Fig. 22. Representations of higher-order interactions. (A) Example of heterogeneous interaction data. (B) Basic building block for pairwise representation: link. (C–F) Pairwise representations: (C) standard graph; (D) bipartite graph; (E) network motifs; (F) cliques. (G) Basic building blocks for higher-order representation: simplices and hyperlinks. (H–J) Simplicial complexes: (H) A set of simplices forms a simplicial complex; (I) This refers to the closure condition of simplicial complexes, which distinguishes genuine group interactions from pairwise interactions; (J) a simplicial complex requires all lower-order parts of a simplex to be present. (K–L) Hypergraph: (K) Relaxing this rule leads to hyperedges; (L) general hypergraph representation. *Source:* The figure is from [218].

viduals not only stimulate activity but also dynamically suppress the behavior of others. This allows the colony to regulate collective activity levels without centralized control, thereby reducing overall energy expenditure and enhancing group-level efficiency [199].

The structural–functional trade-offs observed in biological collectives are mirrored in artificial systems, where network topology plays a key role in shaping control costs. Yan et al. conducted a systematic study on the energy cost of controlling complex networks, revealing that structural heterogeneity can reduce the required control energy [200]. This finding laid a solid theoretical foundation for energy-efficient control of complex networked systems. Sun et al. further investigated the control of nonlinear complex networks and revealed a trade-off between energy consumption and time cost, which depends on the network structure and control parameters [201]. Building on this, Dai et al. found that across various network structures—such as regular graphs, small-world networks, and scale-free networks—increased connectivity tends to accelerate consensus in multi-agent networks but also results in higher energy consumption [202]. This reveals a clear trade-off between convergence speed and energy expenditure. These findings highlight how network topology and control parameters influence convergence speed and energy consumption in coordinated systems.

4.2. *Collective behavior with higher-order interactions*

Classic network models of collective dynamics typically assume that interactions occur exclusively between pairs of individuals, with each link connecting exactly two nodes [203,204]. However, growing empirical evidence from domains such as human behavior [205], ecology [206], and neuroscience [207] suggests that real-world interactions often involve simultaneous influences among multiple agents—a phenomenon inadequately captured by pairwise approximations [208–210]. These interactions, termed "higher-order" interactions, have been shown to not only reshape the structural organization of networks [211–213] but also fundamentally influence their collective dynamical behaviors [214–217].

To model these non-pairwise dependencies, two primary mathematical frameworks have emerged: simplicial complexes and hypergraphs [218–220]. Among these, simplicial complexes offer a mathematically structured and topologically meaningful representation, particularly suited for systems where interactions are not only multi-node but also nested in nature [218–220]. A simplicial complex is built from basic building blocks known as simplices, where a k-simplex corresponds to a simultaneous interaction among $k+1$ nodes. For example, a 2-simplex represents a triadic interaction and takes the form of a filled triangle, as shown in Fig. 22 (G). A defining property of simplicial complexes is that they require the presence of all lower-dimensional faces of any simplex. That is, if a group interaction involves nodes a, b and c, then all pairwise interactions $[a,b],[a,c],[b,c]$, as well as the individual nodes, must also be present in the complex. This hierarchical inclusion structure is shown in Fig. 22 (H), where interactions such as $[a,b,c],[a,d],[c,d],[c,e]$ are represented as 2- and 1-simplices. The simplicial complex formed by these elements contains not only the group interactions but also all their subfaces.

In contrast to the strict inclusion constraints of simplicial complexes, hypergraphs offer a more general and flexible framework for representing higher-order interactions, particularly when group interactions do not imply the existence of all possible lower-order subsets [218,220]. A hypergraph is formally defined as a pair (V, ε), where V is the set of nodes and ε is a set of hyperedges, each of which is a non-empty subset of V representing a multi-node interaction. Unlike simplicial complexes, hypergraphs do not require that all faces of a hyperedge be included, which allows them to directly encode arbitrary group interactions without enforcing nestedness. This modeling flexibility is illustrated in Fig. 22 (K–L), where the same interaction dataset $[a, b, c], [a, d], [c, d], [c, e]$ is represented as a hypergraph. In this case, the hyperedges (shown in Fig. 22 (K)) include only the specified groups, without assuming that all dyadic interactions among group members must also be present. As seen in Fig. 22 (L), this relaxed condition allows the hypergraph to represent interactions like $[a, b, c]$ without implicitly including $[a, b], [a, c]$, or $[b, c]$, which may not be observed in the data. This characteristic makes hypergraphs particularly useful in contexts where group participation is explicit but not necessarily reducible to pairwise connections—for instance, in co-authorship networks, biochemical complexes, or survey responses where multiple participants interact jointly but not necessarily in all possible subgroups [212,221–223].

Higher-order interactions have emerged as a pivotal factor in shaping the dynamics of synchronization within complex systems. Unlike pairwise interactions, which typically produce smooth and continuous transitions toward synchronization, higher-order couplings often give rise to fundamentally different dynamics. These include a variety of nonlinear phenomena—such as abrupt transitions and multistability—that deviate significantly from classical scenarios. For instance, the higher-order Kuramoto model, which incorporates both pairwise (1-simplex) and three-body (2-simplex) interactions, can exhibit a sudden transition from an incoherent to a fully synchronized state at a critical coupling strength, displaying hallmark features of explosive synchronization [224]. This suggests that higher-order structures not only alter synchronization thresholds but also fundamentally reshape the stability landscape of the system. Moreover, it has been shown that substituting a portion of pairwise links with three-body interactions, even under fixed total coupling strength, can significantly enhance synchronization performance [225]. However, higher-order interactions do not universally promote synchronization. In multilayer metapopulation networks, the introduction of three-body coupling can induce desynchronization, disrupting previously stable coherent states maintained by pairwise interactions [226]. These contrasting observations underscore the context-dependent nature of higher-order effects: their impact hinges on parameters such as coupling strength and network topology.

To gain a more systematic understanding of how the structural encoding of higher-order interactions influences synchronization behavior, Zhang et al. developed a unified higher-order Kuramoto model [227]. This framework allows for a controlled comparison between hypergraphs and simplicial complexes under structurally equivalent coupling conditions, providing new insights into the role of multi-node interactions in collective dynamics [227]. The governing dynamics are given by:

$$\dot{\theta}_i = \omega + \frac{\gamma_1}{\langle K^{(1)} \rangle} \sum_{j=1}^{n} A_{ij} \sin(\theta_j - \theta_i) + \frac{\gamma_2}{\langle K^{(2)} \rangle} \sum_{j,k=1}^{n} B_{ijk} \frac{1}{2} \sin(\theta_j + \theta_k - 2\theta_i), \tag{18}$$

where θ_i denotes the phase of node i, and ω is its natural frequency. The parameters γ_1 and γ_2 represent the coupling strengths associated with first-order and second-order interactions, respectively. The interaction structure is defined via adjacency tensors: $A_{ij} = 1$ if nodes i and j are connected via a first-order (pairwise) interaction, and zero otherwise; $B_{ijk} = 1$ if and only if nodes i, j and k participate in a second-order interaction. The generalized degrees are given by $K_i^{(1)} = \sum_{j=1}^{n} A_{ij}$, $K_i^{(2)} = \frac{1}{2} \sum_{j,k=1}^{n} B_{ijk}$, corresponding to the number of first-order and second-order interactions involving node i, respectively. The first summation in the dynamical equation captures conventional pairwise coupling, while the second term accounts for three-body interactions within higher-order structures. The second-order coupling adopts a symmetric form, $\sin(\theta_j + \theta_k - 2\theta_i)$, which reflects a phase alignment tendency induced by multi-node interactions.

A key feature of the model is its structural flexibility—it can be instantiated as either a hypergraph or a simplicial complex, enabling direct comparisons under equivalent interaction strength and connectivity. Fig. 23 reveals that, despite encoding the same set of higher-order interactions, the two representations yield markedly different synchronization dynamics: hypergraphs tend to promote faster and more uniform synchronization, whereas simplicial complexes often lead to delayed or fragmented synchronization trajectories. This highlights that the manner in which higher-order interactions are organized—not merely their presence—can fundamentally influence the collective dynamics of the system. Building upon this, Zhang et al. systematically investigated the impact of higher-order interactions on both linear stability and basin stability of collective dynamics within the hypergraph framework of the Kuramoto model [228]. They found that while higher-order interactions enhance the linear stability of synchronized and twisted states, they significantly reduce the size of their basins of attraction, revealing a trade-off between stability and accessibility in complex networks. This finding enriches the theoretical understanding of how higher-order coupling influences synchronization dynamics.

While the unified Kuramoto model effectively reveals structural effects on synchronization, recent investigations have extended the scope to broader classes of collective phenomena. For example, in the swarmalator framework, which integrates synchronization and spatial self-organization, the inclusion of three-body interactions has led to the emergence of diverse states such as asynchrony, phase waves, and full synchrony [42]. Remarkably, these higher-order couplings enable abrupt transitions from incoherent to ordered states and allow for synchronized patterns to persist even under repulsive pairwise coupling. Similarly, a minimal oscillator model incorporating higher-order terms has been shown to induce anomalous transitions to synchrony, including multistable coexistence among synchronized, desynchronized, and clustered states, as well as slow switching dynamics between them [229]. These findings highlight that the nonlinear coupling between structure and dynamics introduced by higher-order interactions leads to the emergence of diverse collective behaviors.

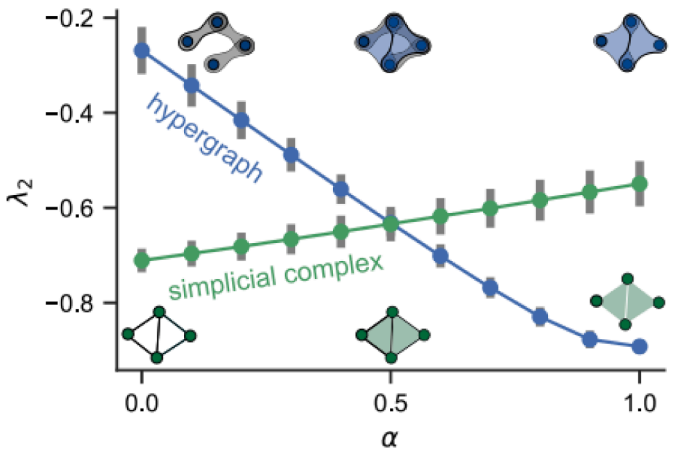

Fig. 23. The effect of higher-order interactions on synchronization differs significantly between random hypergraphs and simplicial complexes. Let $\gamma_1 = 1 - \alpha$ and $\gamma_2 = \alpha$. The maximum transverse Lyapunov exponent λ_2 is plotted against α for random hypergraphs (blue) and simplicial complexes (green). As α is increased, the coupling goes from first-order-only ($\alpha = 0$) to second-order-only ($\alpha = 1$). Each point represents the average over 50 independent hypergraphs or simplicial complexes with $n = 100$ nodes. The error bars represent standard deviations. The shaded groups of nodes indicate hyperedges (blue) and second-order simplicial complexes (green). As the fraction α of second-order (three-body) coupling increases, the maximum transverse Lyapunov exponent λ_2 decreases in hypergraphs (blue), indicating enhanced synchronization stability, whereas it increases in simplicial complexes (green), suggesting reduced stability. *Source:* The figure is from [227].

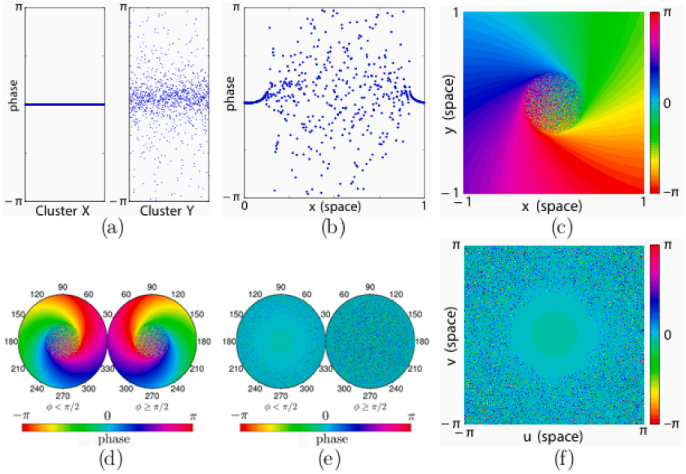

Fig. 24. Examples of chimera states. (a) Chimera state in a system of two point-like clusters. (b) Chimera state in a one-dimensional periodic space (ring). (c) The incoherent region for a spiral chimera state on a two-dimensional infinite plane. (d) 'Spiral' chimera state on a two-dimensional periodic space (sphere). (e) 'Spot' chimera state on a two-dimensional periodic space (sphere). (f) 'Spot' chimera state on a two-dimensional periodic space (flat torus). The points in the figure represent the phase state of each oscillator. *Source:* The figure is from [232].

An intriguing form of collective dynamics is the chimera state, characterized by the coexistence of synchronized and desynchronized regions within the same network. It generally arises from spontaneous symmetry breaking in structurally homogeneous systems [230–232]. Chimera states epitomize the delicate balance between local coherence and global incoherence. As shown in Fig. 24, classical chimera states appear across diverse spatial configurations, including clusters, rings, spheres, and tori [232]. With the growing interest in higher-order interactions, recent studies have explored how these couplings influence the emergence and evolution of chimera states. Notably, it has been demonstrated that such states can emerge solely through the introduction of three-body interactions—without the need for conventional phase-lag mechanisms—positioning higher-order structures as key drivers of chimera formation [233].

The effects of three-body interactions embedded in hypergraphs, as opposed to simplicial complexes, on chimera dynamics have been systematically investigated [234,235]. It has been shown that, in hypergraphs, chimera states tend to emerge in regions of weak lower-order coupling, while in simplicial complexes, they are more associated with zones of strong higher-order coupling [234]. Furthermore, the latter is more conducive to sustaining bistable coexistence between stable chimera and synchronized states. In addition, a novel class of non-stationary chimera, termed "penetrating traveling wave chimera", was discovered in coupled pendulum

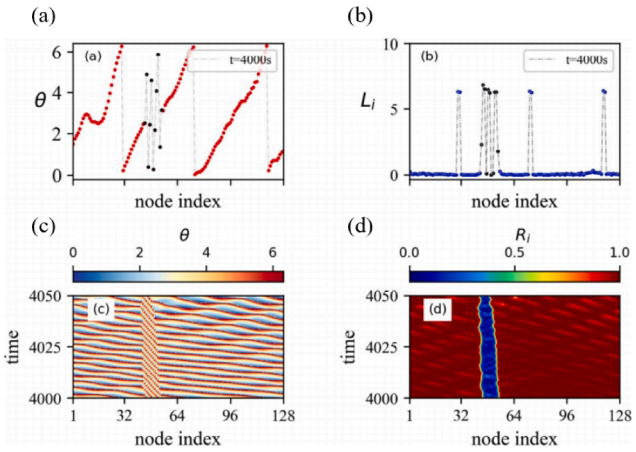

Fig. 25. A penetrable traveling chimera state observed in a nonlocally coupled pendulum network with higher-order interactions and inertia. (a) Red dots mark coherent wave regions, and black dots indicate incoherent drift. (b) The local curvature L_i highlights the distinction between coherent and incoherent domains. (c) Spatiotemporal plot of θ shows ordered wave propagation through disordered regions. (d) Spatiotemporal evolution of the local order parameter R_i reveals the dynamics of synchronization. *Source:* The figure is from [235].

systems with inertia and higher-order interactions [235]. This newly identified state is characterized by the orderly propagation of coherent domains in the form of waves, coexisting with incoherent regions that exhibit random drifting, as illustrated in Fig. 25. This further reveals that the strength of higher-order interactions plays a critical role in the emergence of multistability, while damping coefficients significantly affect the formation, persistence, and evolution of chimera states.

Higher-order interactions are not simply refinements of pairwise models but represent fundamentally different mechanisms governing collective behavior. By allowing simultaneous influences among multiple individuals, frameworks such as hypergraphs and simplicial complexes capture emergent phenomena including cluster synchronization, abrupt transitions between dynamical regimes, and flexible patterns of coordination that cannot be reproduced by conventional network representations. Incorporating higher-order descriptions into modeling efforts enriches our understanding of how biological collectives achieve resilience, adaptability, and functional complexity. They also offer deeper insights into structure–function coupling mechanisms in complex systems and establish a theoretical foundation for addressing practical challenges, such as maintaining synchronization in power grids or understanding coordinated activity in neural ensembles. Continued exploration of these approaches, combined with empirical validation, holds significant promise for uncovering the organizational principles that underlie self-organization across scales.

4.3. Emergence of collective dynamics in temporal networks

While regular, small-world, scale-free, and higher-order networks have substantially enriched our understanding of how structural features shape collective dynamics, these models commonly assume that connections between individuals remain static over time. However, in many real-world systems—such as neural circuits with synaptic plasticity, dynamic social interactions, or time-varying communication topologies—the connectivity itself evolves, often in unpredictable or intermittent ways [236,237]. These temporal fluctuations can critically alter the conditions under which collective behaviors such as synchronization or consensus emerge [238]. To address these limitations, researchers have increasingly turned to temporal networks, which explicitly account for the timing and duration of interactions. This shift in perspective enables the exploration of how not only the network structure, but also the temporal patterns of connectivity, shape the emergence and stability of collective behaviors.

Temporal variations in network topologies have been shown to induce complex collective behaviors that static networks struggle to support. In the context of synchronization dynamics, studies have indicated that even when the average coupling strength is zero, stochastic switching of the interaction networks can realize synchronization with probability one—highlighting the constructive role of random temporal structures [239–241]. Continuing along these lines, subsequent work revealed that periodic switching between network topologies can also regulate system behavior. For instance, Majhi et al. found that when the switching frequency falls within a specific range, the system may exhibit oscillation suppression or chimera states, which are dynamical regimes rarely observed in static networks [242]. These results collectively demonstrate that temporal modulation not only alters network architecture but also serves as a potent mechanism for driving state transitions in dynamical systems.

The significance of temporal structures has also been explored in the context of evolutionary cooperation. Several studies have shown that intermediate interaction rhythms are most conducive to the emergence and stabilization of cooperative strategies, whereas overly static or highly frequent structural perturbations tend to suppress cooperation [243,244], as illustrated in Fig. 26. This indicates that not only the structure of interactions, but also their temporal regularity, plays a critical role in shaping the evolution of collective behavior.

Alongside these theoretical advances, temporal network approaches are increasingly being applied to real-world collective animal behavior. Fisher et al. investigated the social spider *Stegodyphus dumicola*, examining how its social network evolves over time and how

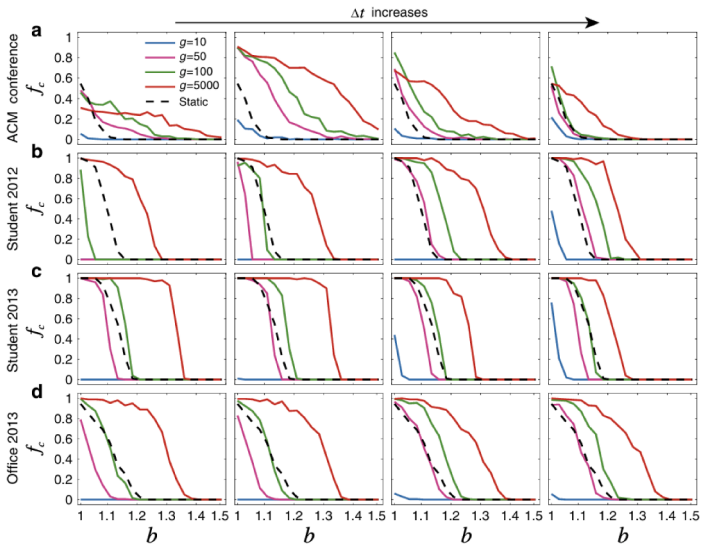

Fig. 26. Temporal networks generally facilitate the evolution of cooperation in real social systems. (a) Attendees at a scientific conference (ACM conference); (b) High school students in Marseilles, France, 2012; (c) High school students in Marseilles, France, 2013; (d) Office workers in France, 2013. The figure illustrates how the cooperation level f_c varies with the temptation parameter b in both temporal and static networks across these four real-world datasets. Cooperation is best sustained at intermediate rhythms. Here, Δt represents the aggregation time window, while b denotes the strength of the temptation to defect, directly influencing the balance between cooperation and defection in the system. The game evolves for g rounds before the network structure is updated to the next snapshot. The parameter g sets the relative timescale of strategy updates versus network changes. *Source:* The figure is from [243].

this affects collective predation behavior [245]. They found that although the network structure fluctuated on the scale of 2–3 days, such structural dynamics did not significantly impact the speed or consistency of group attacks. This observation suggests that temporal variations in network structure do not always translate into behavioral changes, highlighting the importance of distinguishing between structural sensitivity and functional responsiveness in natural systems.

While temporal networks have significantly advanced our understanding of dynamic interactions, their modeling framework remains largely confined to pairwise connections, limiting their capacity to capture the complexity of simultaneous multi-body interactions. To overcome this limitation, researchers have integrated higher-order and temporal characteristics of interactions among individuals by proposing the temporal hypergraph model, which more realistically captures collective behaviors. Iacopini et al. analyzed group dynamics using data collected from preschool children and university first year students, focusing on group formation, transition, and dissolution processes [246]. Their study confirmed the presence of higher-order and temporal patterns in human interactions. They further proposed a model incorporating mechanisms of short-term and long-term social memory, which provides a powerful framework for studying the impact of higher-order temporal interactions on collective dynamics. Subsequently, Xu et al. incorporated evolutionary game theory into the framework of higher-order interactions and developed a temporal higher-order hypergraph model in a multiplayer snowdrift game environment [247]. Their results show that both higher-order structures and temporal variability independently promote cooperation, and that their combination produces significantly enhanced cooperative outcomes.

Furthermore, the influence of temporal and higher-order interactions on neurodynamics has also been studied. Anwar et al. constructed a network of Hindmarsh–Rose neurons interconnected through dynamically evolving triplet interactions and demonstrated that, even in the complete absence of pairwise links, rapidly switching higher-order connections alone can induce full synchronization [248], see Fig. 27. The results on synchronization in time-varying simplicial complexes of coupled Sherman neurons [249] further demonstrate that the time-averaged simplicial complex serves as a reliable indicator of synchronization, provided that the switching among simplicial topologies is sufficiently fast [250]. These findings not only reveal that the coexistence of temporal and higher-order interactions enhances synchronization more effectively than either static higher-order structures or temporal pairwise systems alone, but also highlight the critical role of structural switching speed in achieving coordinated states, offering new insights into the dynamics of complex brain systems [251].

By moving beyond static and pairwise frameworks, temporal approaches provide a powerful lens through which to explore complex coordination phenomena in animal groups, human societies, and neural systems. However, how complex biological systems spontaneously regulate the emergence of collective behaviors through such mechanisms remains poorly understood. Furthermore, extending these insights to cellular and microbial systems—where interactions are inherently dynamic and often involve multiple agents—holds great potential for revealing the organizing principles of collective behavior at microscopic scales and represents a promising direction for future research.

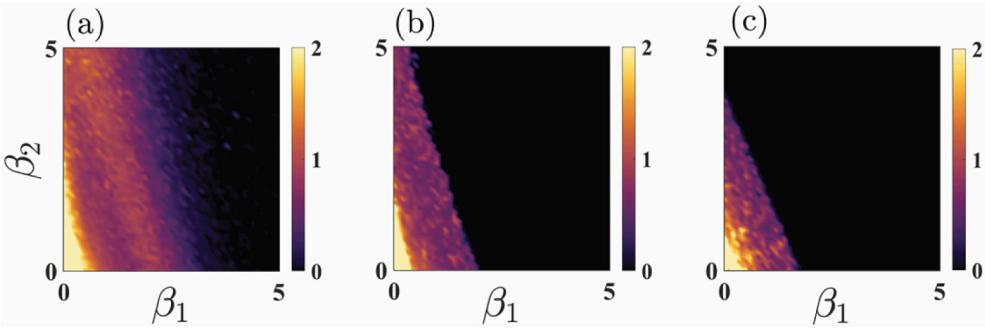

Fig. 27. Effect of 1-simplex (β_1) and 2-simplex (β_2) interaction strengths on neuronal synchronization under different topology switching probabilities. Color maps show average synchronization error for β_1 and β_2 interactions at switching probabilities $p^{(r)} = 10^{-6}, 10^{-3}, 10^{-1}$ from (a) to (c). Dark regions indicate high synchrony. (a) Synchronization requires 1-simplex interactions. (b) Higher β_2 lowers the β_1 threshold for synchronization. (c) Three-body interactions alone ($\beta_1 = 0$) can achieve complete synchronization. *Source:* The figure is from [248].

5. Mechanisms of information transmission

Information transmission forms the backbone of collective behavior, as it enables individuals to adjust their internal states based on cues from neighbors or the group, thereby allowing the collective to maintain coherence and adapt to environmental changes [21,252,253]. In collective systems, however, information is not an abstract quantity: it is embodied in concrete variables such as heading direction, velocity, phase, or chemical signals, and propagates through local interaction networks shaped by spatial, topological, or sensory constraints. Efficient information transfer therefore underpins not only coordinated motion, but also the stability, robustness, and adaptability of collective dynamics across biological scales.

In real-world systems, information transmission is inevitably constrained by multiple factors, including external disturbances, intrinsic noise, limited communication capabilities, and adversarial disruptions [21,31,32,55,254–257]. These constraints can degrade information accuracy, create temporal misalignment, and disrupt interaction structure, collectively undermining coordination and, in extreme cases, precipitating the loss of coherent collective motion. A comprehensive understanding of how such constraints modulate information transmission is therefore key to explaining the stability and adaptability of collective motion.

In the following, we focus not on how information is generated or encoded, but on how information transmission is modulated by noise, time delays, and intentional attacks. We first examine the role of noise in collective systems, drawing on classical frameworks such as the Vicsek and Cucker–Smale models to illustrate how stochasticity—shaped by network structure—can both disrupt and facilitate coordination, induce phase transitions, and generate complex dynamical patterns including vortex formation and bistable switching. Empirical evidence from locust swarms, bacterial colonies, and robotic collectives is reviewed to highlight the constructive and destructive roles of noise across diverse networked systems. Next, we explore the modulatory effects of time delay on networked collective dynamics. Beginning with the delayed Vicsek model, we explore its effects on information flow dynamics and system evolution. It then turn to the delayed Cucker–Smale model to analyze how the interplay between delay and network topology influences the emergence of flocking. Biological networks such as biofilms and neural circuits are discussed to illustrate delay-driven pattern formation and multistability. Finally, we discuss intentional attacks as a form of adversarial interference with information transmission, examining their mechanisms, consequences, and mitigation strategies, and outlining coordinated approaches to enhance the resilience of collective behavior.

5.1. Noise

Noise is ubiquitous in the collective motion of biological systems, ranging from animal groups and microbial colonies to cellular populations. By introducing stochastic perturbations at the level of individual behavior, noise fundamentally reshapes how information—such as directional cues, velocity alignment, or signaling states—is transmitted through local interaction networks. As a result, noise plays a central role in determining whether collective systems maintain coherence, undergo transitions between dynamical states, or adapt to fluctuating environments [21,32,54,55,93,258]. Importantly, noise should not be viewed merely as a disruptive factor: depending on its intensity, origin, and interaction structure, it can either degrade information accuracy or enhance collective coherence by promoting sensitivity and adaptability.

In collective dynamics, noise is typically classified into two main types: extrinsic noise and intrinsic noise [21,32,55,258]. Extrinsic noise arises from fluctuations in the external environment, such as turbulent fluid flows affecting plankton, or variations in light and temperature altering the migratory behavior of cells. These environmental perturbations can impair sensory accuracy or disrupt signal perception, thereby influencing the precision of local interactions and the resulting global patterns. In contrast, intrinsic noise stems from stochasticity inherent to individual agents, including neuronal firing variability, molecular-level randomness, or fluctuations in internal decision-making processes. Although intrinsic noise originates locally, it can accumulate through interactions among individuals and ultimately modulate group-level behavior.

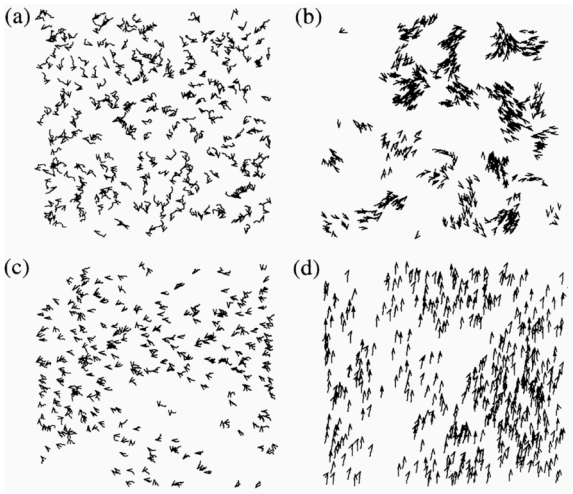

Fig. 28. Particle velocities in the Vicsek model (1) as a function of density and noise. (a) Initial disordered state; (b) Low density and low noise: formation of local clusters; (c) High density and high noise: disordered motion; (d) High density and low noise: emergence of global order. *Source:* The figure is from [54].

From a modeling perspective, noise can further be classified as either additive or multiplicative [147–150,259,260]. Additive noise represents random fluctuations that are independent of the system's state and is commonly used to model external disturbances. Multiplicative noise is dependent on the current state of the system, and its intensity often varies as a function of variables such as velocity or concentration. This distinction is crucial for understanding how noise shapes information transmission in collective systems: while additive noise tends to uniformly blur signals, multiplicative noise can selectively amplify or suppress fluctuations depending on the local collective state, thereby leading to qualitatively different macroscopic behaviors. Importantly, this state-dependent modulation allows noise to regulate not only collective order, but also the reliability, reach, and adaptability of information flow across the interaction network.

A seminal contribution to understanding the role of noise in collective dynamics is the aforementioned Vicsek model [54], which explicitly incorporates angular noise to represent randomness in the motion direction of individual particles. This model has become a cornerstone for studying phase transitions between disordered and ordered states in systems of self-propelled particles (SPPs). Under conditions of low particle density and high noise intensity, the system typically exhibits a disordered state in which individuals form small clusters with randomly oriented movements (Fig. 28(a-c)). In contrast, increasing the particle density or reducing the noise intensity drives the system toward a more ordered state, where particles progressively align their velocities and move collectively in a spontaneously selected direction (Fig. 28(d)).

Beyond regulating the emergence of order, noise plays a crucial role in enabling transitions between collective states. This mechanism is clearly illustrated by studies of locust swarms inspired by the Vicsek model [55]. In this framework, N particles move along a line, with each particle adjusting its velocity and direction based on local interactions. The state of each particle is described by its position $x_i(t)$ and velocity $v_i(t)$, with updates governed by:

$$\begin{cases} x_i(t+1) = x_i(t) + v_0 v_i(t) \\ v_i(t+1) = \alpha v_i(t) + (1-\alpha) G(\langle v(t) \rangle_i) + \xi_i. \end{cases} \tag{19}$$

Here, v_0 is the fixed speed, and α determines the relative weight that the particle assigns to its own velocity and to that of its neighbors in deciding its velocity. For locusts, α reflects their tendency to maintain directional persistence in the absence of conspecifics. The term $\langle v(t) \rangle_i$ denotes the local average velocity of neighbors within the interaction range, while ξ_i is a noise term representing stochastic fluctuations due to environmental perturbations. The function $G(u)$ describes how an individual adjusts its velocity to match local group dynamics.

It has been shown by Buhl et al. that at low densities, noise disrupts directional alignment, leading to random and disordered movement patterns. As density increases, local interactions become more dominant. This allows the group to overcome the effects of noise and form a stable, coordinated marching structure, as illustrated in Fig. 29. Notably, in intermediate-density regimes, noise can induce spontaneous switching of the collective direction, revealing a nontrivial role of stochasticity in reshaping the collective behavior.

To further investigate the role of noise in directional switching, Yates et al. introduced a revised model that assumes locusts may respond to low group alignment by increasing the noisiness of their movement [32]. The key finding is that the mean switching time between collective directions increases exponentially with individual density, dramatically reducing the overall turning rate, as illustrated in Fig. 30. Surprisingly, under low alignment conditions, although the level of noise in individual movement increases, this does not disrupt the global coordination of the group; rather, it facilitates the transition to a highly aligned ordered state. This

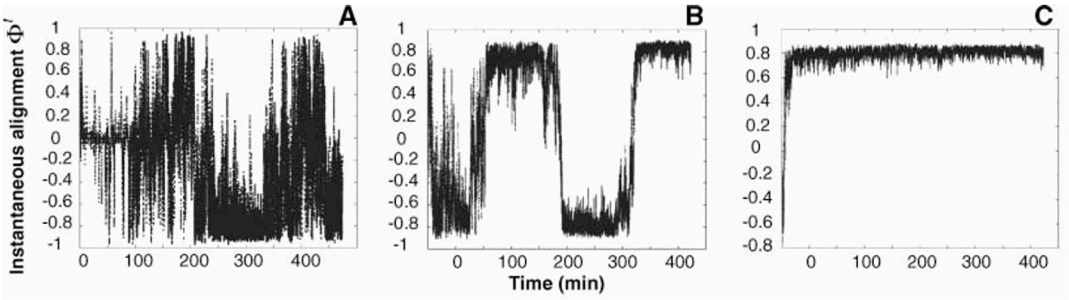

Fig. 29. Change in instantaneous alignment Φ^I over time for three different densities of experimentally observed locust swarms: (A) Low density $N = 7$; (B) Intermediate density $N = 20$; (C) High density $N = 60$. At low densities, alignment occurs sporadically after disordered motion; at intermediate densities, rotational motion with frequent direction changes is observed; at high densities, locusts adopt a consistent rotational direction. *Source:* The figure is from [55].

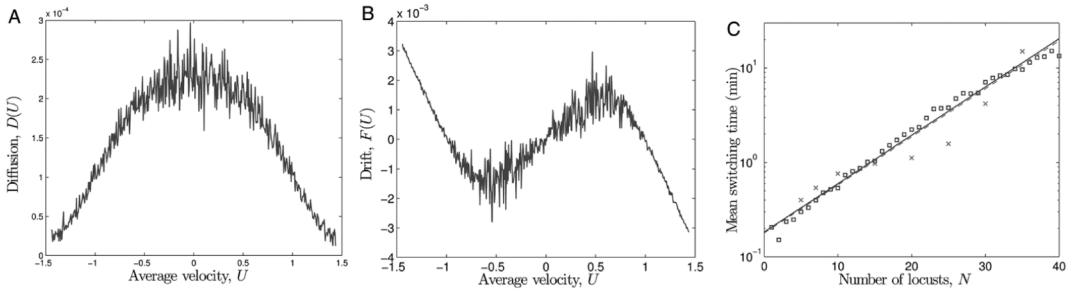

Fig. 30. Analysis of the revised SPP model for locust swarm behavior. (A) The diffusion coefficient peaks near zero velocity. (B) The drift function shows a bistable landscape. (C) As individual density increases, the mean switching time grows exponentially, leading to a significant decrease in the group's overall turning rate. *Source:* The figure is from [32].

supports the view that noise plays a constructive role in self-organized collective motion and offers important theoretical insights into the dynamical mechanisms underlying biological group behavior.

Beyond directional motion, noise-induced switching between distinct collective states has also been observed in a broader class of biological and artificial systems. For example, Biancalani et al. simulated foraging dynamics in ant colonies and found that noise promotes bistable switching between two competing food sources, further quantifying the average switching times between these states [34]. Similarly, Kolpas et al. reported that stochastic fluctuations can drive repeated transitions between two stable macroscopic states: one in which the group remains stationary while individuals move relative to each other, and another in which the entire group translates in a specific direction [261].

While noise-induced switching often occurs between competing collective states, increasing stochasticity can also destabilize entire classes of collective motion and drive transitions to different modes of motion. In doing so, noise enriches the behavioral repertoire of collective systems. For example, Erdmann et al. found that noise can induce a transition from translational to rotational motion in groups [262]. As shown in Fig. 31, increasing noise intensity destabilizes translational motion, ultimately causing a transition to a rotational state. Similarly, Chen et al. observed that noise can induce vortex reversal [33], where the rotational direction of a particle swarm suddenly changes as illustrated in Fig. 32(b). Moreover, noise can induce complex motion patterns—such as turning, vortex formation, and group merging—by altering the local dynamics of the system [263]. More recently, Huang et al. showed that spatially structured noise can drive the collective behavior of chiral active particles [264]. The particles spontaneously aggregate in low-noise regions, forming self-organized patterns such as vortex and orbital polarization.

At smaller biological scales, noise also plays a constructive role in shaping collective behavior. Experiments on dense bacterial suspensions have shown that, despite stochastic and non-periodic individual motion, bacteria can spontaneously form stable elliptical trajectories, exhibiting large-scale collective order [11], illustrated in Fig. 7(c) and (d). In this process, noise does not merely act as a perturbation; instead, it serves as a crucial driving force that sustains and shapes collective behavior. Moderate noise perturbs individual trajectories and promotes bacterial collective oscillations in dense bacterial suspensions by inducing chiral symmetry breaking through local interactions. Similarly, in cellular regulatory networks such as Notch–Delta signaling pathway, noise facilitates the correction of disordered patterns by allowing cells to switch into their appropriate states, thereby enhancing the stability of tissue-level structures [265]. However, when noise intensity exceeds a critical threshold, the system becomes unstable, resulting in frequent transitions between ordered and disordered states.

Inspired by biological collectives, engineered systems also exploit noise to achieve robust coordination. Li et al. introduced the concept of "particle robotics" based on statistical mechanics principles [266]. This system consists of numerous simple, loosely coupled "particles", each lacking an independent identity and the ability to move autonomously. Instead, the particles move via uniform

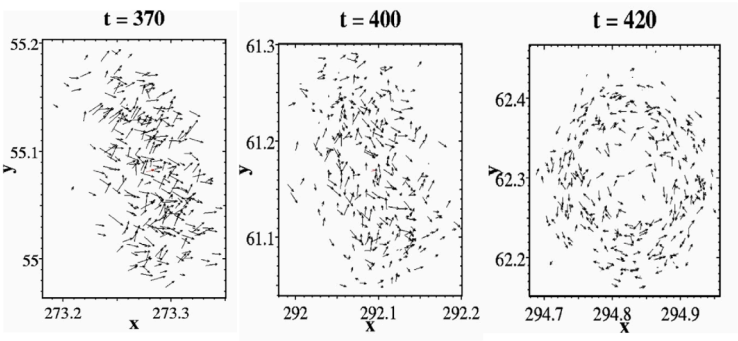

Fig. 31. Three sequential snapshots from numerical simulations of a 300-particle swarm, showing the transition from translational to rotational motion driven by increasing noise. Snapshots correspond to $t = 370$, $t = 400$, and $t = 420$. *Source:* The figure is from [262].

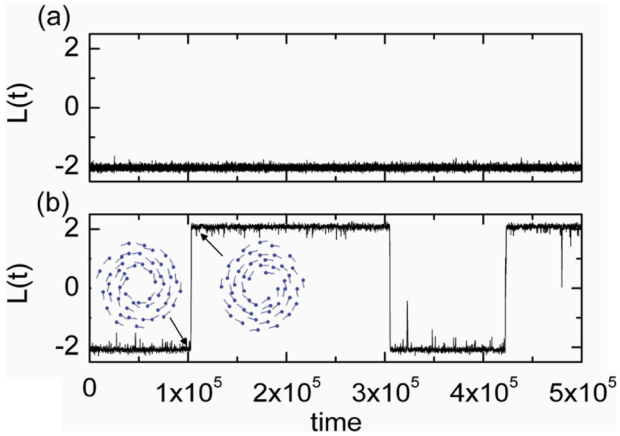

Fig. 32. Numerical simulation of a two-dimensional self-propelled particle model showing the evolution of average angular momentum $L(t)$ over time. The system contains 40 particles, with noise intensities $D = 0.32$ (a) and $D = 0.37$ (b). $L > 0$ indicates counterclockwise rotation, and $L < 0$ indicates clockwise rotation. Panel (b) shows two stable vortex states: clockwise and counterclockwise. *Source:* The figure is from [33].

volumetric oscillations regulated by a global signal, a mechanism clearly depicted in Fig. 33(e), where each particle periodically expands and contracts to coordinate collective dynamics. Although the motion of individual particles is inherently random, the coordinated collective behavior allows the entire system to achieve stable locomotion, object transport, and even phototaxis—highlighting how complexity emerges from simplicity through collective dynamics.

In addition to spatial models and biological case studies, network-based consensus models provide an abstract yet powerful approach to understanding collective behavior in the presence of noise. These models focus not on the physical positions of individuals but on how their internal states, such as opinion or direction, evolve through interactions with neighboring agents in a network. In this context, collective behavior emerges from the network structure and information flow rather than spatial proximity, and becomes increasingly complex under the influence of noise. A landmark contribution in this direction was made by Olfati-Saber et al., who developed a rigorous graph-theoretic framework for analyzing consensus in multi-agent networks [151]. By addressing solvability conditions and proposing effective control strategies, they analytically demonstrated that multi-agent systems can achieve consensus provided the network topology is strongly connected.

In realistic multi-agent networks, communication among agents is inevitably affected by noise, making it essential to examine its impact on consensus dynamics [267–273]. Following the foundational work of Olfati-Saber et al., a number of studies have demonstrated that noise significantly affects the convergence rate of consensus. It has been shown that noise can facilitate the emergence of consensus under certain conditions [267,270,273]. The effects of noise on consensus have been studied across various network topologies, revealing that both the network structure and noise intensity critically influence the coordinated behavior of multi-agent systems [274–276].

Related insights have also been obtained from flocking models with distance-dependent communication, most notably the Cucker–Smale (C–S) framework [50]. In the classical C–S model, each agent aligns its velocity with others through an influence function that decays with inter-agent distance, yielding an effectively weighted interaction network whose weights evolve in time as agents move. Extensive analytical and numerical studies have shown that stochastic perturbations can significantly affect the emergence and stability of flocking, influencing alignment dynamics and the persistence of coherent collective motion [147,148,150,259,260]. From a network-level perspective, the influence of noise is inherently non-monotonic: weak noise may have little effect, intermediate noise

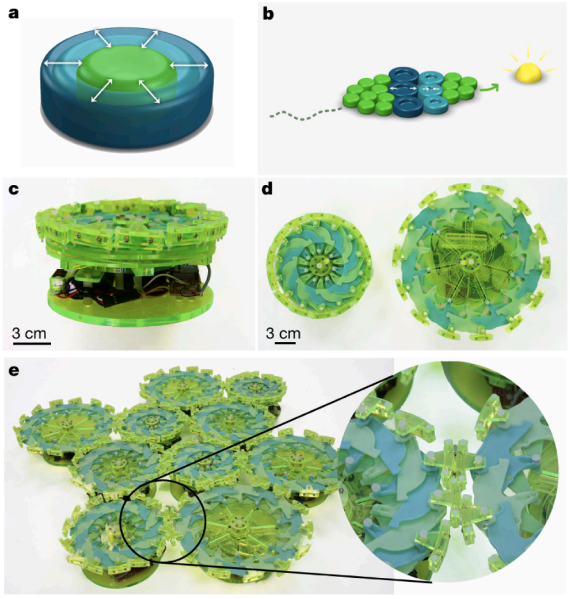

Fig. 33. A particle robot is composed of many loosely coupled individual "particles". (a) Each individual particle is capable of radial expansion and contraction, enabling dynamic deformation; (b) Multiple particles form a collective structure through loose coupling and exhibit phototactic motion under light guidance; (c) An oblique view of a single particle is presented; (d) The particle is shown in both contracted and expanded states for comparison; (e) The particles are loosely coupled using dangling magnets, allowing for flexible interactions. The particles achieve movement through uniform volumetric oscillations, which are modulated by a global signal. *Source:* The figure is from [266].

levels can enhance coherence and coordination, and strong noise disrupts information integration and prevents consensus [28,150,277,278]. These studies challenge the conventional view that noise is universally detrimental to collective behavior and highlight the critical interplay between noise intensity and network structure in shaping collective dynamics.

Although the above studies primarily report macroscopic noise-induced phenomena, these effects can be understood through a small number of underlying information-level mechanisms [147,150,259]. First, noise modulates the fidelity of locally transmitted information by introducing uncertainty in individual perception and response, thereby limiting the accuracy with which directional or state information is propagated through the collective. Second, moderate noise enables information renewal by allowing the system to escape from locally stable but informationally outdated collective states, facilitating spontaneous switching and adaptive reorganization. Third, noise effectively reshapes the range and efficiency of information propagation by altering interaction strengths, alignment responses, and network connectivity patterns. Together, these mechanisms explain the seemingly paradoxical role of noise in collective systems, whereby stochastic fluctuations can both disrupt coordination and enhance information transmission, adaptability, and robustness across diverse biological and artificial collectives [32,34,55].

5.2. Time delay

In collective motion, interactions between individuals are rarely instantaneous. Instead, they are often influenced by time delays arising from finite information transmission speeds and the internal processes of perception, computation, and execution [279–283]. These delays can be categorized into transmission delay and response delay [31,150,151,284,285]. Transmission delay refers to the time required for an individual to receive information from neighboring individuals, while response delay denotes the time needed for an individual to process the received information and adjust its state accordingly.

Time delays therefore pose a fundamental challenge in modeling collective behavior. The standard Vicsek model simplifies reality by assuming that individuals respond instantaneously to the real-time states of their neighbors, thereby neglecting the intrinsic lags in perception, information processing, and motor execution. To overcome this limitation, time-delayed Vicsek models were proposed [31,133,286–288], enabling individuals to adjust their direction based on delayed rather than instantaneous neighbor information.

To address the limitation imposed by finite information transmission speed, Sun et al. developed a delayed Vicsek-type model in which individuals adjust their direction based on the velocities of their neighbors at time $t-\tau$ [31]. The model is formulated as follows:

$$\begin{cases} \mathrm{d}x_i(t) = v_i(t)\mathrm{d}t, \\ \mathrm{d}v_i(t) = [\mathrm{sign}(U_{i,R}(t-\tau)) - v_i(t-\tau)]\mathrm{d}t + \eta \mathrm{d}W_i. \end{cases} \tag{20}$$

Here, $x_i(t)$ and $v_i(t)$ denote the position and velocity of individual i at time t, respectively. The interaction is confined within a finite perception radius R, such that an individual only interacts with neighbors located within this range. The neighbor set is defined as

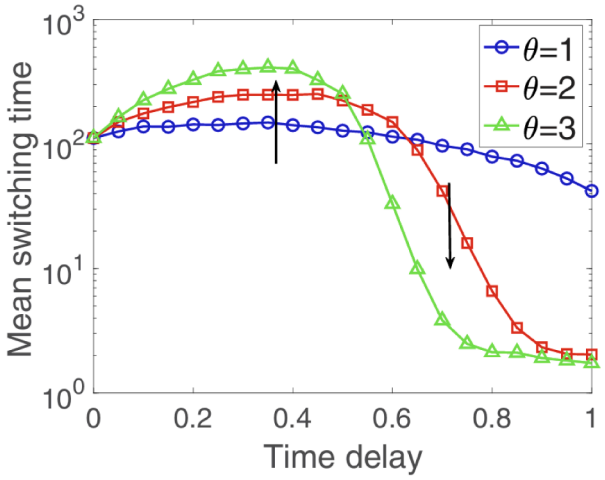

Fig. 34. The mean switching time as a function of the response delay τ for the system (20), with the transmission delay $\omega = \theta\tau$ for $\theta = 1, 2, 3$. For smaller response delays, an increase in propagation delay typically leads to a longer average switching time. However, for larger response delays, longer transmission delays may result in more frequent switching. *Source:* The figure is from [31].

$J_{i,R}(t) = \{j \mid |x_i - x_j| \le R\}$, and the average velocity of this set is given by:

$$U_{i,R}(t) = \frac{1}{|J_{i,R}(t)|} \sum_{j \in J_{i,R}(t)} v_j(t).$$

The function $\mathrm{sign}(\cdot)$ ensures alignment of an individual's direction with the average heading of its neighbors. The noise term $\eta \mathrm{d}W_i$ models random fluctuations due to environmental disturbances, sensory limitations, or internal noise, with η representing the noise intensity and $\mathrm{d}W_i$ denoting a standard Wiener process. When $\tau = 0$, the model reduces to the original Vicsek model, in which individuals align with their neighbors based on instantaneous information. However, when $\tau > 0$, individuals are influenced by the past states of their neighbors, meaning their directional adjustments are based on delayed rather than instantaneous information. In [31], the transmission delay ω is introduced to describe finite propagation speed and is parameterized as $\omega = \theta\tau$.

The effect of transmission delay on the average switching time depends critically on the magnitude of the response delay: for small response delays, lengthening the transmission delay tends to slow down switching, whereas for large response delays, further increases in transmission delay can actually accelerate the switching frequency [31]. This result is clearly illustrated in Fig. 34. Related extensions incorporating nonlinear coupling further reveal that response and transmission delays affect switching through distinct mechanisms, and that stronger nonlinear interactions induce non-monotonic changes in the average switching time [289].

In addition to its effects on switching statistics, time delay also alters the mode of information propagation. Geiß et al. demonstrated that information transmission exhibits delay-dependent regimes [30]: under short delays, information spreads diffusively, whereas longer delays induce a transition to linear propagation with significantly accelerated information flow. Moreover, adaptive adjustment of time delays has been shown to enhance collective responsiveness, improving response speed by approximately 1.6 times and reducing convergence time by nearly 38% within the reported parameter regimes [285].

While time delay plays a role in shaping information transmission and responsiveness, it has also emerged as a critical modulatory factor in governing the dynamical states and stability of collective behavior. Forgoston et al. demonstrated that time delay can induce transitions in collective motion, such as shifts from translational to rotational states and the onset of global oscillatory behavior [133]. Sun et al. found that moderate delays, under specific conditions, can enhance the stability of collective motion by supporting the emergence and maintenance of coherent group structures [286]. In contrast, Piwowarczyk et al. and Holubec et al. observed that while short delays tend to strengthen alignment and cohesion, longer delays often disrupt coordination and may ultimately lead to a breakdown of collective order [287,288]. Similarly, Pakpour et al. showed that reaction delays can trigger order–disorder transitions in active matter systems [290]. The finding that these delays destabilize collective motion highlights the non-equilibrium nature of such systems.

Recent studies have further demonstrated that delay can also drive structural state changes and spatial pattern formation in active particle systems. As shown in Fig. 35, increasing the delay can cause particle systems to spontaneously organize into shell-like structures with distinct inner and outer layers, which may exhibit counter-rotating dynamics [291]. At short delays, particles typically form densely packed hexagonal crystals; however, as the delay increases, the system undergoes a series of dynamic transitions, including shear-induced changes in the crystal structure and the emergence of satellite-like rotational formations around a central core [292]. With further increases in delay, the system evolves into a dynamic cluster structure that exhibits periodic changes resembling a "breathing" effect and displays overall dynamics characteristic of glass-like states [293].

From the perspective of network science, time delay modulates collective switching in a manner that depends strongly on the underlying interaction topology. In swarming systems defined on fixed network topologies, Xiao et al. [44] systematically investigated

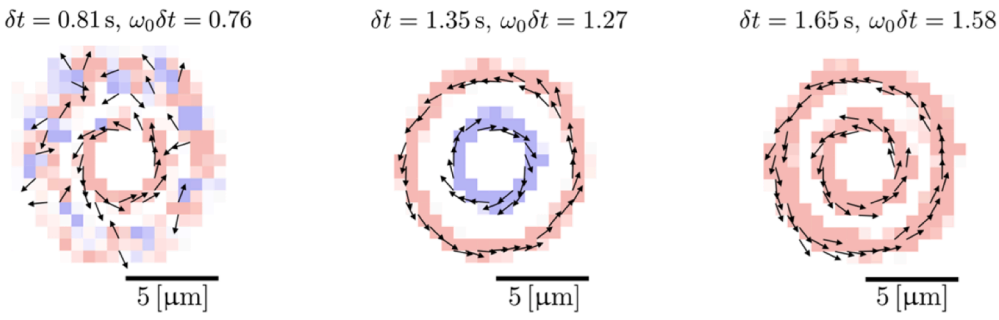

Fig. 35. The average velocity field of active particles at different time delays. The arrows indicate the average direction of motion, with the color gradient representing the velocity magnitude. The scale bar corresponds to 5 μm. δt represents the time delay in the feedback response of the microswimmer to the target position, while $\omega_0\delta t$ represents the influence of the delay on the microswimmer's rotational behavior. Specifically, $\omega_0 = v_0/R$ is the microswimmer's natural angular velocity, v_0 is the swimming speed of the microswimmer, and R is the distance between the microswimmer and the target particle. (a) At $\delta t = 0.81$s, the spontaneous rotation of the inner shell is continuously disrupted by the non-rotating outer shell. (b) At $\delta t = 1.35$s, the inner and outer shells are counter-rotating. (c) At $\delta t = 1.65$s, both shells are co-rotating. *Source:* The figure is from [291].

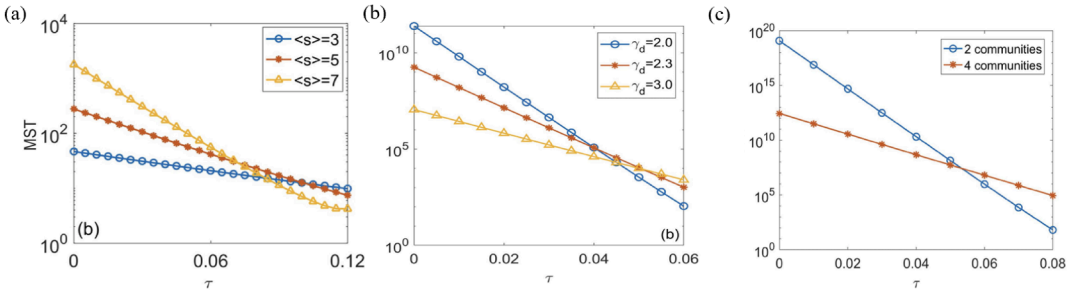

Fig. 36. Mean switching time (MST) as a function of the time delay τ for directional switching in swarming networked systems with different topologies: (a) Erdős–Rényi networks with average degrees $\langle s\rangle = 3, 5, 7$; (b) Scale-free networks with degree exponents $\gamma_d = 2.0, 2.3, 3.0$; (c) Modular networks with 2 and 4 communities. *Source:* The figure is from [44].

the effect of time delay on directional switching, considering both homogeneous Erdős–Rényi and heterogeneous scale-free network structures. In homogeneous Erdős–Rényi networks, a higher mean degree suppresses direction switching under short delays but promotes it when delays are long. In scale-free networks, greater degree heterogeneity accelerates switching for small delays but inhibits it under large delays. In networks with strong community structure, increased clustering enhances switching at short delays but impairs it under longer delays, see Fig. 36. These results indicate that although the dependence of switching time on the delay is monotonic for fixed network parameters, network topology determines whether increasing delay effectively promotes or suppresses collective switching across different delay regimes.

Related delay-topology dependencies have also been reported in other networked collective systems. Wang et al. [294] showed that network topology, coupling strength, and information transmission delay jointly influence synchronization in neuronal networks, with scale-free networks exhibiting heightened sensitivity to delay due to their heterogeneous connectivity. In addition, Yu et al. demonstrated that time delay can induce stochastic resonance phenomena in small-world neuronal networks, further highlighting how delayed interactions can qualitatively alter collective responses in networked systems. [295].

Beyond fixed network structures, delayed interactions can also be studied in systems with dynamically evolving interaction weights, where effective connectivity depends on agent states rather than prescribed links. This class of systems is exemplified by the Cucker–Smale framework [150,296–299], in which coupling strengths decay with inter-agent distance. In such models, time delays do not preclude the emergence of flocking but introduce memory effects that modify agents' trajectories, long-term velocities, and sensitivity to past states [296]. When stochastic noise is present, moderate delays can even facilitate flocking under low-noise conditions [150]. In contrast, large, heterogeneous, or time-varying delays tend to slow convergence, induce transient disorder, or destabilize alignment, with their effects depending on both delay variability and interaction strength [297,298]. Overall, these studies indicate that in dynamically weighted interaction networks, the impact of time delay arises from a competition between alignment strength, noise intensity, and the temporal mismatch introduced by delayed feedback, such that coherent flocking remains possible provided delays are sufficiently bounded and interactions remain robust.

In addition to connectivity patterns and interaction weights, structural hierarchy represents a further level of organization that shapes delay effects in collective systems. In an extended C–S model, a structured leadership hierarchy is introduced, wherein higher-level agents exert influence over lower-level ones [299,300]. It has been shown that, in such hierarchically organized systems, moderate time delays do not disrupt group coherence, and velocity alignment can still be achieved efficiently. However, when

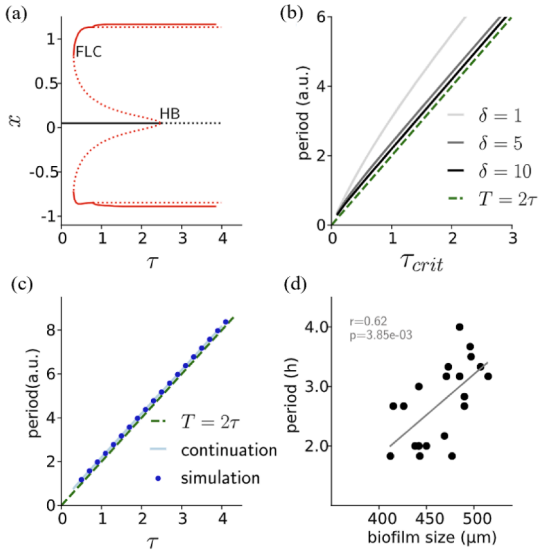

Fig. 37. Impact of time delay on subcritical Hopf bifurcation dynamics in the biofilm growth model. (a) The black solid line denotes the stable equilibrium state prior to the onset of oscillations. The black dashed line (HB, Hopf bifurcation) marks the point where oscillations emerge. The red curves (FLC, Fold of Limit Cycles) indicate the boundary of limit cycle existence, with the solid red line representing stable limit cycles and the dashed red line representing unstable ones. (b) Oscillation period versus critical delay τ_{crit} for different stress degradation rates δ (δ = 1, 5, 10). Here, T denotes the oscillation period, and the green dashed line ($T = 2\tau$) shows the analytical prediction. (c) Numerical relationship between the oscillation period and the time delay for the same parameter values as in (a). (d) Experimental measurements of the oscillation onset period as a function of biofilm radius, showing that larger biofilms oscillate with longer periods (correlation coefficient $r = 0.62$). *Source:* The figure is from [301].

delays become excessive, the system may exhibit instability or even a breakdown of coordinated motion. This balance between structural leadership and dynamic responsiveness offers theoretical insights into how flocking behavior emerges and persists in general networked systems with time-delayed interactions.

While much of the literature on time-delayed collective behavior has focused on macroscopic systems [279–283], such as animal groups or robotic swarms, recent research has shown that analogous collective behaviors can also emerge in microscopic systems, including bacterial colonies, developing tissues, and neuronal networks [301–304]. Although these systems may not exhibit physical displacement or trajectory coordination in the traditional sense, they do display hallmark features of collective behavior, such as synchronization, pattern formation, and dynamic state transitions, all of which are critically shaped by time delay. For instance, in bacterial biofilms, delay-induced ionic feedback between peripheral and interior cells gives rise to a subcritical Hopf bifurcation. This leads to bistable oscillatory dynamics, with periods that scale linearly with the delay—highlighting its dual role as both a trigger and a modulator of group-level rhythms [301], as shown in Fig. 37. Similar delay-mediated mechanisms operate in developmental systems. For example, in vertebrate somitogenesis, time-delayed juxtacrine coupling facilitates the formation and directional propagation of phase waves, enabling coordinated segmentation even without centralized control [303].

Similar delay-induced mechanisms have also been identified in microscopic collective systems, particularly in neuronal networks, further supporting the generality of time-delay effects across scales. In bursting neuronal networks, time delay has been shown to induce phase-flip bifurcations, which lead to abrupt transitions between synchronous and asynchronous states, as depicted in Fig. 38. These transitions are shaped by the system's intrinsic multi-timescale bursting dynamics and are robust across different coupling types, including both electrical and chemical synapses [305]. Moreover, in neuronal systems with electrical autapses and heterogeneous delays, delay diversity has been shown to facilitate the emergence of complex spatial patterns such as spiral and target waves, as shown in Fig. 39. Depending on spatial interaction strength and delay distribution, these patterns may either enhance or disrupt global synchrony. Under appropriate conditions, they can also act as pacemaker-like structures, stabilizing coordination across the network [306].

Taken together, the diverse phenomena reviewed in this section indicate that the impact of time delay on collective systems can be understood through a small number of underlying mechanisms. First, time delay introduces a memory-like coupling that mixes past and present information, which may stabilize coordination for moderate delays but destabilize alignment when feedback becomes outdated [31,133,286–288]. Second, delay generates phase lags in local interaction loops, enabling oscillations, switching, and resonance-like amplification when intrinsic and interaction timescales align [289,290,301,305]. Third, by effectively altering who influences whom at a given time, delay reshapes information pathways through evolving interaction patterns, giving rise to non-monotonic and system-dependent responses of coherence, synchronization, and switching to the delay magnitude [44,150,299,300]. These mechanisms unify delay-induced effects observed across macroscopic swarms, networked systems, and microscopic biological and active matter collectives.

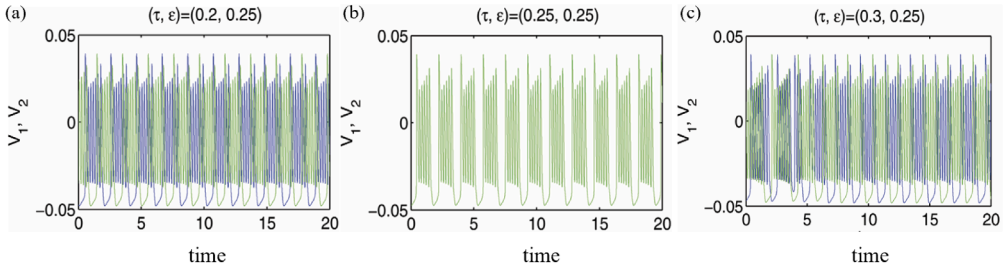

Fig. 38. Phase-flip transitions induced by time delay in a pair of coupled bursting neurons. Panels (a)–(c) show the membrane potentials V_1 and V_2 of two coupled neurons, obtained from numerical simulations of the neuronal model. At coupling strength $\epsilon = 0.25$, as the time delay τ is varied from 0.2 to 0.25 and then to 0.3, the system undergoes phase transitions from out-of-phase to in-phase and back to out-of-phase states. *Source:* The figure is from [305].

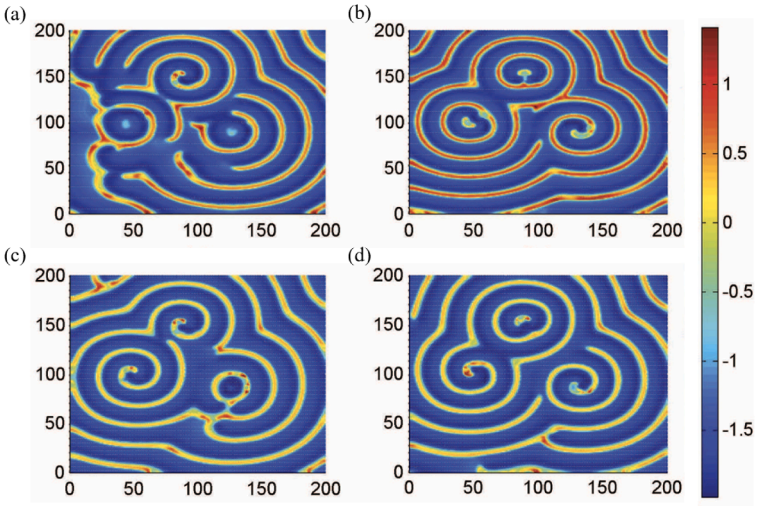

Fig. 39. Time delay diversity effects on spiral wave dynamics in a neuronal network with electrical autapses. Despite the apparent similarity of wave structures in panels (a) to (d), an increase in time delay range results in more complex patterns. In panel (a), a narrow time delay range produces simpler spiral waves, while in panels (b) and (c), wavefront collisions create more intricate spiral configurations. Panel (d) shows that with a broader time delay range, spiral waves become more stable and dominant in the network. *Source:* The figure is from [306].

5.3. Intentional attacks

Collective behavior in both biological and engineered systems relies critically on the integrity and reliability of information transmission among interacting individuals. Beyond random noise or inherent time delays, intentional and non-random disruptions of information flow—whether arising from external interference, internal malfunction, or the selective loss of key components—can pose particularly severe challenges to coordination and stability. Unlike random perturbations or delays, such disruptions often compromise the integrity, accuracy, or availability of information flow, thereby undermining collective coordination and stability [254,307]. Systematically understanding the impact of these intentional disruptions is therefore of considerable theoretical and practical significance for the design of resilient coordination mechanisms.

Similar vulnerability patterns emerge across biological and ecological systems, where attacks such as the selective removal of influential individuals, misinformation propagation, or habitat disruption can trigger abrupt behavioral shifts in structured collectives [308]. These disruptions may push the system past critical thresholds, leading to the breakdown of coordinated behavior. For instance, in migratory bird flocks, the removal of experienced leader individuals can cause navigation failures and group fragmentation, while in wolf packs, the loss of alpha individuals disrupts the entire social hierarchy and cooperative hunting strategies [309]. Such selective disruptions of key individuals can propagate through biological networks, compromising the stability and coordination of collective systems and potentially leading to cascading failures with systemic consequences.

Inspired by these naturally occurring structural vulnerabilities, extensive research has investigated intentional disruptions in engineered swarm systems, where network structure plays a decisive role in determining system-level resilience. These engineered attacks can be viewed as deliberately amplifying structural fragilities that already exist in naturally evolved collective systems. In UAV swarm networks, for example, each agent functions as both a communication and an information-processing node; disruptions

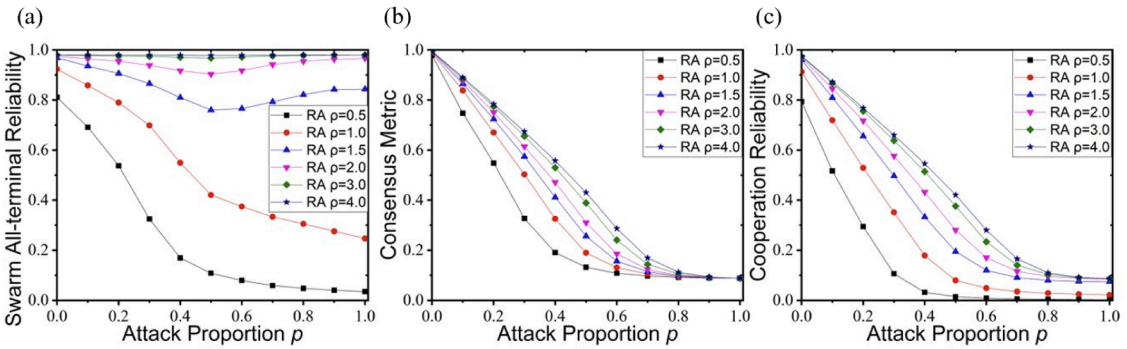

Fig. 40. Impact of random attack (RA) on swarm system reliability under varying densities. The simulations are based on the Vicsek model of collective motion. The plots illustrate (a) all-terminal connectivity, (b) consensus metric, and (c) cooperation reliability as functions of attack proportion p. Results are shown for six density levels ρ, with other parameters set as: number of agents $N = 100$, noise strength $\eta = 0.1\pi$, agent speed $v = 0.03$, and communication radius $r = 1$. *Source:* The figure is from [314].

such as malicious attacks, network congestion, or node failures can trigger cascading failures across communication and information layers, severely degrading system stability and reliability.

Early studies on swarm resilience primarily focused on static network properties. Komareji et al. investigated the structural determinants of consensus resilience in dynamic collective behavior by constructing a time-evolving signaling network [255]. Within a small-world network topology, they revealed that the system's resilience is strongly correlated with the out-degrees of nodes, indicating that more densely connected agents enhance overall robustness. Building on these insights, Huang et al. proposed a theoretical framework for evaluating the robustness of fully interdependent networks under such intentional attacks [310], which was further generalized by Dong et al. to partially dependent systems [311] and later to network-of-networks architectures [312], showing that protecting key hubs can substantially improve systemic stability.

However, such static models may fall short in capturing the complexities of real-world swarm systems, which are often dynamic and heterogeneous in nature [313]. In real-world applications, failures are rarely random but often result from intentional attacks targeting critical hubs—high-degree or highly central nodes—or occasionally from peripheral nodes, especially in cases where core components are well-protected [310]. Addressing this limitation, Liu et al. proposed a temporal network-based framework to assess swarm system reliability under malicious attacks [314], demonstrating that attacks guided by degree and centrality measures cause substantially greater degradation than random attacks. Under random attacks, the effect of attack proportion on swarm reliability depends strongly on network density. As shown in Fig. 40, systems with higher agent density exhibit greater resilience in terms of all-terminal connectivity, consensus, and cooperation reliability as attack levels increase. This density-dependent robustness highlights the importance of connectivity redundancy in mitigating the impact of non-uniform disruptions.

Across both biological and engineered systems, selective disruptions often induce abrupt, nonlinear transitions rather than gradual performance degradation. To investigate such transitions, classical resilience analysis often models system dynamics using simplified one-dimensional nonlinear differential equations, such as $\dot{x} = f(\beta, x)$, where $f(\beta, x)$ describes the system's dynamics and β represents variations in environmental conditions. Critical state transitions can then be examined via bifurcation analysis with respect to the tunable parameter β [315,316]. However, real-world systems are rarely so simple. They typically consist of numerous interacting components, complex weighted connections, and multidimensional control parameters, and are often modeled as networked dynamical systems. By applying dimensional reduction techniques and mean-field theory, complex networked systems can be mapped to low-dimensional representations. The resilience of the original high-dimensional system can then be quantitatively assessed through bifurcation analysis of the reduced dynamical model [316,317]. While such reduced-order approaches offer valuable insight into the onset of critical transitions, they often rely on strong homogeneity and mean-field assumptions, which may limit their applicability to highly heterogeneous or adaptive collectives.

To enhance the resilience of collective systems against intentional attacks, comprehensive defense strategies must operate across multiple system layers. At the structural level, network analyses based on centrality measures (e.g., node degree, betweenness centrality) can identify critical hub nodes whose compromise would most severely degrade system performance [310,312]. These core nodes can then be preferentially protected through redundancy, isolation, or enhanced security measures to mitigate the risk of functional collapse. At the detection and response layer, real-time intrusion detection algorithms and trust-based mechanisms enable continuous monitoring of node behavior and communication link integrity [318]. Machine learning approaches can be employed to establish baseline behavioral patterns and detect anomalies that may indicate ongoing attacks. Once detected, compromised nodes or links must be rapidly isolated to prevent attack propagation, while alternative communication pathways are activated to maintain system functionality. Finally, at the control layer, robust control laws and distributed fault-tolerant algorithms are essential for maintaining system coordination even under partial compromise [319–321]. These approaches typically incorporate redundancy in control decision-making, consensus protocols that can tolerate a certain fraction of malicious nodes, and adaptive mechanisms that can reconfigure system behavior in response to detected attacks. Taken together, these multi-layered defense strategies reflect an inherent trade-off between robustness, efficiency, and implementation complexity. Their integration provides a systematic approach

to mitigating intentional disruptions, while also highlighting the need for adaptive and scalable resilience frameworks capable of addressing increasingly sophisticated attack scenarios.

6. Collective decision-making and emergence of collective intelligence

The fascination of group behavior lies not only in how individuals aggregate to form groups that exhibit behaviors distinct from those of individuals acting alone, but also in the fact that many collective systems possess the capacity for collective decision-making—that is, a social or organizational group can reach decisions that reflect the overall preferences or interests of its members through interactions among individuals. Such collective decision-making processes are widely regarded as a core manifestation of collective intelligence, whereby group-level interactions enable performance, accuracy, or adaptability that exceeds those of isolated individuals. Across a wide range of biological and artificial systems, decision-making is not confined to isolated agents but emerges through local interactions, social influence, and feedback processes that span multiple scales [322]. Whether in ant colonies choosing nest sites [323,324], bird flocks adjusting flight paths [325], or robotic swarms coordinating movement [326], collective decisions are shaped by a dynamic interplay between individual information, social connectivity, and environmental cues.

This section presents an overview of how individual-level decision-making mechanisms scale to generate emergent collective intelligence. It begins by reviewing key processes that support decentralized coordination, including rule-based heuristics, quorum sensing, and leadership dynamics—mechanisms observed across biological systems, from cellular migration to animal societies [322,327]. The discussion then shifts to network-level factors, highlighting how individual heterogeneity and patterns of social connectivity influence information flow and shape collective outcomes. Finally, we summarize major modeling approaches to collective decision-making, including agent-based models, Bayesian inference frameworks, and neural network architectures. These computational approaches provide a powerful means of capturing the core mechanisms that drive collective decision-making [328,329].

6.1. Mechanisms of decision-making

Collective decision-making represents one of the most fundamental aspects of group behavior, enabling organisms to coordinate their actions without centralized control. From microbial colonies responding to environmental gradients to complex animal societies choosing migration routes, the ability to reach consensus through local interactions has evolved independently across diverse biological systems [322,330]. Understanding these mechanisms is crucial for comprehending how individual-level information processing scales up to produce coherent group-level behaviors and emergent collective intelligence [331,332].

The most fundamental form of collective decision-making occurs through decentralized processes, where consensus emerges from local interactions without requiring any individual to have complete information about the group's state or the environment [322]. These processes typically rely on simple behavioral rules that, when applied by multiple individuals simultaneously, generate complex group-level patterns and decisions. A canonical example of decentralized decision-making is found in honeybee swarms during nest site selection [333,334]. Scout bees independently evaluate potential sites and advertise them via waggle dances, with dance intensity reflecting site quality. Through local recruitment and quorum sensing, the swarm collectively converges on the best option without central control. Similarly, in the ant species *Leptothorax albipennis*, individuals evaluate nest quality independently and recruit others based on their personal assessments. Once a quorum threshold is surpassed, the colony initiates relocation [323,324]. In fish schools, individuals align their movements with informed neighbors, and simulations show that decision accuracy increases with group size [335,336], as illustrated in Fig. 41. Collectively, these cases show that simple local interactions, coupled with the integration of individual and socially shared information, are sufficient to generate coherent group-level decisions in the absence of centralized control.

Microbial communities, despite lacking nervous systems, also display sophisticated collective decision-making capabilities. For instance, the slime mold *Physarum polycephalum* achieves adaptive decision-making through repeated sampling and local information integration [337]. Phage populations exhibit density-dependent life cycle decisions via nonlinear feedback mechanisms [338], while bacterial communities coordinate actions like biofilm formation and resource allocation through chemical signals and quorum sensing [339]. In *Myxococcus xanthus*, collective migration is regulated by the Frz signaling pathway, providing a clear example of how individual-level decisions contribute to large-scale coordinated movements in microbial communities [340]. These microbial systems demonstrate that collective decisions can emerge through local sensing, chemical communication, and feedback regulation, even in the absence of a nervous system.

While decentralized coordination is common, many collective decisions still depend on influential individuals. Many biological systems exhibit asymmetries in knowledge or behavior, leading to the emergence of leaders. Theoretical models show that groups can reach a shared movement direction even when only a few individuals are informed [327], highlighting the importance of leadership in consensus formation. Empirical studies further reveal that leadership takes multiple forms across animal groups. In stickleback fish schools, bolder individuals frequently initiate movements, whereas more cautious individuals tend to follow [341]. In pigeon flocks, directional changes propagate from leaders to followers, forming a stable hierarchical structure in which a few individuals have a greater influence on the formation of the group's movement direction [66]. Privileged access to information can also give rise to leadership: during ant emigration, workers familiar with higher-quality nest sites guide the colony toward better options [342].

Importantly, leadership is not always fixed. In sheep herds, leadership is transient and context dependent, with movements initiated by individuals whose momentary state or environmental cues grant temporary influence, yet still ensuring cohesion and directional accuracy [343], as shown in Fig. 42. Recent multi-timescale analyses further reveal that leadership is not fixed but reorganizes dynamically over time, with different individuals emerging as leaders at different temporal scales [344].

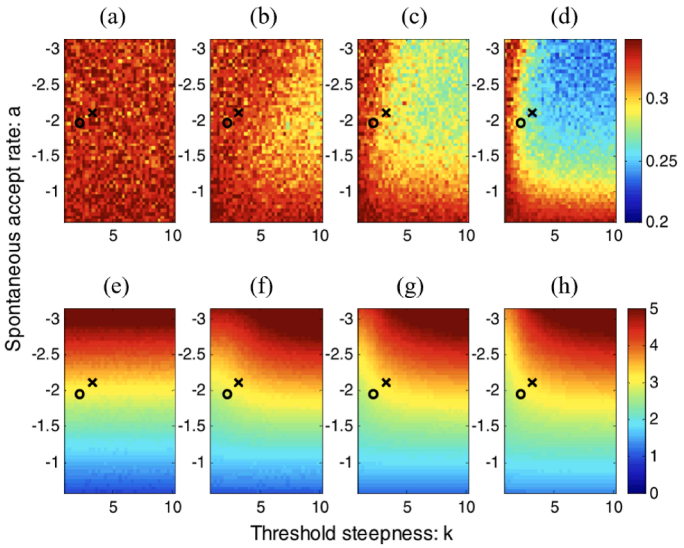

Fig. 41. Accuracy and speed of individual decision-making from model simulations across group sizes ($n = 2, 4, 8, 16$). Vertical axis: spontaneous accept rate (a, log-transformed); horizontal axis: threshold steepness (k). Subplots (a–d) show decision accuracy, and (e–h) show decision speed. Black "×" marks best-fit parameters in the absence of a predator; circles mark best-fit parameters in the presence of a predator. *Source:* The figure is from [335].

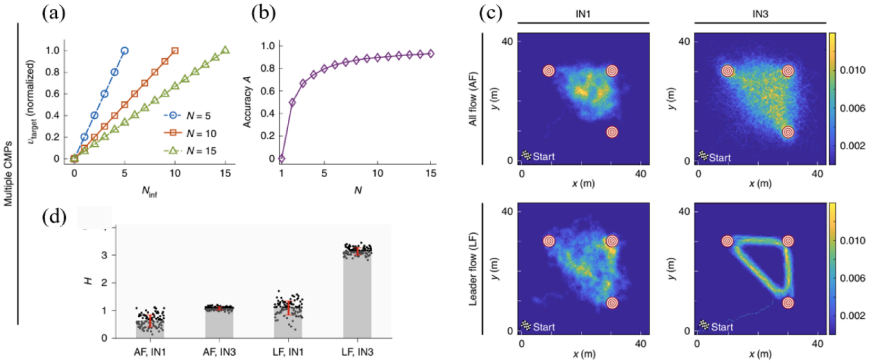

Fig. 42. Intermittent collective motion enhances cohesion and information pooling in sheep. (a) Average normalized speed toward the target (v_{target}) as a function of the number of informed individuals (N_{inf}) for groups of different sizes ($N = 5, 10, 15$). (b) Navigation accuracy A increases with group size, indicating improved information integration when leadership rotates across individuals. (c) Simulation of multiple-target exploration under two interaction networks (IN1: fully connected, IN3: hierarchical directed) and two information flow strategies (AF: all informed individuals continuously share information; LF: only the temporary leader shares information). (d) Exploration performance H shows that the leader-follower strategy combined with IN3 yields the highest efficiency. *Source:* The figure is from [343].

Similar phenomena are observed at the cellular level. During collective cell migration, transient leader cells emerge in response to external cues and are replaced by others when environmental conditions change [345–347], as illustrated in Fig. 43. In many tissues, subpopulations of cells polarize into distinct "leader" or "pioneer" phenotypes that actively guide trailing "follower" cells [348]. Leader cells typically exhibit pronounced morphological polarity, heightened responsiveness to extracellular guidance cues, and elevated cytoskeletal dynamics compared to follower cells. A well-characterized example is tip–stalk cell differentiation during angiogenesis, in which genetically programmed tip cells lead less motile stalk cells to collectively form functional, lumenized vascular structures [349]. Such leader-driven coordination not only ensures efficient directional migration but also supports the formation of complex branched vascular networks that are essential for tissue perfusion and function.

When group members hold conflicting preferences, leadership can mediate consensus. Using high-precision GPS tracking of pigeon pairs, Biro et al. found that when the conflict between two birds' directional preferences was small, individuals averaged their routes. However, when the conflict exceeded a critical threshold, the pair either split or one bird assumed the role of leader [325]. Field studies of wild baboons further illustrate this, where individuals follow multiple initiators when their directions align, and shift to follow the majority when conflict arises [350] (see Fig. 44). Notably, theoretical work by Couzin et al. suggested that the presence of "uninformed" or "information-neutral" individuals can help prevent minority opinions from disproportionately influencing

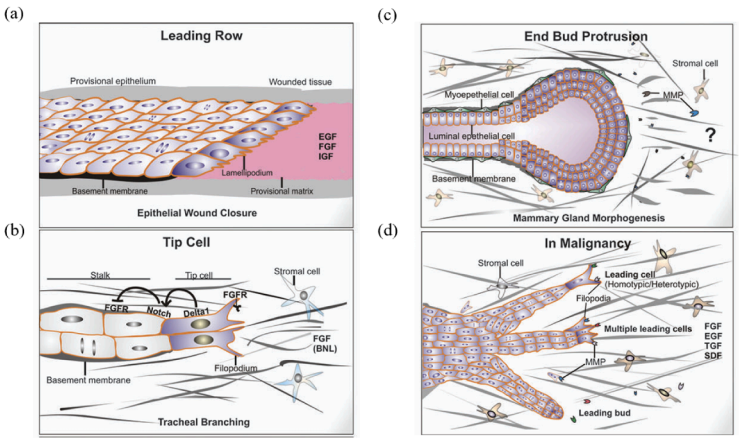

Fig. 43. Diversity of leading edge morphology and function in collective cell migration. (a) Multicellular leading row drives epithelial wound closure. (b) One or two tip cells guide tracheal branching via FGF/Notch signaling. (c) Mammary terminal end buds protrude collectively during ductal morphogenesis. (d) In malignancy, multiple heterogeneous leader cells drive invasive collective migration through 3D stromal environments. *Source:* The figure is from [345].

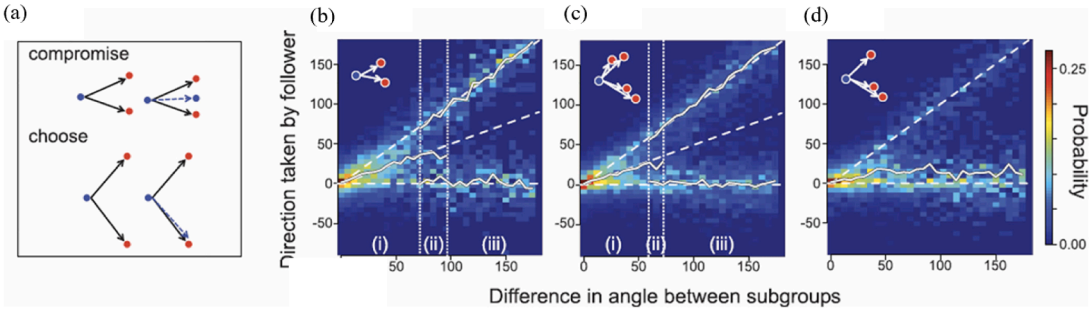

Fig. 44. Collective decision-making in baboons under directional conflict. (a) As the angular difference between initiators increases, follower decisions transition from compromise (taking the intermediate direction) to choosing a single direction. (b–d) illustrate this transition: groups tend to compromise at small angular differences but favor the majority direction when the difference is large. Solid white lines show the median of the directions taken for each mode, while dashed white lines represent the expected direction when compromising (middle line) or choosing (top/bottom lines). Red dots denote initiators, and blue dots denote followers. *Source:* The figure is from [350].

group decisions, thereby promoting fairer and more democratic outcomes [37]. These findings highlight the importance of leaders in facilitating coordination and promoting democratic decision-making within the group.

6.2. Connectivity and individual influence in decision-making

Influence in collective decision-making emerges from the interplay between individual differences and social connectivity. In collective decision-making, individual heterogeneity shapes how influence is distributed and expressed within groups, while social connectivity determines the pathways through which that influence propagates. Early models often assumed homogeneity among individuals, overlooking the widespread differences in personality traits, behavioral responsiveness, and information sensitivity observed in real-world systems. However, a growing body of empirical and theoretical research has shown that such diversity not only affects how social information is adopted but also significantly shapes the efficiency of opinion integration and group coordination [327,351,352]. Meanwhile, an individual's connectivity constrains the reach and amplification of influence in the network, shaping their role in information transmission and decision-making [353–355]. Highly connected individuals tend to possess greater social influence and structural centrality, making them more likely to play dominant roles in shaping collective opinions. In contrast, individuals with lower connectivity are more susceptible to external influence and exhibit greater variability in their decisions. Therefore, understanding the interplay between individual differences and network structure is essential for revealing the dynamic mechanisms underlying group behavior.

At the individual level, heterogeneity generates unequal influence by shaping behavioral tendencies and spatial positioning. In sheep populations, bold individuals, who are relatively less influenced by social attraction, and shy individuals, who are more responsive to conspecifics and local crowding, tend to exhibit distinct spatial distribution patterns across vegetation patches [356]. These personality-related differences become increasingly pronounced as group size grows, ultimately altering the dynamics of collective decision-making. Comparable effects appear in other taxa. In social insects, differences in nest-site evaluation enhance decision accu-

racy at the colony level [357]; in Trinidadian guppies, stable group-level personality differences accounted for most of the variation in collective behaviors, including leadership–follower dynamics and decision-making processes [358]; and in wild great tits, individuals with reactive personalities were more likely to engage in group activities, while proactive individuals tended to forage independently on the periphery of the group [359]. These empirical patterns are mirrored in theoretical work. Mann's rational-agent model demonstrates that individuals facing greater uncertainty rely more heavily on social information, whereas those with strong or divergent preferences selectively discount it. Notably, minority subgroups with distinct goals can influence collective outcomes, even without structural asymmetries in the group [352].

While individual traits lay the foundation for behavioral influence, the structure of the social network often determines how such influence propagates. Transitions from centralized to distributed network topologies can trigger qualitative shifts in group decision-making dynamics [360]. In centralized networks, a few key individuals dominate decision-making, whereas distributed structures support more balanced information flow and the emergence of shared consensus. Network-level mathematical properties further shape consensus formation. Bruggeman demonstrated that the speed of reaching consensus is closely tied to a network's algebraic connectivity [355]. Higher algebraic connectivity was found to promote more efficient information diffusion, thus accelerating agreement across the network. Moreover, Hu and Shu proposed a kinetic model that incorporates agents' connectivity and opinion preferences [361]. They found that highly connected individuals exert greater influence yet are more resistant to opinion change, serving as stabilizing anchors within the decision-making process.

Importantly, empirical studies suggest that stabilizing or anchoring roles in collective decision-making need not arise solely from high connectivity or structural centrality. In multispecies octopus–fish hunting groups, leadership and influence are distributed across functionally distinct roles rather than concentrated in the most active or mobile individuals [362]. Detailed trajectory analyses revealed that goatfish frequently initiate movement and exploration, effectively guiding where the group searches, whereas the octopus disproportionately determines whether and when collective movement occurs by inhibiting or anchoring group motion. Despite not being the primary initiator, the octopus emerges as a key decision-making node through its capacity to constrain collective transitions, illustrating that individual influence can be exerted through inhibitory control rather than information propagation alone.

Empirical work in primate societies provides striking real-world evidence of how social connectivity impacts collective decisions. Fratellone et al. conducted field observations and social network analyses on a group of Tibetan macaques (*Macaca thibetana*) in the Huangshan Mountains of China, revealing that social bonds among females were significantly stronger than those among males, characterized by more preferential associations, higher centrality, and tighter clustering in the network [363]. After controlling for group size, they further demonstrated that groups with a higher proportion of females initiated and progressed through collective decisions more rapidly, indicating that social connectivity directly facilitates the efficiency of group-level decision-making.

While highly connected networks often accelerate consensus formation, rapid convergence may not always align with optimal collective performance, particularly in complex adaptive landscapes. Experimental evidence indicates that communication network structure significantly shapes collaborative learning outcomes: in complex problem-solving tasks, networks that support efficient yet distributed information exchange consistently outperform poorly connected or overly centralized configurations [364]. Rather than relying on mechanical imitation, individuals flexibly adjust their use of social information in response to feedback and contextual cues. Further agent-based investigations by Reia and colleagues suggest that in multi-peaked landscapes, hierarchical and modular network architectures tend to achieve superior performance, in part by limiting the rapid diffusion of locally suboptimal strategies and thereby reducing the risk of collective lock-in [365]. In contrast, non-modular scale-free and random networks are more susceptible to information cascades and premature convergence. These findings highlight that network topology influences not only the speed of convergence, but also the stability and adaptiveness of collective outcomes in complex environments.

More generally, these findings point to an inherent structural trade-off in networked decision systems. Network structure can alter collective problem-solving performance by shaping the balance between exploration and exploitation, thereby influencing both the speed and accuracy with which groups converge on effective solutions. Highly integrated networks may accelerate convergence but risk premature lock-in, whereas modular or partially decentralized structures can preserve diversity, sustain adaptive search, and enhance robustness in complex task environments. Such trade-offs imply that no network topology is universally optimal; rather, optimality is contingent upon environmental complexity and the distribution of uncertainty across agents.

6.3. Modeling collective decision-making

Understanding how individual-level behavioral rules give rise to coordinated group decisions is a central challenge in the study of collective systems. Over the past two decades, theoretical models have played a crucial role in bridging this gap, revealing how simple interaction rules, probabilistic inference, and neural computation can generate complex group-level patterns. These approaches, rooted in behavioral ecology, statistical physics, and network science, provide mechanistic explanations for empirical observations and offer predictive tools applicable across biological and artificial collectives.

A foundational approach to modeling group coordination comes from self-organized interaction rules. Couzin et al. proposed a widely influential model in which individuals update their movement direction by combining short-range repulsion, mid-range alignment, and long-range attraction [327]. These simple local rules generate cohesive and flexible collective motion. Specifically, if one or more neighbors fall within a short-range repulsion zone (defined by distance threshold α), then the desired movement direction is updated to avoid collisions:

$$d_i(t+\Delta t) = -\sum_{j\neq i} \frac{c_j(t)-c_i(t)}{|c_j(t)-c_i(t)|}, \tag{21}$$

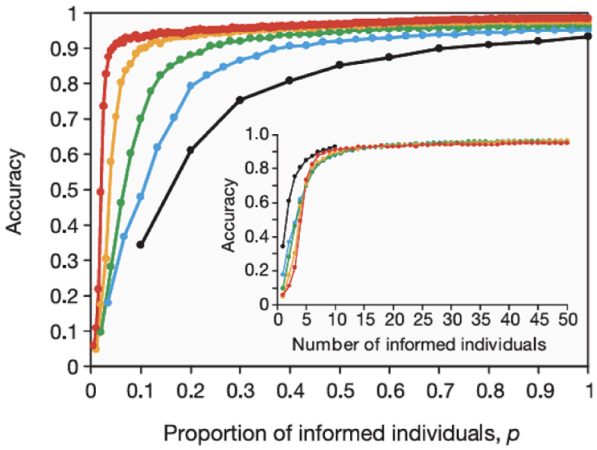

Fig. 45. The relationship between group accuracy and the proportion of informed individuals, p, in the self-organizing collective movement model (21)–(23), shown for different group sizes: $N = 10$ (black), $N = 30$ (blue), $N = 50$ (green), $N = 100$ (yellow), and $N = 200$ (red). The results show that in larger groups, only a small proportion of informed individuals is needed to achieve high-precision group movement. *Source:* The figure is from [327].

where d_i represents a desired direction of travel. If no neighbors are detected within this region, the individual will tend to become attracted to and aligned with its neighbors:

$$d_i(t+\Delta t) = \sum_{j\neq i}\left(\frac{c_j(t)-c_i(t)}{|c_j(t)-c_i(t)|}+\frac{v_j(t)}{|v_j(t)|}\right). \tag{22}$$

This composite vector $\mathbf{d}_i(t+\Delta t)$ is then normalized to obtain a unit movement direction $\hat{\mathbf{d}}_i(t+\Delta t) = \mathbf{d}_i(t+\Delta t)/\left|\mathbf{d}_i(t+\Delta t)\right|$.

To incorporate informed individuals, the model assumes that a subset of agents possesses a preferred direction $\mathbf{g}_i$. Their movement results from a weighted combination of social cues and personal information:

$$\mathbf{d}_i'(t+\Delta t) = \frac{\hat{\mathbf{d}}_i(t+\Delta t)+\omega\mathbf{g}_i}{\left\|\hat{\mathbf{d}}_i(t+\Delta t)+\omega\mathbf{g}_i\right\|}. \tag{23}$$

This formulation captures how informed individuals trade off social influence ($\hat{\mathbf{d}}_i$) against private directional knowledge ($\mathbf{g}_i$) via the parameter ω. When $\omega = 0$, informed individuals behave identically to uninformed ones, relying entirely on local social interactions. As ω increases, the influence of the preferred direction $\mathbf{g}_i$ becomes more dominant. When $\omega > 1$, informed individuals prioritize personal information over neighbor cues.

They demonstrated that a small proportion of informed individuals can effectively guide the entire group, even when preferences conflict. The group tends to reach consensus, typically aligning with the majority's direction. Coordination accuracy is measured by the angular deviation between the group's average heading and the intended goal (ranging from 0 for perfect alignment to 1 for random movement). As illustrated in Fig. 45, group accuracy increases with the proportion of informed individuals, particularly in larger groups.

Building on this rule-based framework, subsequent work across taxa has shown that collective decisions can be implemented through diverse mechanisms while relying on similar principles of local interaction and information pooling. For instance, quorum responses in fish shoals enable rapid consensus once the number of committed individuals exceeds a critical threshold [335]. High-resolution GPS tracking of wild baboons further indicates shared decision-making in group movement: large directional conflicts are typically resolved by selecting one direction, whereas smaller conflicts lead to compromise [350]. More generally, theory suggests that group composition and interaction structure influence which consensus outcome emerges [366].

Complementing rule-based collective motion models, Arganda et al. proposed a unified Bayesian framework to account for cross-species variation in collective decision strategies [328]. The core idea of this model is that individuals, when making decisions, rely not only on their own sensory information but also on the choices made by others in the group. For clarity, we describe the two-option case (x vs. y), while the same logic can be extended to multiple alternatives (Fig. 46).

In this framework, decision-making is cast as Bayesian inference: individuals estimate the probability that each option is "good" by combining non-social (private) information with social evidence derived from others' observed choices. Specifically, for the two-option case (x vs. y), the probability that option x is good is

$$P(x \text{ is good}) = \frac{1}{1+as^{-(n_x-kn_y)}}. \tag{24}$$

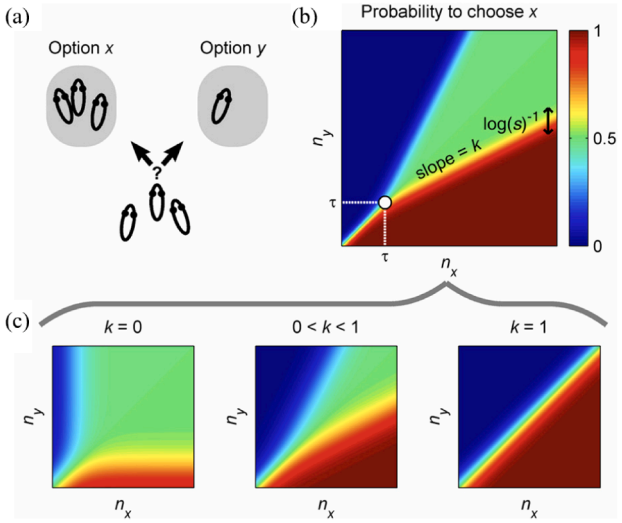

Fig. 46. A general decision-making rule based on Bayesian estimation in animal collectives. (a) Schematic illustration of a binary collective decision-making scenario. (b) The probability of choosing option x (P_x), obtained by substituting the estimation from Eq. (24) into Eq. (25), plotted as a function of the number of individuals committed to options x (n_x) and y (n_y). The model predicts qualitatively different regimes for small vs. large group sizes, with a clear separation at the critical point τ. The width of the transition region scales with $\log(s)^{-1}$. (c) Influence of different values of the sensitivity parameter k on the probability of choosing x. *Source:* The figure is from [328].

Here n_x and n_y denote the numbers of individuals currently choosing options x and y, respectively. The parameter a captures the quality of non-social information, whereas s controls the reliability of social information conveyed by others' choices. The parameter k is a balancing parameter that controls the influence of individuals choosing the alternative option.

Based on this Bayesian estimation, individuals select among options via probability matching, i.e., the probability of choosing an option is proportional to its inferred goodness. In the two-option case, the probability of choosing x is

$$P(x) = \frac{P(x \text{ is good})}{P(x \text{ is good}) + P(y \text{ is good})}. \tag{25}$$

This implies that the probability of choosing an option depends not only on its perceived "goodness" but also on the distribution of others' choices. Social information therefore plays a central role, as the decision is dynamically adjusted according to the changing behaviors of other group members. This decision-making mechanism enables individuals to make more accurate choices in complex and uncertain environments, while also explaining the diversity of decision-making behaviors observed in animal groups.

This decision-making model has since been adopted and extended across a range of settings to account for collective behavior in diverse taxa. For example, Vicente-Page et al. found that smaller groups exhibit greater decision accuracy in dynamic environments, underscoring the enhanced influence of social information when group size is limited [367]. Pérez-Escudero et al. generalized the approach to three alternatives, showing that Bayesian estimation continues to capture collective choices in complex decision spaces [368]. Calovi et al. further connected the framework to the interaction rules in fish burst-and-coast swimming, illustrating how components such as attraction and alignment can be integrated within a unified collective decision-making architecture [369].

From the perspective of network science, Sridhar et al. proposed a neural decision-making model to study how individuals make decisions when faced with multiple spatial options [329]. They showed that multi-option spatial choice can emerge from dynamics on an interaction network of direction-tuned neural units. In this formulation, neural populations are treated as nodes on a ring-organized interaction network, with coupling strengths determined by angular similarity between preferred directions.

In this model, the animal's brain is represented as a system of N interacting units (nodes), formally analogous to spins in an Ising-type model. Each spin i corresponds to a direction-tuned neural unit with a preferred direction $\hat{\rho}_i$ and a binary activity state $\sigma_i \in \{0, 1\}$ (inactive/active). Presented goals act as directional inputs that bias activity on this ring-attractor-like network. The collective state of the network is captured by an Ising-like Hamiltonian,

$$H = -\frac{k}{N} \sum_{j \neq i} J_{ij} \sigma_i \sigma_j, \tag{26}$$

where k is the number of available options, J_{ij} is the interaction strength between units i and j, and σ_i and σ_j are the states of the units. The interaction strength J_{ij} depends on the angular difference between preferred directions and is defined as $J_{ij} = \cos\left(\pi \left(\frac{|\theta_{ij}|}{\pi}\right)^{\mu}\right)$. Here, θ_{ij} is the angular difference between spins i and j, and μ is the tuning parameter that controls the range of interactions.

When $\mu = 1$, the system exhibits a Euclidean "cosine-shaped" interaction, while for $\mu < 1$, the network shows more localized excitation. The final movement direction of the individual is determined by the weighted sum of the goal vectors $\hat{\rho}_i$ of all active spins,

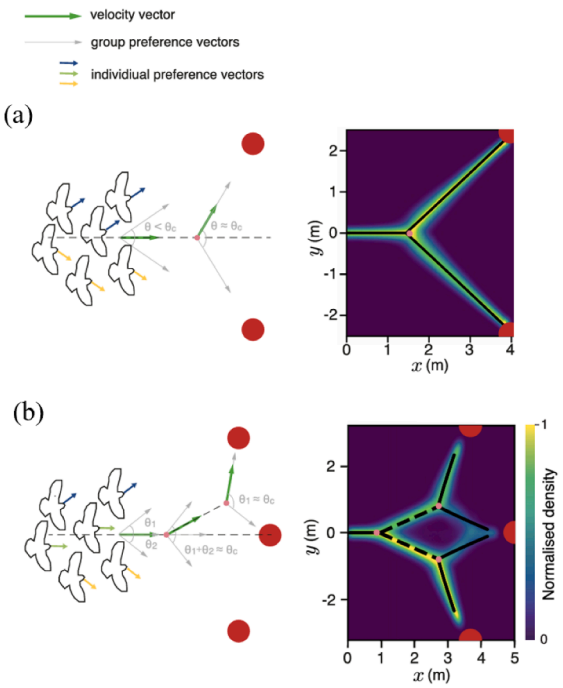

Fig. 47. Consensus decision-making in simulations of animal groups. (a) In a two-choice scenario, the group compromises and moves along the average direction. (b) In a three-choice scenario, bifurcated paths emerge due to angular summation of competing preferences. The density plots show trajectories adopted by the centroid of the animal group for 500 replicate simulations where the groups do not split. The black lines represent the phase transition function fit to the trajectories, revealing the dynamic changes in the decision-making process. For the three-choice case (b), the dashed line is the bisector of the angle between the central target and the corresponding side target at the first bifurcation point. Red dots represent the target positions. *Source:* The figure is from [329].

represented by the following equation:

$$\vec{V} = \frac{v_0}{N} \sum_{i=1}^{N} \hat{\rho}_i \sigma_i, \tag{27}$$

where v_0 is the proportionality constant. The goal vector $\hat{\rho}_i$ of spin i now points from the agent's updated position toward its preferred goal, incorporating directional noise. Within this framework, Sridhar et al. showed that when animals are confronted with multiple spatially distributed options, they simplify complex multi-alternative decisions by sequentially reducing them to a series of binary choices, as shown in Fig. 47. This behavior arises from ring-attractor dynamics characterized by local excitation and global inhibition, and reflects geometric principles that shape spatial attention and choice.

While the preceding models mainly describe how individuals coordinate under fixed interaction rules, studies of human collective intelligence typically focus on repeated task settings in which strategies can change through feedback and learning over time. Extending collective decision-making frameworks to such iterated settings, a growing body of work has explored how social interaction structures shape group performance in complex problem-solving environments [364,370–372]. Employing agent-based and minimal computational models, these studies highlight how network topology and information flow regulate collective outcomes through mechanisms such as selective imitation, social learning, and shared information repositories. By capturing exploration–exploitation trade-offs and the diffusion of successful strategies across repeated interactions, these models illuminate how simple local rules can give rise to sustained collective adaptation and improved group-level outcomes.

6.4. Collective navigation and the emergence of collective intelligence

Having reviewed representative mechanistic models of collective decision-making, we now turn to a widely studied application: collective navigation. From a physical perspective, collective navigation can be formulated as a distributed information-processing problem, in which multiple agents acquire noisy, local measurements of their environment and integrate this information through interaction networks to generate coherent, large-scale motion. Such processes are widespread in nature, ranging from large-scale seasonal migration in northern bald ibis to homeward navigation in Pacific salmon, as well as smaller-scale behaviors such as locating new food sources, moving up and down the water column, or finding new shelters [373–375].

In such contexts, individuals face noisy environmental information and limited local sensing, and in some cases may even lack memory; collective mechanisms can help overcome these constraints [375]. Through local interactions, collective motion enables

the integration of distributed information and exploits feedback between movement and environmental cues to reduce these limitations [330,375]. As collective experience accumulates, navigation routes can be progressively refined, leading to cumulative improvements in performance [376]. Collective navigation thus offers a concrete and intuitive example of how individual-level constraints can be transformed into group-level accuracy, robustness, and adaptability—key hallmarks of collective intelligence [330,375].

To explain how animal groups achieve such coordination, researchers have proposed a range of theoretical mechanisms underlying collective navigation. Among the most widely studied are the many-wrongs principle and leadership [375]. These mechanisms offer contrasting perspectives on how individuals contribute to group-level movement decisions under uncertainty. The many wrongs principle suggests that individuals make noisy or imperfect estimates of direction, but by averaging across many such estimates, the group can achieve higher navigational accuracy. Originally proposed by Simons [377], this principle implies that larger group sizes inherently lead to improved performance due to statistical averaging. Empirical support for this idea comes from early field studies on migrating birds, which found that directional accuracy increased with group size in species such as white storks [378] and skylarks [379]. More recent GPS-tracking experiments have provided rigorous validation of this mechanism [325,380].

In contrast, the leadership mechanism is based on informational asymmetry. It posits that a small number of well-informed or experienced individuals can effectively guide the entire group's trajectory. Couzin et al. demonstrated that even if leaders represent only a small fraction of the population, effective coordination from followers allows them to significantly influence the group's overall navigational path [327]. Such leadership phenomena have been widely observed in various social animals, including collective flight in pigeon flocks [66] and nest-site selection in honeybees [381]. The many-wrongs principle and leadership provide two fundamental, often complementary, routes to collective navigation. By converting individual noise and informational asymmetry into higher accuracy, robustness, and efficiency, they exemplify the emergence of collective intelligence in complex natural environments.

While collective navigation is commonly associated with animals, microbial systems can also exhibit sophisticated group-level coordination. A notable example is *Paenibacillus vortex* (*P. vortex*), a self-lubricating bacterium capable of coordinated movement via flagella-driven swarming and potential pili-based twitching [382]. Its navigation relies on the interplay between attractive and repulsive chemotactic cues, enabling coordinated group movement across various complex terrains [383]. When grown on hard surfaces, the colony organizes into dense pioneer cell clusters that are propelled forward by repulsive chemical signals secreted by rear cells. When grown on soft surfaces, *P. vortex* organizes into snake-like foraging swarms that extend outward, with widths reaching hundreds of cells [383].

The group-level navigation of *P. vortex* is not merely reactive but demonstrates features of decision-making and optimization. Upon detection of extracellular material at a distance, the bacteria employ collective navigation (chemotaxis), reorienting the entire swarm towards the detected signal. As depicted in Fig. 48 (a-d), directional changes in the moving swarm occur when signals from distant sources are detected. Remarkably, when encountering scattered patches of extracellular material, the swarm can spontaneously split and reunite, as shown in Fig. 48(e-h), reflecting its capacity for self-organized adaptation. These findings suggest that *P. vortex* achieves not only collective changes in propagation but also demonstrates a sophisticated optimization strategy that likely evolved to enhance survival in complex environments [383].

Beyond biology, collective navigation principles have increasingly inspired artificial multi-agent systems designed to operate without centralized control. One such example is the bacteria-inspired swarm model proposed by Shklarsh et al., which simulates cooperative cargo transport through complex terrains [384]. In this model, agents interact with a shared payload through different physical coupling mechanisms that emulate biological coordination strategies. Specifically, the study investigates three distinct configurations: a rope-like model, characterized by loose but persistent connectivity that allows flexible movement; a spring-like model, which introduces elastic tension to enhance cohesion; and an elastic-stick model, which provides semi-rigid linkages with constrained flexibility. These coupling strategies were found to give rise to markedly different swarm behaviors, with phase transitions occurring between uncoordinated group splitting and cohesive collective delivery, depending on the interaction strength and environmental complexity. As shown in Fig. 49, these outcomes underscore how simple local rules can generate complex transport dynamics at the group level.

Inspired by biological navigation, collective navigation strategies have been extensively applied to unmanned aerial vehicle (UAV) systems, where swarms of autonomous agents perform coordinated tasks in the absence of centralized control [136,326,385,386]. In these systems, agents rely on local sensing, short-range communication, and distributed decision-making to execute path planning and collision avoidance. Navigation architectures based on local interaction rules and swarm intelligence have demonstrated superior robustness, scalability, and environmental adaptability, offering viable solutions for complex missions such as exploration, surveillance, and search-and-rescue operations.

The feasibility of decentralized information processing and coordination has been validated through real-world robotic systems. For instance, Zhou et al. developed a decentralized navigation framework for micro aerial robot swarms that enables fully autonomous operation in cluttered natural environments [136]. Each drone is capable of locally optimal real-time trajectory planning using only onboard sensors, with limited broadcasting of planned paths to nearby agents for collision avoidance and coordination. The system was successfully demonstrated in dense bamboo forests as illustrated in Fig. 50, where it exhibited effective obstacle avoidance, reciprocal yielding, and emergent group-level coordination. In addition, Wang et al. introduced a bio-inspired navigation strategy based on visual perception and heterogeneous swarming [386]. In this framework, only a subset of agents possess knowledge of the navigation goal, while the remaining agents follow based on local perception cues. This approach enables fully decentralized migration of aerial robot swarms without inter-agent communication, and exhibits strong scalability and environmental adaptability.

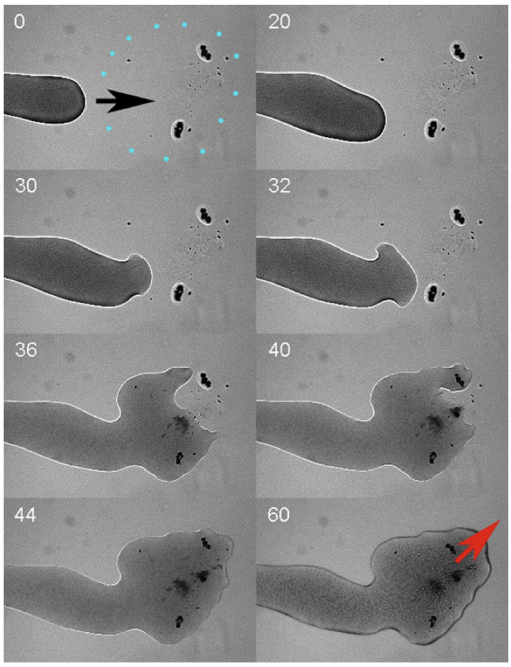

Fig. 48. An illustration of the "swarming intelligence" of the *P. vortex* bacteria when responding to extracellular material. Area of extract outlined in blue dots with direction of cell mass elongation shown by the black arrow. Dark marks inside the area of the extract are disturbances due to the toothpick contacting the agar. During 0–32 s, directional changes in the moving swarm are initiated upon detection of signals from distant extracellular sources. During 36–60 s, upon encountering scattered patches of extracellular material, the swarm demonstrates adaptability by spontaneously splitting and subsequently reuniting. *Source:* The figure is from [383].

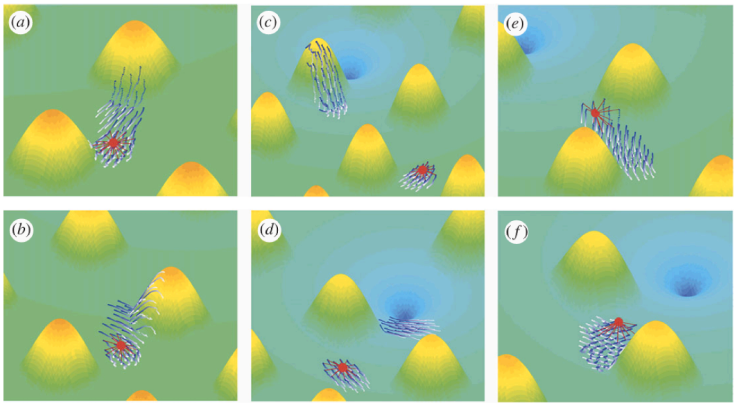

Fig. 49. Simulated swarm navigation under three agent–cargo coupling mechanisms in a bacteria-inspired swarm model. The panels illustrate cargo transport in complex terrains using (left) rope-like, (middle) spring-like, and (right) elastic-stick models. The yellow regions represent obstacles or terrain features that the agents navigate through. The cargo is marked by the red circle. The agent–cargo bonds are marked by red lines. The agents are marked by the blue to white lines indicating their current (blue) to past (white) locations. The figure demonstrates distinct collective behaviors—such as group splitting, coordinated delivery, and failure to transport—emerging from different coupling strategies. *Source:* The figure is from [384].

7. Applications in engineering

In nature, phenomena such as the schooling of fish, flocking of birds, and coordinated movements of insect swarms exhibit collective behaviors that are highly coordinated, robust, and adaptive. These complex yet orderly group dynamics typically operate without centralized control and instead emerge from simple local interaction rules based on individual-level perception. Such rules include neighbor alignment, attraction–repulsion mechanisms, and velocity matching strategies [48,49]. Together, these principles provide fundamental insights into how large-scale coordination can arise in distributed systems.

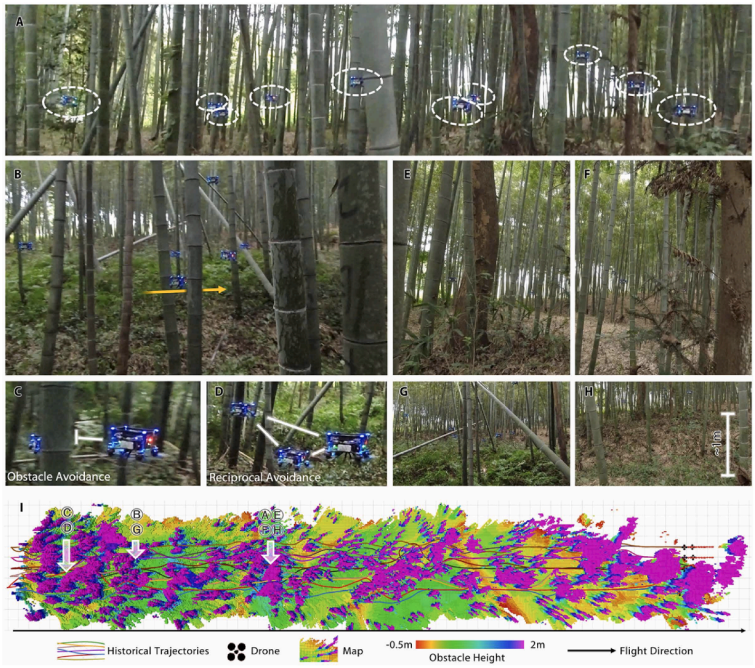

Fig. 50. Autonomous navigation of a multi-drone system in dense bamboo forests. (A–H) Real-world flight scenes showing obstacle avoidance, tight-gap traversal, and challenging terrain. (I) Combined trajectories and maps from ten drones illustrate distributed exploration, mapping, and decision-making in highly cluttered natural environments. *Source:* The figure is from [136].

Inspired by these mechanisms, bio-inspired swarm robotic systems have become a key paradigm for achieving autonomy, scalability, and fault tolerance in complex and dynamic environments [387]. Aerial drone swarms, aquatic robotic fish, and terrestrial mobile robots increasingly rely on locally distributed sensing and interaction rules to coordinate motion, adapt to environmental changes, and perform cooperative tasks. Such systems have demonstrated remarkable versatility across applications including exploration, environmental monitoring, disaster response, and collective transport, particularly in scenarios where decentralized decision-making and robustness are essential [388,389].

This section reviews how the physical and dynamical principles underlying natural collective behavior can be implemented in aquatic and aerial robotic systems. We first discuss biomimetic robotic fish and swarm-robotic control inspired by local coordination rules and hydrodynamic coupling, followed by bio-inspired formation and coordination strategies in UAV swarms. These examples illustrate how biological collectives inform the design of scalable and robust engineered multi-agent systems.

7.1. Biomimetic robotic fish and swarm robotics control

Aquatic animals, particularly fish, exhibit elegant and highly efficient swimming behaviors that enable them to adapt to complex and dynamic environments with ease. These biological locomotion strategies have long served as a rich source of inspiration for underwater robotic systems [390]. In schooling fish, coherent collective motion can emerge without centralized control: empirical and modeling studies suggest that individuals rely primarily on local sensing and interactions with a limited number of nearby neighbors to achieve global alignment and stable spatial organization [53,143,391]. A common formulation is the repulsion–alignment–attraction zonal model, which assumes strong repulsion at very short range to prevent collisions, velocity alignment at intermediate range, and attraction toward the group at longer range [49]. Inspired by these principles, robotic fish swarms often employ neighborhood-based distributed controllers that convert local neighbor measurements (e.g., relative positions and velocities) into control actions, enabling formation keeping and coherent navigation under decentralized and communication-limited settings [392].

Beyond the aforementioned kinematic neighborhood interaction rules, a growing body of empirical and theoretical studies has demonstrated that hydrodynamic interactions also play a crucial role in shaping the performance of collective swimming [86,393]. As each individual propels itself through the water, it generates complex, unsteady wake vortices that alter the local flow field and pressure distribution experienced by its neighbors. These fluid-mediated forces can be either beneficial or detrimental to group performance. Evidence from both natural fish schools and biomimetic robotic fish formations indicates that individuals can benefit from favorable flow structures, such as by entering the low-pressure region of a leader's wake or synchronizing tail beats under suitable spatial arrangements [86,394,395]. These strategies have been shown to reduce energy expenditure, enhance propulsion efficiency, and improve formation stability.

To more comprehensively understand how hydrodynamic coupling contributes to improvements in energy efficiency and formation stability, previous studies have identified several representative mechanisms, including wake capture, drafting, channeling

effects, and vortex synchronization [393,394,396,397]. In staggered or diamond-shaped formations, individuals can enter the low-pressure region within the leader's wake or exploit periodic vortex rings, thereby reducing the propulsive effort required for forward motion [86,398]. Under appropriate phase-synchronization conditions, trailing individuals can further achieve coherent coupling with neighboring vortex structures, leading to enhanced propulsive efficiency [396,397]. These mechanisms not only account for the energy-saving phenomena widely observed in natural fish schools but also provide a theoretical foundation for designing energy-efficient formation strategies in biomimetic underwater robotic systems.

Building on the macroscopic hydrodynamic mechanisms, recent experiments and bio-inspired robotic models have further advanced these hypotheses to the level of testable behavioral and control mechanisms. Li et al. proposed a "vortex phase-matching" mechanism, arguing that followers adjust their tail-beat rhythm according to the distance to the neighbor ahead, synchronizing their tail motions with the direction of vortices shed by the neighbor. This allows them to exploit the wake more effectively and reduce energy expenditure. Experiments on goldfish pair swimming have also confirmed this pattern: even when the fish's vision or lateral line sensing is impaired, such phase matching still persists [87]. In addition, the experiments of Thandiackal and Lauder showed that brook trout actively enter the thrust wake generated by a flapping bioinspired foil and maintain an in-line following position, thereby reducing tail-beat frequency and decreasing pressure drag on the head. Their tail-beat motions also synchronize with the oscillatory rhythm of the incoming vortices, reflecting another form of hydrodynamic coupling based on vortex structures [395]. These results suggest that hydrodynamic coupling influences not only whether a group can maintain its formation, but also the cost of doing so, thereby tightly linking the energy-sharing mechanisms observed in biological collectives with the endurance-optimization goals of bio-inspired engineering systems.

7.2. Formation of UAVs

In recent years, bio-inspired strategies have not only yielded remarkable results in underwater systems but have also gradually extended into aerial domains, particularly in the study of UAV swarms. Compared to a single UAV, swarm systems exhibit higher efficiency, fault tolerance, and adaptability, making them especially suitable for high-risk missions such as surveillance, disaster response, and cooperative mapping [399]. However, achieving effective collaboration within UAV swarms presents a core challenge: how to coordinate globally and adapt dynamically under the absence of centralized control, relying solely on local perception and interaction among agents. To address this issue, researchers have sought inspiration from nature, developing a range of decentralized and distributed control methods based on phenomena such as bird flight formation and insect group behavior.

Collective behavior observed in natural systems provides critical insights for the control of UAV swarms. Taking bird flocking as an example, V-shaped formations exhibit clear global structure that arises from three simple local rules: separation, alignment, and cohesion [48]. This mechanism not only enhances formation stability but also improves energy efficiency and information transmission [400]. Likewise, insect swarms such as locust clouds and bee colonies demonstrate the advantages of decentralized regulation and scalability [49]. These natural systems exhibit key properties—distributed decision-making, local sensing, emergent behavior, dynamic topology, and fault tolerance—which directly inform the theoretical foundation and methodological guidance for UAV swarm system design.

Building on the natural mechanisms observed in collective animal behavior, researchers first started from the local interaction rules of bird flocks and pursued bio-inspired formation control studies driven by the Boids model. Hauert et al. implemented decentralized flocking demonstrations on small fixed-wing UAVs by adopting Reynolds' Boids rules [401]. Vicsek et al. further validated a multi-copter decentralized formation architecture structurally consistent with the Boids principles, enabling stable and autonomous swarm flight [402]. Saska introduced a stabilization and navigation method for UAV swarms that enables them to follow predefined paths through complex, obstacle-filled environments, relying on flocking-based stabilization rules derived from avian group behavior [403]. Although these approaches laid the foundation for bio-inspired formation control, the resulting swarm configurations typically exhibit parallel or loosely organized structures, making it difficult to achieve more desirable and constrained formations required in engineering tasks—such as linear formations. This limitation has driven further investigation into more complex biological interaction mechanisms.

In further studies inspired by bird flocks, pigeon swarms are seen as a representative example of collective intelligence, noted for their strong self-organizing ability and adaptability. Interactions among pigeons can generally be categorized into two modes: egalitarian interactions and hierarchical interactions. The former assumes that all individuals follow the same set of rules and interact uniformly with neighbors within their perceptual range [2], whereas the latter emphasizes the dominant influence of a small subset of leaders, forming explicit leader–follower structures. Through the coordinating effects of hierarchical networks, such structures enable the flock to maintain coherent formation even in the presence of decision-making delays. Based on GPS tracking data of pigeon flights, Nagy et al. identified a pronounced hierarchical order within flocks [66], providing direct evidence for layered leader–follower organization. At the same time, studies have shown that pigeons do not consistently adhere to purely egalitarian or strictly hierarchical strategies; instead, they dynamically switch their following patterns in response to flight conditions [404–406]. These insights provide valuable guidance for engineering applications in multi-agent system control, particularly in UAV formation control [407–409].

Building on these interaction principles—especially those derived from pigeon flocks—recent studies have developed several representative bio-inspired control approaches. Fan et al. proposed a hybrid swarm-intelligence control strategy that enables UAVs to maintain formation integrity while performing cooperative obstacle avoidance [410]. Li et al. integrated virtual-leader formation control with pigeon flocking principles and introduced a hierarchical early-warning mechanism, allowing UAV swarms to adaptively adjust their formation to prevent collisions in complex environments [408]. Shen et al. introduced a hierarchical topology pigeon-inspired optimization algorithm and combined it with receding-horizon control for multi-UAV formation [411], achieving improved

stability and adaptability. Zhang introduced a decentralized UAV-swarm control framework that operationalizes pigeon-inspired interaction patterns into a hierarchical–egalitarian switching mechanism, enabling compact formation maintenance while achieving rapid, collective obstacle avoidance [412].

Overall, these pigeon-inspired control strategies translate hierarchical structures, adaptive following, and biologically grounded interaction rules into practical decentralized formation mechanisms for UAV swarms. However, challenges remain in achieving precise task-driven formations, coping with sensing and communication constraints, and ensuring scalability in dense or uncertain environments. These limitations indicate that pigeon-inspired approaches may need to be complemented with optimization-based, graph-theoretic, or learning-driven methods to fully support complex real-world UAV swarm applications.

8. Conclusions and discussions

Collective behavior is a pervasive phenomenon in both animal ecology and cell biology, where individuals within a group coordinate their actions to achieve common goals [6,21]. Understanding how such coordination emerges in complex systems has profound implications and can inform the development of advanced technologies in robotics, swarm intelligence, and autonomous systems. Network science has proven to be a powerful tool for studying these systems, offering insights into how the structural properties of networks influence collective dynamics [413,414]. By analyzing the intricate relationships between network topology and behavior, we can gain a deeper understanding of the mechanisms that drive coordination in both ecological and cellular contexts. Therefore, in this review, we have examined the interplay between network structure and the emergence of collective behavior.

After highlighting the diverse manifestations of collective behavior in animal and cellular systems, this review has presented both microscopic and macroscopic modeling approaches aimed at capturing their underlying dynamics. From a network science perspective, we have emphasized the pivotal role of network topology in shaping the coordination, stability, and adaptability of collective behavior. We have further explored how information transmission is influenced by noise, time delays, and intentional attacks, and how these factors modulate collective dynamics. The processes of decision-making and the emergence of collective intelligence were also discussed, with particular attention paid to the ways in which local interactions among individuals give rise to effective group-level decisions. Finally, we reviewed practical applications of collective behavior, demonstrating how bio-inspired principles of collective behavior can enhance the performance of multi-robot systems and UAV coordination. Taken together, this review offers new perspectives for understanding collective behavior in both natural and artificial systems and highlights its broad potential for real-world applications.

The diverse collective phenomena observed across animal ecology and cell biology are increasingly understood to arise from a common set of organizing principles [204,322,330]. In both domains, information transmission, collective decision-making and robustness emerge from local interactions among individuals or cells, shaped by structured and time-varying patterns of connectivity [110,167,236,327]. This perspective naturally motivates a unified, network-based framework for comparing collective dynamics across biological scales. From this viewpoint, differences in physical substrates and characteristic length scales do not preclude fundamental commonalities in the underlying collective dynamics. Rather, coordinated behavior in both animals and cells arises through local interactions coupled by temporal connectivity, enabling groups to integrate information, coordinate motion or migration, and maintain coherence under uncertainty [6,54,151]. Biological differences primarily influence how coordination is physically implemented—through sensory-mediated interactions in animal groups [2,49] and through biochemical or mechanical coupling in cellular systems [167]—while the network-level functional roles that support collective dynamics remain largely conserved.

This unifying perspective links collective behavior across three interconnected levels of description: local interaction rules, network architecture, and emergent collective states. At the microscopic level, collective dynamics are governed by local interaction rules that specify how individuals or cells respond to their neighbours and to external cues. In animal collectives, these rules typically involve attraction–repulsion interactions, alignment, and selective attention to neighbours, modulated by sensory constraints such as limited fields of view and finite reaction delays [31,49]. In cellular collectives, analogous local rules are implemented through adhesion, contact inhibition, chemotaxis and mechanical coupling, with information transmitted via biochemical signaling and force propagation [6,57,159]. Despite these mechanistic differences, strikingly similar collective patterns emerge across the two domains. Local coupling can suppress fluctuations, whether through alignment interactions in animal groups or junctional and mechanical coupling in tissues. Weak directional cues can be amplified into coherent collective motion or migration, as seen in minority-informed navigation in animal groups and chemotactic or mechanotactic biases in cellular systems. Moreover, nonlinear local responses can give rise to threshold-like collective switching, manifesting as quorum responses in animal collectives or as biochemical and mechanical thresholds in tissues [54,158,197,327,345].

At the mesoscopic level, collective behavior is shaped by the structure and dynamics of the interaction network—that is, by who interacts with whom, with what strength, and over what timescales [204]. In animal groups, interaction networks may be organized by spatial proximity, social relationships, leadership hierarchies or topological interaction rules, and often evolve dynamically as groups move and reorganize [71,73]. In cellular systems, connectivity is defined by contact networks, junctional coupling, and mechanical or biochemical pathways, all of which are actively remodeled during processes such as collective migration, growth and morphogenesis [110,167]. Crucially, these interaction networks are rarely static. Both animal and cellular collectives exhibit temporal connectivity, in which links continuously appear, disappear or change weight as individuals move, respond to signals, or remodel their local environment [236,243]. Rather than being a secondary complication, such temporal variability often constitutes a central element of collective function, shaping the speed and reliability of information transmission, the emergence of coherent motion, and the robustness of coordinated responses to perturbations [238].

At the macroscopic level, the interplay between local interaction rules and network structure gives rise to emergent collective states and functional outcomes. In animal groups, these manifest as alignment and polarization, milling, collective navigation, coordinated escape, and group-level decision-making [322,375]. In cellular systems, emergent behaviors include collective migration, wound closure, and developmental patterning [6,108]. Strikingly, many of these emergent patterns can be quantified using a common set of dynamical descriptors. Metrics such as order parameters, correlation lengths, response times, propagation speeds, and robustness measures (including resilience to noise, delays, or perturbations) provide a shared quantitative framework. This convergence suggests that tools from network science and statistical physics offer a unified language for comparing collective dynamics across biological scales [54,167,203].

These cross-scale parallels naturally raise a deeper question: why do animal groups and cellular assemblies, despite their different biological mechanisms, often converge on similar ways of coordinating? From an evolutionary perspective, collective behavior across biological scales does not arise solely to achieve coordination, but rather to solve recurrent ecological challenges that directly influence survival and fitness. Among the most fundamental of these tasks are the reliable localization of food sources, the rapid avoidance of predators or harmful conditions, and the minimization of energetic expenditure under persistent environmental uncertainty [8,34,199,252]. These challenges recur across organismal and cellular systems, despite their vastly different physical and biological substrates.

At the organismal scale, collective foraging allows animal groups to pool noisy sensory information to detect weak or spatially extended resource gradients, while coordinated motion and rapid alignment enable fast collective responses to predation threats [252,415,416]. At the cellular scale, analogous pressures arise during chemotaxis, tissue morphogenesis, and immune responses, where groups of cells must collectively detect biochemical cues, respond coherently to stress or damage, and maintain functional integrity at minimal metabolic cost [6,383]. In both cases, evolution tunes interaction strengths, response thresholds, and network connectivity to amplify relevant signals while suppressing noise.

Crucially, energetic efficiency constrains these solutions [74,327]. Strong or global coupling can accelerate information transfer, but incurs metabolic and communication costs; sparse or local interactions conserve energy but risk fragmentation. Evolution therefore favors decentralized, dynamically reconfigurable networks that balance responsiveness, robustness, and efficiency. The resulting collective strategies—distributed sensing, nonlinear decision thresholds, and adaptive connectivity—represent evolutionarily stable solutions to shared ecological challenges, explaining why animal collectives and cellular assemblies converge on similar forms of coordination despite operating at different biological scales.

From this perspective, the conceptual and dynamical features highlighted in this review—temporal connectivity, distributed decision-making, and resilience to perturbations—are unlikely to be mere coincidences across scales. They likely reflect convergent solutions to a common challenge: coordinating effectively in noisy, resource-limited environments without central control. This evolutionary and network-based viewpoint points to clear directions for future research. A central goal is to uncover the universal principles and mechanisms underlying collective dynamics. With advances in high-resolution, multimodal, and long-duration data collection, principled model selection and robust reconstruction of interaction networks have become increasingly feasible and necessary to link observed dynamics to underlying mechanisms. At the same time, AI and data-driven methods provide unprecedented tools to infer behavioral rules, capture nonlinear and high-dimensional dynamics, and enable predictive modeling. These capabilities make it timely to study open systems with individual turnover and to investigate cooperation and coordination under energetic–informational constraints, revealing universal principles and informing the design of bio-inspired collectives. In the following, we outline several concrete directions for future research.

With the rapid growth of multimodal, multiscale, and long-duration collective motion data, developing principled approaches for selecting models that connect data to mechanism has emerged as an important research direction. Rapid advances in imaging, tracking, and computer vision have generated unprecedented spatiotemporal data on collective behavior across animal groups and cellular assemblies. Yet, despite this abundance of data, identifying which modeling framework best captures the underlying interaction mechanisms remains an open challenge. Numerous models—ranging from alignment-based dynamics to attraction–repulsion schemes—have been proposed [49,50,54,140], but their relative validity is often difficult to assess empirically. This difficulty is amplified by partial observability, strong stochasticity, and the fact that distinct microscopic interaction rules can produce similar macroscopic patterns, severely limiting model identifiability and complicating model comparison in collective systems. Although model selection is a well-established task in statistics [417], and has been extensively applied in ecology [418], engineering [419], and epidemiology [420], it remains comparatively underdeveloped in the context of collective animal and cellular behavior. Developing systematic model-comparison pipelines that integrate standardized datasets, uncertainty-aware parameter inference, and predictive validation under noise and partial observability therefore represents a critical avenue for future research.

The reconstruction of interaction networks that underpin collective dynamics remains a central challenge. Across ecological, cellular, and social systems, network structure profoundly shapes system-level behavior [214–216]. The increasing availability of high-resolution temporal and spatial data now enables inference of these networks using advanced mathematical and statistical approaches [421]. Yet, principled network reconstruction remains hampered by noise, temporal variability, and heterogeneity, and existing methods often conflate correlation with causation [422]. Crucially, collective behavior observed over long time scales can differ qualitatively from that inferred under static or short-time assumptions: interaction networks may reorganize as population structure evolves, while leadership and social influence can shift across temporal scales. Failing to account for this temporal dimension fundamentally limits our understanding of collective dynamics, as demonstrated by long-term studies linking network structure to kinship and familiarity [195], and by analyses showing that different individuals emerge as leaders at different temporal resolutions [344]. Developing robust inference frameworks that connect observed collective dynamics to underlying interaction topologies, explicitly account for temporal persistence and network evolution, and reveal latent variables is therefore essential. Such advances

are critical for bridging theory and experiment, enabling predictive models of complex systems, and guiding targeted interventions. In this sense, reconstructing interaction networks lies at the heart of understanding how network structure shapes collective behavior.

The rapid advancement of artificial intelligence provides a novel, data-driven perspective for studying collective behavior, offering powerful new tools and opportunities to uncover underlying mechanisms, particularly in capturing nonlinear, high-dimensional, and time-varying patterns [423]. Unlike traditional models, AI-based approaches can autonomously infer behavioral rules and interaction motifs from large-scale empirical and simulated datasets, delivering both mechanistic insight and practical applications [424,425]. Crucially, these methods enable predictive modeling, allowing researchers to anticipate system trajectories, assess stability, and design targeted interventions. With biological and ecological systems increasingly accessible through high-resolution temporal and spatial data, and analytical techniques—from statistical inference to machine learning—continuing to evolve [426], an unprecedented opportunity arises to reveal the fundamental principles governing collective behavior.

A particularly important frontier is to move from closed, conserved-number descriptions of collective behavior to open collective systems in which individuals are continuously born, die, divide, or enter and leave the group. Most existing frameworks assume fixed population sizes, overlooking how demographic flux influences system evolution [49,54]. In microbial and cellular communities, birth–death dynamics not only occur frequently but can also stabilize or generate patterns. Incorporating these dynamics reveals novel behaviors and scaling laws [427,428], exemplified by the concept of "Malthusian flocks", which exhibit critical phenomena distinct from traditional conserved-number models. This motivates the development of collective dynamics frameworks that explicitly capture individual turnover, particularly when combined with network-based and data-driven approaches that can track how turnover continuously reshapes interaction structure and density over time.

Another promising future direction is the development of unified frameworks that integrate theory, data-driven modeling, and experiments to understand the emergence of collective cooperation [429–432]. When individuals have access only to local information and adapt their behavior based on local feedback, cooperation can still emerge, yet it may become unstable or collapse under certain conditions. While data-driven approaches are increasingly effective at inferring individual behavioral rules and predicting system-level dynamics, their full potential lies in providing controllable platforms to systematically explore how noise, changes in interaction networks, and individual turnover shape cooperative behavior. By combining these approaches with mechanism-oriented theoretical analysis, it is possible to integrate feedback at the individual level with collective-scale feedback, identify thresholds governing the emergence, stability, and collapse of cooperation, and explore whether these principles hold across different systems, scales, and structures.

Understanding the resilience of collective coordination under strong disturbances and adversarial conditions remains a major challenge. While self-organized collective motion is relatively well understood in idealized or weakly perturbed settings [54,327], real collectives operate in noisy, fluctuating, and sometimes hostile environments, where coordination can fail and must be actively maintained [433–435]. Failures can arise when interaction links are broken, information propagation is impeded, or influence concentrates on a few bottleneck individuals [313]. Future research should aim to identify common failure modes and the mechanisms that enhance resilience—such as redundant information pathways, adaptive network reorganization, and rapid local feedback—and connect these to measurable network features and dynamical indicators to predict collapse and design robust, functional collectives.

Future research should focus on understanding how multi-species collectives, often characterized by rich population structure, achieve coordinated behavior and reliable collective decisions despite differences in sensory modalities, interaction rules, and behavioral tendencies. While most studies have focused on single-species groups, real-world collectives often involve multiple species or distinct agent types. Field studies of mixed-species bird flocks, for example, show that individuals can exploit heterospecific foraging information, with certain species playing a disproportionately large role in information transmission [436]. Cohesion is maintained through stable, non-random social associations influenced by dominance hierarchies and body size [437], and coordinated responses can emerge even when species rely on partially distinct local decision heuristics [438]. These observations indicate that population structure—shaped by species composition, role differentiation, and asymmetric influence—plays a central role in mediating information flow and collective coordination [439]. Addressing this challenge requires models that accommodate species-specific interaction and decision rules, together with inference methods to quantify cross-species influence—identifying key information brokers, measuring information flow between species, and tracking how these contributions shift across ecological or social contexts.

Finally, collective coordination is not cost-free: achieving robust and responsive behavior typically requires both energetic and informational investment, highlighting the need to study efficiency–robustness trade-offs explicitly. Energetic efficiency and cost constraints are likely central to shaping collective dynamics and may also provide a unifying link between biological systems and engineered swarms [440,441]. While collective motion inherently incurs energetic expenditure, biological systems such as fish schools, bird flocks, and cellular assemblies often achieve remarkable coordination with high efficiency. A key open question is whether these behaviors can be captured by effective cost functions that balance energy use against robustness, responsiveness, and information flow under noise and environmental variability. Identifying these constraints and the resulting trade-offs could bridge biological optimization with physically grounded principles of collective organization, inform the design of efficient artificial intelligent systems, and provide insights for the development of intelligent algorithms.

Declaration of competing interest

The authors declare the following financial interests/personal relationships which may be considered as potential competing interests:

Yongzheng Sun reports financial support was provided by National Natural Science Foundation of China. Yongzheng Sun reports financial support was provided by China Scholarship Council. Yongzheng Sun reports financial support was provided by Shenzhen

Science and Technology Program. Yongzheng Sun reports was provided by Fundamental Research Funds for the Central Universities. If there are other authors, they declare that they have no known competing financial interests or personal relationships that could have appeared to influence the work reported in this paper.

Acknowledgements

We gratefully acknowledge Prof. Tamás Vicsek and Dr. Yuan Yin for valuable discussions and constructive comments during the revision of this review. This work was supported by the National Natural Science Foundation of China (Grant No. 12271519), the China Scholarship Council (Grant No. 202306420026), the Shenzhen Science and Technology Program (Grant No. JCYJ20240813101300001), and the Fundamental Research Funds for the Central Universities (Grant Nos. 2023ZDYQ11005 and 2024KYJD2002). For the purpose of open access, the authors have applied a CC BY public copyright licence to any author accepted manuscript arising from this submission.

References

[1] Delcourt J, Bode N WF, Denoël M. Collective vortex behaviors: diversity, proximate, and ultimate causes of circular animal group movements. Q Rev Biol 2016;91(1):1–24.
[2] Ballerini M, Cabibbo N, Candelier R, Cavagna A, Cisbani E, Giardina I, et al. Empirical investigation of starling flocks: a benchmark study in collective animal behaviour. Anim Behav 2008;76(1):201–15.
[3] Cavagna A, Giardina I, Grigera TS. The physics of flocking: correlation as a compass from experiments to theory. Phys Rep 2018;728:1–62.
[4] Parrish JK, Edelstein-Keshet L. Complexity, pattern, and evolutionary trade-offs in animal aggregation. Science 1999;284(5411):99–101.
[5] Couzin ID, Franks NR. Self-organized lane formation and optimized traffic flow in army ants. Proc R Soc Lond Ser B Biol Sci 2003;270(1511):139–46.
[6] Friedl P, Gilmour D. Collective cell migration in morphogenesis, regeneration and cancer. Nat Rev Mol Cell Biol 2009;10(7):445–57.
[7] Clark AG, Vignjevic DM. Modes of cancer cell invasion and the role of the microenvironment. Curr Opin Cell Biol 2015;36:13–22.
[8] Friedl P, Alexander S. Cancer invasion and the microenvironment: plasticity and reciprocity. Cell 2011;147(5):992–1009.
[9] Jayathilake PG, Gupta P, Li B, Madsen C, Oyebamiji O, González-Cabaleiro R, et al. A mechanistic individual-based model of microbial communities. PLoS ONE 2017;12(8):e0181965.
[10] Nagarajan K, Ni C, Lu T. Agent-based modeling of microbial communities. ACS Synth Biol 2022;11(11):3564–74.
[11] Chen C, Liu S, Shi X-q, Chaté H, Wu Y. Weak synchronization and large-scale collective oscillation in dense bacterial suspensions. Nature 2017;542(7640):210–14.
[12] Helbing D, Farkas I, Vicsek T. Simulating dynamical features of escape panic. Nature 2000;407(6803):487–90.
[13] Colaiori F, Castellano C. Interplay between media and social influence in the collective behavior of opinion dynamics. Phys Rev E 2015;92(4):042815.
[14] Li L, Jiao S, Shen Y, Liu B, Pedrycz W, Chen Y, et al. A two-stage consensus model for large-scale group decision-making considering dynamic social networks. Inf Fusion 2023;100:101972.
[15] Luo Q, Duan H. Distributed UAV flocking control based on homing pigeon hierarchical strategies. Aerosp Sci Technol 2017;70:257–64.
[16] Han W, Wang J, Wang Y, Xu B. Multi-UAV flocking control with a hierarchical collective behavior pattern inspired by sheep. IEEE Trans Aerosp Electron Syst 2024;60(2):2267–76.
[17] Dorigo M, Theraulaz G, Trianni V. Swarm robotics: past, present, and future [point of view]. Proc IEEE 2021;109(7):1152–65.
[18] Ko H, Lauder G, Nagpal R. The role of hydrodynamics in collective motions of fish schools and bioinspired underwater robots. J R Soc Interf 2023;20(207):20230357.
[19] De R, Chakraborty D. Collective motion: influence of local behavioural interactions among individuals. J Biosci 2022;47(3):48.
[20] Miguel MC, Parley JT, Pastor-Satorras R. Effects of heterogeneous social interactions on flocking dynamics. Phys Rev Lett 2018;120(6):068303.
[21] Vicsek T, Zafeiris A. Collective motion. Phys Rep 2012;517(3–4):71–140.
[22] Liu Q-X, Rietkerk M, Herman P MJ, Piersma T, Fryxell JM, van de Koppel J. Phase separation driven by density-dependent movement: a novel mechanism for ecological patterns. Phys Life Rev 2016;19:107–21.
[23] Ouellette NT. A physics perspective on collective animal behavior. Phys Biol 2022;19(2):021004.
[24] Amaral L AN, Ottino JM. Complex networks: augmenting the framework for the study of complex systems. Eur Phys J B 2004;38:147–62.
[25] Strogatz SH. Exploring complex networks. Nature 2001;410(6825):268–76.
[26] Ji P, Wang Y, Peron T, Li C, Nagler J, Du J. Structure and function in artificial, zebrafish and human neural networks. Phys Life Rev 2023;45:74–111.
[27] Papo D, Buldú JM. Does the brain behave like a (complex) network? i. dynamics. Phys Life Rev 2024;48:47–98.
[28] Jhawar J, Guttal V. Noise-induced effects in collective dynamics and inferring local interactions from data. Philos Trans R Soc B 2020;375(1807):20190381.
[29] Pimentel JA, Aldana M, Huepe C, Larralde H. Intrinsic and extrinsic noise effects on phase transitions of network models with applications to swarming systems. Phys Rev E-Stat Nonlinear Soft Matter Phys 2008;77(6):061138.
[30] Geiß D, Kroy K, Holubec V. Signal propagation and linear response in the delay vicsek model. Phys Rev E 2022;106(5):054612.
[31] Sun Y, Li W, Li L, Wen G, Azaele S, Lin W. Delay-induced directional switches and mean switching time in swarming systems. Phys Rev Res 2022;4(3):033054.
[32] Yates CA, Erban R, Escudero C, Couzin ID, Buhl C, Kevrekidis IG, et al. Inherent noise can facilitate coherence in collective swarm motion. Proc Natl Acad Sci 2009;106(14):5464–9.
[33] Chen H, Hou Z. Noise-induced vortex reversal of self-propelled particles. Phys Rev E 2012;86(4):041122.
[34] Biancalani T, Dyson L, McKane AJ. Noise-induced bistable states and their mean switching time in foraging colonies. Phys Rev Lett 2014;112(3):038101.
[35] Dyer J RG, Johansson A, Helbing D, Couzin ID, Krause J. Leadership, consensus decision making and collective behaviour in humans. Philos Trans R Soc B Biol Sci 2009;364(1518):781–9.
[36] Dussutour A, Beekman M, Nicolis SC, Meyer B. Noise improves collective decision-making by ants in dynamic environments. Proc R Soc B Biol Sci 2009;276(1677):4353–61.
[37] Couzin ID, Ioannou CC, Demirel G, Gross T, Torney CJ, Hartnett A, et al. Uninformed individuals promote democratic consensus in animal groups. Science 2011;334(6062):1578–80.
[38] Pasquaretta C, Battesti M, Klenschi E, Bousquet C AH, Sueur C, Mery F. How social network structure affects decision-making in drosophila melanogaster. Proc R Soc B Biol Sci 2016;283(1826):20152954.
[39] Oscar L, Li L, Gorbonos D, Couzin ID, Gov NS. A simple cognitive model explains movement decisions in zebrafish while following leaders. Phys Biol 2023;20(4):045002.
[40] Tu S-Y, Sayed AH. Distributed decision-making over adaptive networks. IEEE Trans Signal Process 2013;62(5):1054–69.
[41] Bazazi S, Pfennig KS, Handegard NO, Couzin ID. Vortex formation and foraging in polyphenic spadefoot toad tadpoles. Behav Ecol Sociobiol 2012;66:879–89.
[42] Anwar MS, Sar GK, Perc M, Ghosh D. Collective dynamics of swarmalators with higher-order interactions. Commun Phys 2024;7(1):59.
[43] Escudero C, Yates CA, Buhl C, Couzin ID, Erban R, Kevrekidis IG, et al. Ergodic directional switching in mobile insect groups. Phys Rev E-Stat Nonlinear Soft Matter Phys 2010;82(1):011926.
[44] Xiao R, Li W, Zhao D, Sun Y. Directional switches in network-organized swarming systems with delay. Chaos Interdiscip J Nonlinear Sci 2023;33(4):043143.

[45] Strömbom D. Collective motion from local attraction. J Theor Biol 2011;283(1):145–51.
[46] Hernandez-Ortiz JP, Stoltz CG, Graham MD. Transport and collective dynamics in suspensions of confined swimming particles. Phys Rev Lett 2005;95(20):204501.
[47] Nishiguchi D, Shiratani S, Takeuchi KA, Aranson IS. Vortex reversal is a precursor of confined bacterial turbulence. Proc Natl Acad Sci 2025;122(11):e2414446122.
[48] Reynolds CW. Flocks, herds and schools: a distributed behavioral model. In: Proceedings of the 14th annual conference on computer graphics and interactive techniques. 1987, p. 25–34.
[49] Couzin ID, Krause J, James R, Ruxton GD, Franks NR. Collective memory and spatial sorting in animal groups. J Theor Biol 2002;218(1):1–11.
[50] Cucker F, Smale S. Emergent behavior in flocks. IEEE Trans Automat Contr 2007;52(5):852–62.
[51] Pearce D JG, Miller AM, Rowlands G, Turner MS. Role of projection in the control of bird flocks. Proc Natl Acad Sci 2014;111(29):10422–6.
[52] Bastien R, Romanczuk P. A model of collective behavior based purely on vision. Sci Adv 2020;6(6):eaay0792.
[53] Herbert-Read JE, Perna A, Mann RP, Schaerf TM, Sumpter D JT, Ward A JW. Inferring the rules of interaction of shoaling fish. Proc Natl Acad Sci 2011;108(46):18726–31.
[54] Vicsek T, Czirók A, Ben-Jacob E, Cohen I, Shochet O. Novel type of phase transition in a system of self-driven particles. Phys Rev Lett 1995;75(6):1226.
[55] Buhl C, Sumpter D JT, Couzin ID, Hale JJ, Despland E, Miller ER, et al. From disorder to order in marching locusts. Science 2006;312(5778):1402–6.
[56] Rasa G, Baker RE, Kulesa PM, Maini PK. Modelling collective cell migration: neural crest as a model paradigm. J Math Biol 2020;80(1):481–504.
[57] Carmona-Fontaine C, Matthews HK, Kuriyama S, Moreno M, Dunn GA, Parsons M, et al. Contact inhibition of locomotion in vivo controls neural crest directional migration. Nature 2008;456(7224):957–61.
[58] Baker RE, Crossley RM, Falco C, Martina-Perez SF. Modelling collective cell migration in a data-rich age: challenges and opportunities for data-driven modelling.2025; arXiv preprint arXiv:250419974 .
[59] Japaridze A, Struijk V, Swamy K, Rosłoń I, Shoshani O, Dekker C, et al. Synchronization of e. coli bacteria moving in coupled microwells. Small 2025;21(3):2407832.
[60] Lega J, Passot T. Hydrodynamics of bacterial colonies: a model. Phys Rev E 2003;67(3):031906.
[61] Cremer J, Segota I, Yang C-y, Arnoldini M, Sauls JT, Zhang Z, et al. Effect of flow and peristaltic mixing on bacterial growth in a gut-like channel. Proc Natl Acad Sci 2016;113(41):11414–19.
[62] Bajec IL, Heppner FH. Organized flight in birds. Anim Behav 2009;78(4):777–89.
[63] Mirzaeinia A, Hassanalian M, Lee K, Mirzaeinia M. Energy conservation of v-shaped swarming fixed-wing drones through position reconfiguration. Aerosp Sci Technol 2019;94:105398.
[64] Cristiani E, Menci M, Papi M, Brafman L. An all-leader agent-based model for turning and flocking birds. J Math Biol 2021;83(4):45.
[65] Potts WK. The chorus-line hypothesis of manoeuvre coordination in avian flocks. Nature 1984;309(5966):344–5.
[66] Nagy M, Ákos Z, Biro D, Vicsek T. Hierarchical group dynamics in pigeon flocks. Nature 2010;464(7290):890–3.
[67] Nagy M, Vásárhelyi G, Pettit B, Roberts-Mariani I, Vicsek T, Biro D. Context-dependent hierarchies in pigeons. Proc Natl Acad Sci 2013;110(32):13049–54.
[68] Jolles JW, King AJ, Manica A, Thornton A. Heterogeneous structure in mixed-species corvid flocks in flight. Anim Behav 2013;85(4):743–50.
[69] King AJ, Sueur C, Huchard E, Cowlishaw G. A rule-of-thumb based on social affiliation explains collective movements in desert baboons. Anim Behav 2011;82(6):1337–45.
[70] Moussaïd M, Perozo N, Garnier S, Helbing D, Theraulaz G. The walking behaviour of pedestrian social groups and its impact on crowd dynamics. PLoS ONE 2010;5(4):e10047.
[71] Croft DP, James R, Krause J. Exploring animal social networks. Princeton University Press; 2008.
[72] Hemelrijk CK, Kunz H. Density distribution and size sorting in fish schools: an individual-based model. Behav Ecol 2005;16(1):178–87.
[73] Bode N WF, Wood AJ, Franks DW. The impact of social networks on animal collective motion. Anim Behav 2011;82(1):29–38.
[74] Ling H, Mclvor GE, van der Vaart K, Vaughan RT, Thornton A, Ouellette NT. Costs and benefits of social relationships in the collective motion of bird flocks. Nat Ecol Evol 2019;3(6):943–8.
[75] Storms RF, Carere C, Zoratto F, Hemelrijk CK. Complex patterns of collective escape in starling flocks under predation. Behav Ecol Sociobiol 2019;73:1–10.
[76] Carere C, Montanino S, Moreschini F, Zoratto F, Chiarotti F, Santucci D, et al. Aerial flocking patterns of wintering starlings, sturnus vulgaris, under different predation risk. Anim Behav 2009;77(1):101–7.
[77] Olson RS, Hintze A, Dyer FC, Knoester DB, Adami C. Predator confusion is sufficient to evolve swarming behaviour. J R Soc Interf 2013;10(85):20130305.
[78] Papadopoulou M, Hildenbrandt H, Sankey D WE, Portugal SJ, Hemelrijk CK. Emergence of splits and collective turns in pigeon flocks under predation. R Soc Open Sci 2022;9(2):211898.
[79] Papadopoulou M, Hildenbrandt H, Storms RF, Carere C, Verhulst S, Hemelrijk CK. Mechanisms driving collective escape patterns in starling flocks. BioRxiv 2024;:2024–10 https://doi.org/10.1101/2024.10.27.620514.
[80] Kasumyan AO, Pavlov DS. Evolution of schooling behavior in fish. J Ichthyol 2018;58:670–8.
[81] Lopez U, Gautrais J, Couzin ID, Theraulaz G. From behavioural analyses to models of collective motion in fish schools. Interf Focus 2012;2(6):693–707.
[82] Ruxton GD, et al. Living in groups. Oxford University Press; 2002.
[83] Pavlov DS, Kasumyan AO, et al. Patterns and mechanisms of schooling behavior in fish: a review. J Ichthyol 2000;40(2):S163.
[84] Turesson H, Brönmark C. Predator–prey encounter rates in freshwater piscivores: effects of prey density and water transparency. Oecologia 2007;153:281–90.
[85] Krausz RR. Living in groups. Trans Anal J 2013;43(4):366–74.
[86] Weihs D. Hydromechanics of fish schooling. Nature 1973;241(5387):290–1.
[87] Li L, Nagy M, Graving JM, Bak-Coleman J, Xie G, Couzin ID. Vortex phase matching as a strategy for schooling in robots and in fish. Nat Commun 2020;11(1):5408.
[88] Li L, Ravi S, Xie G, Couzin ID. Using a robotic platform to study the influence of relative tailbeat phase on the energetic costs of side-by-side swimming in fish. Proc R Soc A 2021;477(2249):20200810.
[89] Fang D, Huang Z, Zhang J, Hu Z, Tan J. Flow pattern investigation of bionic fish by immersed boundary–lattice boltzmann method and dynamic mode decomposition. Ocean Eng 2022;248:110823.
[90] Fang D, Zhang J, Huang Z. Modal analysis on mechanism of bionic fish swimming by dynamic mode decomposition. Ocean Eng 2023;273:113897.
[91] Becco C, Vandewalle N, Delcourt J, Poncin P. Experimental evidences of a structural and dynamical transition in fish school. Physica A 2006;367:487–93.
[92] Tunstrøm K, Katz Y, Ioannou CC, Huepe C, Lutz MJ, Couzin ID. Collective states, multistability and transitional behavior in schooling fish. PLoS Comput Biol 2013;9(2):e1002915.
[93] Jhawar J, Morris RG, Amith-Kumar UR, Danny Raj M, Rogers T, Rajendran H, et al. Noise-induced schooling of fish. Nat Phys 2020;16(4):488–93.
[94] Franks NR, Gomez N, Goss S, Deneubourg J-L. The blind leading the blind in army ant raid patterns: testing a model of self-organization (hymenoptera: formicidae). J Insect Behav 1991;4:583–607.
[95] Biesmeijer JC, Seeley TD. The use of waggle dance information by honey bees throughout their foraging careers. Behav Ecol Sociobiol 2005;59:133–42.
[96] Beekman M, Sumpter D JT, Ratnieks F LW. Phase transition between disordered and ordered foraging in pharaoh's ants. Proc Natl Acad Sci 2001;98(17):9703–6.
[97] Sayin S, Couzin-Fuchs E, Petelski I, Günzel Y, Salahshour M, Lee C-Y, et al. The behavioral mechanisms governing collective motion in swarming locusts. Science 2025;387(6737):995–1000.
[98] Néda Z, Ravasz E, Brechet Y, Vicsek T, Barabási A-L. The sound of many hands clapping. Nature 2000;403(6772):849–50.
[99] Néda Z, Ravasz E, Vicsek T, Brechet Y, Barabási A-L. Physics of the rhythmic applause. Phys Rev E 2000;61(6):6987.
[100] Sun Y, Ruan J, Li W. Synchronization of the applause with leaders. Acta Phys Sin 2008;57(12):7547–54.
[101] Proksch S, Reeves M, Spivey M, Balasubramaniam R. Coordination dynamics of multi-agent interaction in a musical ensemble. Sci Rep 2022;12(1):421.

[102] Lender A, Perdikis D, Gruber W, Lindenberger U, Müller V. Dynamics in interbrain synchronization while playing a piano duet. Ann NY Acad Sci 2023;1530(1):124–37.
[103] Dyer J RG, Ioannou CC, Morrell LJ, Croft DP, Couzin ID, Waters DA, et al. Consensus decision making in human crowds. Anim Behav 2008;75(2):461–70.
[104] Moussaïd M, Helbing D, Theraulaz G. How simple rules determine pedestrian behavior and crowd disasters. Proc Natl Acad Sci 2011;108(17):6884–8.
[105] Sieben A, Schumann J, Seyfried A. Collective phenomena in crowds-where pedestrian dynamics need social psychology. PLoS ONE 2017;12(6):e0177328.
[106] Gu F, Guiselin B, Bain N, Zuriguel I, Bartolo D. Emergence of collective oscillations in massive human crowds. Nature 2025;638(8049):112–19.
[107] Srinivasan S, Kaplan CN, Mahadevan L. A multiphase theory for spreading microbial swarms and films. Elife 2019;8:e42697.
[108] Maini PK, McElwain DLS, Leavesley DI. Traveling wave model to interpret a wound-healing cell migration assay for human peritoneal mesothelial cells. Tissue Eng 2004;10(3–4):475–82.
[109] McDougall S, Dallon J, Sherratt J, Maini P. Fibroblast migration and collagen deposition during dermal wound healing: mathematical modelling and clinical implications. Philos Trans R Soc A Math Phys Eng Sci 2006;364(1843):1385–405.
[110] Schumacher LJ, Kulesa PM, McLennan R, Baker RE, Maini PK. Multidisciplinary approaches to understanding collective cell migration in developmental biology. Open Biol 2016;6(6):160056.
[111] Vaughan RB, Trinkaus JP. Movements of epithelial cell sheets in vitro. J Cell Sci 1966;1(4):407–13.
[112] Friedl P. Prespecification and plasticity: shifting mechanisms of cell migration. Curr Opin Cell Biol 2004;16(1):14–23.
[113] Ghysen A, Dambly-Chaudière C. The lateral line microcosmos. Genes & Development 2007;21(17):2118–30.
[114] Landman KA, Simpson MJ, Newgreen DF. Mathematical and experimental insights into the development of the enteric nervous system and hirschsprung's disease. Develop Growth Differ 2007;49(4):277–86.
[115] Painter KJ, Bloomfield JM, Sherratt JA, Gerisch A. A nonlocal model for contact attraction and repulsion in heterogeneous cell populations. Bull Math Biol 2015;77:1132–65.
[116] Luparello C, Mauro M, Lazzara V, Vazzana M. Collective locomotion of human cells, wound healing and their control by extracts and isolated compounds from marine invertebrates. Molecules 2020;25(11):2471.
[117] Byrne HM, Alarcon T, Owen MR, Webb SD, Maini PK. Modelling aspects of cancer dynamics: a review. Philos Trans R Soc A Math Phys Eng Sci 2006;364(1843):1563–78.
[118] Smallbone K, Gatenby RA, Gillies RJ, Maini PK, Gavaghan DJ. Metabolic changes during carcinogenesis: potential impact on invasiveness. J Theor Biol 2007;244(4):703–13.
[119] Chen H-Y, Hsiao Y-T, Liu S-C, Hsu T, Woon W-Y, I L. Enhancing cancer cell collective motion and speeding up confluent endothelial dynamics through cancer cell invasion and aggregation. Phys Rev Lett 2018;121(1):018101.
[120] Yin Y, Waters SL, Baker RE. The influence of cell phenotype on collective cell invasion into the extracellular matrix. Bull Math Biol 2026;88(1):13.
[121] Pollacco JJ, Baker RE, Maini PK. Collective invasion: when does domain curvature matter?2024; arXiv preprint arXiv:240608291 .
[122] Liu Y, Suh K, Maini PK, Cohen DJ, Baker RE. Parameter identifiability and model selection for partial differential equation models of cell invasion. J R Soc Interf 2024;21(212):20230607.
[123] Mehta P, Gregor T. Approaching the molecular origins of collective dynamics in oscillating cell populations. Curr Opin Genet Develop 2010;20(6):574–80.
[124] Tu BP, McKnight SL. Metabolic cycles as an underlying basis of biological oscillations. Nat Rev Mol Cell Biol 2006;7(9):696–701.
[125] Hubaud A, Regev I, Mahadevan L, Pourquié O. Excitable dynamics and yap-dependent mechanical cues drive the segmentation clock. Cell 2017;171(3):668–82.
[126] Liu J, Prindle A, Humphries J, Gabalda-Sagarra M, Asally M, Lee D-yD, et al. Metabolic co-dependence gives rise to collective oscillations within biofilms. Nature 2015;523(7562):550–4.
[127] Tozzini V. Coarse-grained models for proteins. Curr Opin Struct Biol 2005;15(2):144–50.
[128] De A, Chen W, Li H, Wright JR, Lamendella R, Lukin DJ, et al. Bacterial swarmers enriched during intestinal stress ameliorate damage. Gastroenterology 2021;161(1):211–24.
[129] Celikkanat H, Şahin E. Steering self-organized robot flocks through externally guided individuals. Neur Comput Appl 2010;19:849–65.
[130] Zhao H, Liu H, Leung Y-W, Chu X. Self-adaptive collective motion of swarm robots. IEEE Trans Autom Sci Eng 2018;15(4):1533–45.
[131] Bahaidarah M, Rekabi-Bana F, Marjanovic O, Arvin F. Swarm flocking using optimisation for a self-organised collective motion. Swarm Evol Comput 2024;86:101491.
[132] Mier-y Teran-Romero L, Forgoston E, Schwartz IB. Coherent pattern prediction in swarms of delay-coupled agents. IEEE Trans Rob 2012;28(5):1034–44.
[133] Forgoston E, Schwartz IB. Delay-induced instabilities in self-propelling swarms. Phys Rev E-Stat Nonlinear Soft Matter Phys 2008;77(3):035203.
[134] Dorigo M, Floreano D, Gambardella LM, Mondada F, Nolfi S, Baaboura T, et al. Swarmanoid: a novel concept for the study of heterogeneous robotic swarms. IEEE Rob Autom Magaz 2013;20(4):60–71.
[135] Szwaykowska K, Romero L M-y-T, Schwartz IB. Collective motions of heterogeneous swarms. IEEE Trans Autom Sci Eng 2015;12(3):810–18.
[136] Zhou X, Wen X, Wang Z, Gao Y, Li H, Wang Q, et al. Swarm of micro flying robots in the wild. Sci Rob 2022;7(66):eabm5954.
[137] Meng W, He Z, Su R, Yadav PK, Teo R, Xie L. Decentralized multi-UAV flight autonomy for moving convoys search and track. IEEE Trans Contr Syst Technol 2016;25(4):1480–7.
[138] Yao P, Xie Z, Ren P. Optimal UAV route planning for coverage search of stationary target in river. IEEE Trans Control Syst Technol 2017;27(2):822–9.
[139] Zhang G, Shang B, Chen Y, Moyes H. Smartcavedrone: 3d cave mapping using UAVs as robotic co-archaeologists. In: 2017 International conference on unmanned aircraft systems (ICUAS). IEEE; 2017, p. 1052–7.
[140] Qiu F, Hu X. Modeling group structures in pedestrian crowd simulation. Simul Modell Pract Theory 2010;18(2):190–205.
[141] Lukeman R, Li Y-X, Edelstein-Keshet L. Inferring individual rules from collective behavior. Proc Natl Acad Sci 2010;107(28):12576–80.
[142] Lukeman R. Ordering dynamics in collectively swimming surf scoters. J Theor Biol 2014;355:151–9.
[143] Katz Y, Tunstrøm K, Ioannou CC, Huepe C, Couzin ID. Inferring the structure and dynamics of interactions in schooling fish. Proc Natl Acad Sci 2011;108(46):18720–5.
[144] Ginelli F, Peruani F, Pillot M-H, Chaté H, Theraulaz G, Bon R. Intermittent collective dynamics emerge from conflicting imperatives in sheep herds. Proc Natl Acad Sci 2015;112(41):12729–34.
[145] Ha S-Y, Liu J-G. A simple proof of the cucker-smale flocking dynamics and mean-field limit. Commun Math Sci 2009;7(2):297–325.
[146] Motsch S, Tadmor E. A new model for self-organized dynamics and its flocking behavior. J Stat Phys 2011;144:923–47.
[147] Ha S-Y, Lee K, Levy D. Emergence of time-asymptotic flocking in a stochastic cucker-smale system. Commun Math Sci 2009;7(2):453–69.
[148] Ton TV, Linh N TH, Yagi A. Flocking and non-flocking behavior in a stochastic cucker–smale system. Anal Appl 2014;12(01):63–73.
[149] Ahn SM, Ha S-Y. Stochastic flocking dynamics of the cucker–smale model with multiplicative white noises. J Math Phys 2010;51(10):103301.
[150] Erban R, Haskovec J, Sun Y. A cucker–smale model with noise and delay. SIAM J Appl Math 2016;76(4):1535–57.
[151] Olfati-Saber R, Murray RM. Consensus problems in networks of agents with switching topology and time-delays. IEEE Trans Automat Contr 2004;49(9):1520–33.
[152] Tanner HG, Jadbabaie A, Pappas GJ. Flocking in fixed and switching networks. IEEE Trans Automat Contr 2007;52(5):863–8.
[153] Chakraborty D, Bhunia S, De R. Survival chances of a prey swarm: how the cooperative interaction range affects the outcome. Sci Rep 2020;10(1):8362.
[154] He S-Q, Yin X, Liang D, Chang Z, Xu G-K. Spontaneous oscillation in collective microswimmers: insights from a chiral self-propelled rod model. Phys Rev E 2025;111(1):014411.
[155] Pal S, Melnik R. Nonlocal models in biology and life sciences: sources, developments, and applications. Phys Life Rev 2025;53:24–75.
[156] Montell DJ. Morphogenetic cell movements: diversity from modular mechanical properties. Science 2008;322(5907):1502–5.
[157] Crossley RM, Johnson S, Tsingos E, Bell Z, Berardi M, Botticelli M, et al. Modeling the extracellular matrix in cell migration and morphogenesis: a guide for the curious biologist. Front Cell Dev Biol 2024;12:1354132.
[158] Szabó B, Szöllösi GJ, Gönci B, Jurányi Z, Selmeczi D, Vicsek T. Phase transition in the collective migration of tissue cells: experiment and model. Phys Rev E-Stat Nonlinear Soft Matter Phys 2006;74(6):061908.

[159] Arboleda-Estudillo Y, Krieg M, Stühmer J, Licata NA, Muller DJ, Heisenberg C-P. Movement directionality in collective migration of germ layer progenitors. Curr Biol 2010;20(2):161–9.
[160] Lu F, Zhong M, Tang S, Maggioni M. Nonparametric inference of interaction laws in systems of agents from trajectory data. Proc Natl Acad Sci 2019;116(29):14424–33.
[161] Zhong M, Miller J, Maggioni M. Data-driven discovery of emergent behaviors in collective dynamics. Physica D 2020;411:132542.
[162] Zhu Q, Ma H, Lin W. Detecting unstable periodic orbits based only on time series: when adaptive delayed feedback control meets reservoir computing. Chaos Interdiscip J Nonlinear Sci 2019;29(9).
[163] Gauthier DJ, Bollt E, Griffith A, Barbosa W AS. Next generation reservoir computing. Nat Commun 2021;12(1):5564.
[164] Li X, Zhu Q, Zhao C, Duan X, Zhao B, Zhang X, et al. Higher-order granger reservoir computing: simultaneously achieving scalable complex structures inference and accurate dynamics prediction. Nat Commun 2024;15(1):2506.
[165] Duan X-Y, Ying X, Leng S-Y, Kurths J, Lin W, Ma H-F. Embedding theory of reservoir computing and reducing reservoir network using time delays. Phys Rev Res 2023;5(2):L022041.
[166] Yan M, Huang C, Bienstman P, Tino P, Lin W, Sun J. Emerging opportunities and challenges for the future of reservoir computing. Nat Commun 2024;15(1):2056.
[167] Brückner DB, Broedersz CP. Learning dynamical models of single and collective cell migration: a review. Rep Prog Phys 2024;87(5):056601.
[168] Selmeczi D, Li L, Pedersen L II, Nrrelykke SF, Hagedorn PH, Mosler S, et al. Cell motility as random motion: a review: cell motility as random motion. Eur Phys J Spec Top 2008;157:1–15.
[169] Passucci G, Brasch ME, Henderson JH, Zaburdaev V, Manning ML. Identifying the mechanism for superdiffusivity in mouse fibroblast motility. PLoS Comput Biol 2019;15(2):e1006732.
[170] Zienkiewicz AK, Ladu F, Barton D AW, Porfiri M, Di Bernardo M. Data-driven modelling of social forces and collective behaviour in zebrafish. J Theor Biol 2018;443:39–51.
[171] Sarfati R, Peleg O. Chimera states among synchronous fireflies. Sci Adv 2022;8(46):eadd6690.
[172] Sarfati R, Hayes JC, Sarfati É, Peleg O. Spatio-temporal reconstruction of emergent flash synchronization in firefly swarms via stereoscopic 360-degree cameras. J R Soc Interf 2020;17(170):20200179.
[173] Bishwal J PN, et al. Estimation in interacting diffusions: continuous and discrete sampling. Appl Math 2011;2(9):1154–8.
[174] Gomes SN, Stuart AM, Wolfram M-T. Parameter estimation for macroscopic pedestrian dynamics models from microscopic data. SIAM J Appl Math 2019;79(4):1475–500.
[175] Della Maestra L, Hoffmann M. The LAN property for mckean–vlasov models in a mean-field regime. Stoch Process Appl 2023;155:109–46.
[176] Brunton SL, Proctor JL, Kutz JN. Discovering governing equations from data by sparse identification of nonlinear dynamical systems. Proc Natl Acad Sci 2016;113(15):3932–7.
[177] Messenger DA, Wheeler GE, Liu X, Bortz DM. Learning anisotropic interaction rules from individual trajectories in a heterogeneous cellular population. J R Soc Interf 2022;19(195):20220412.
[178] Raissi M, Perdikaris P, Karniadakis GE. Physics-informed neural networks: a deep learning framework for solving forward and inverse problems involving nonlinear partial differential equations. J Comput Phys 2019;378:686–707.
[179] Chen R TQ, Rubanova Y, Bettencourt J, Duvenaud DK. Neural ordinary differential equations. Adv Neural Inf Process Syst 2018;31.
[180] Lagergren JH, Nardini JT, Baker RE, Simpson MJ, Flores KB. Biologically-informed neural networks guide mechanistic modeling from sparse experimental data. PLoS Comput Biol 2020;16(12):e1008462.
[181] O'Loan OJ, Evans MR. Alternating steady state in one-dimensional flocking. J Phys A Math Gen 1999;32(8):L99.
[182] Raymond JR, Evans MR. Flocking regimes in a simple lattice model. Phys Rev E-Stat Nonlinear Soft Matter Phys 2006;73(3):036112.
[183] DEUTSCH A. Towards analyzing complex swarming patterns in biological systems with the help of lattice-gas cellular automata. J Biol Syst 1995;3(04):947–55.
[184] Deutsch A. Orientation-induced pattern formation: swarm dynamics in a lattice-gas automaton model. Int J Bifurcation Chaos 1996;6(09):1735–52.
[185] Bussemaker HJ, Deutsch A, Geigant E. Mean-field analysis of a dynamical phase transition in a cellular automaton model for collective motion. Phys Rev Lett 1997;78(26):5018.
[186] Deutsch A. A new mechanism of aggregation in a lattice-gas cellular automaton model. Math Comput Model 2000;31(4–5):35–40.
[187] Watts DJ, Strogatz SH. Collective dynamics of 'small-world'networks. Nature 1998;393(6684):440–2.
[188] Barahona M, Pecora LM. Synchronization in small-world systems. Phys Rev Lett 2002;89(5):054101.
[189] Wang XF, Chen G. Synchronization in small-world dynamical networks. Int J Bifurcation Chaos 2002;12(01):187–92.
[190] Barabási A-L, Albert R. Emergence of scaling in random networks. Science 1999;286(5439):509–12.
[191] Ojer J, Pastor-Satorras R. Flocking dynamics mediated by weighted social networks. Phys Rev E 2022;106(4):044601.
[192] Griffiths SW, Magurran AE. Schooling decisions in guppies (poecilia reticulata) are based on familiarity rather than kin recognition by phenotype matching. Behav Ecol Sociobiol 1999;45:437–43.
[193] Croft DP, Krause J, James R. Social networks in the guppy (poecilia reticulata). Proc R Soc Lond Ser B Biol Sci 2004;271(suppl_6):S516–S519.
[194] Croft DP, James R, Ward A, Botham MS, Mawdsley D, Krause J. Assortative interactions and social networks in fish. Oecologia 2005;143:211–19.
[195] Ozogány K, Kerekes V, Fülöp A, Barta Z, Nagy M. Fine-scale collective movements reveal present, past and future dynamics of a multilevel society in przewalski's horses. Nat Commun 2023;14(1):5096.
[196] Ward A JW, Schaerf TM, Burns A, Lizier JT, Crosato E, Prokopenko M, et al. Cohesion, order and information flow in the collective motion of mixed-species shoals. R Soc Open Sci 2018;5(12):181132.
[197] Atkinson S, Williams P. Quorum sensing and social networking in the microbial world. J R Soc Interf 2009;6(40):959–78.
[198] Ling H, Mclvor GE, van der Vaart K, Vaughan RT, Thornton A, Ouellette NT. Local interactions and their group-level consequences in flocking jackdaws. Proc R Soc B 2019;286(1906):20190865.
[199] Porfiri M, Abaid N, Garnier S. Socially driven negative feedback regulates activity and energy use in ant colonies. PLoS Comput Biol 2024;20(11):e1012623.
[200] Yan G, Ren J, Lai Y-C, Lai C-H, Li B. Controlling complex networks: how much energy is needed? Phys Rev Lett 2012;108(21):218703.
[201] Sun Y-Z, Leng S-Y, Lai Y-C, Grebogi C, Lin W. Closed-loop control of complex networks: a trade-off between time and energy. Phys Rev Lett 2017;119(19):198301.
[202] Dai H, Li W, Yang C, Wen G, Sun Y. Time and energy costs for consensus of multi-agent networks with undirected and directed topologies. IEEE Trans Network Sci Eng 2021;8(4):3380–91.
[203] Boccaletti S, Latora V, Moreno Y, Chavez M, Hwang D-U. Complex networks: structure and dynamics. Phys Rep 2006;424(4–5):175–308.
[204] Newman M. Networks. Oxford University Press; 2018.
[205] Cencetti G, Battiston F, Lepri B, Karsai M. Temporal properties of higher-order interactions in social networks. Sci Rep 2021;11(1):7028.
[206] Grilli J, Barabás G, Michalska-Smith MJ, Allesina S. Higher-order interactions stabilize dynamics in competitive network models. Nature 2017;548(7666):210–13.
[207] Petri G, Expert P, Turkheimer F, Carhart-Harris R, Nutt D, Hellyer PJ, et al. Homological scaffolds of brain functional networks. J R Soc Interf 2014;11(101):20140873.
[208] Lambiotte R, Rosvall M, Scholtes I. From networks to optimal higher-order models of complex systems. Nat Phys 2019;15(4):313–20.
[209] Battiston F, Amico E, Barrat A, Bianconi G, Ferraz de Arruda G, Franceschiello B, et al. The physics of higher-order interactions in complex systems. Nat Phys 2021;17(10):1093–8.
[210] Battiston F, Petri G. Higher-order systems. Springer; 2022.
[211] Estrada E, Rodríguez-Velázquez JA. Subgraph centrality and clustering in complex hyper-networks. Physica A 2006;364:581–94.
[212] Benson AR, Abebe R, Schaub MT, Jadbabaie A, Kleinberg J. Simplicial closure and higher-order link prediction. Proc Natl Acad Sci 2018;115(48):E11221–E11230.
[213] Contisciani M, Battiston F, De Bacco C. Inference of hyperedges and overlapping communities in hypergraphs. Nat Commun 2022;13(1):7229.

[214] Bick C, Ashwin P, Rodrigues A. Chaos in generically coupled phase oscillator networks with nonpairwise interactions. Chaos Interdiscip J Nonlinear Sci 2016;26(9):094814.
[215] Skardal PS, Arenas A. Higher order interactions in complex networks of phase oscillators promote abrupt synchronization switching. Commun Phys 2020;3(1):218.
[216] Zhang Y, Latora V, Motter AE. Unified treatment of synchronization patterns in generalized networks with higher-order, multilayer, and temporal interactions. Commun Phys 2021;4(1):195.
[217] Mihara A, Kuwana CM, Budzinski RC, Muller LE, Medrano-T RO. Bifurcations and collective states of kuramoto oscillators with higher-order interactions and rotational symmetry breaking. Chaos Interdiscip J Nonlinear Sci 2025;35(3):033133.
[218] Battiston F, Cencetti G, Iacopini I, Latora V, Lucas M, Patania A, et al. Networks beyond pairwise interactions: structure and dynamics. Phys Rep 2020;874:1–92.
[219] Berge C. Hypergraphs: combinatorics of finite sets. Elsevier; 1984.
[220] Majhi S, Perc M, Ghosh D. Dynamics on higher-order networks: a review. J R Soc Interf 2022;19(188):20220043.
[221] Li X, Wang G, Wei D. Dynamical evolution behavior of scientific collaboration hypernetwork. AIP Adv 2022;12(11):115117.
[222] Aguirre-Guerrero D, Bernal-Jaquez R. A methodology for the analysis of collaboration networks with higher-order interactions. Mathematics 2023;11(10):2265.
[223] Liu X, Wang X, Wu J, Xia K. Hypergraph-based persistent cohomology (HPC) for molecular representations in drug design. Brief Bioinform 2021;22(5):bbaa411.
[224] Millán AP, Torres JJ, Bianconi G. Explosive higher-order kuramoto dynamics on simplicial complexes. Phys Rev Lett 2020;124(21):218301.
[225] Skardal PS, Arola-Fernández L, Taylor D, Arenas A. Higher-order interactions can better optimize network synchronization. Phys Rev Res 2021;3(4):043193.
[226] Pal PK, Anwar MS, Ghosh D. Desynchrony induced by higher-order interactions in triplex metapopulations. Phys Rev E 2023;108(5):054208.
[227] Zhang Y, Lucas M, Battiston F. Higher-order interactions shape collective dynamics differently in hypergraphs and simplicial complexes. Nat Commun 2023;14(1):1605.
[228] Zhang Y, Skardal PS, Battiston F, Petri G, Lucas M. Deeper but smaller: higher-order interactions increase linear stability but shrink basins. Sci Adv 2024;10(40):eado8049.
[229] León I, Muolo R, Hata S, Nakao H. Higher-order interactions induce anomalous transitions to synchrony. Chaos Interdiscip J Nonlinear Sci 2024;34(1):013105.
[230] Abrams DM, Strogatz SH. Chimera states for coupled oscillators. Phys Rev Lett 2004;93(17):174102.
[231] Majhi S, Bera BK, Ghosh D, Perc M. Chimera states in neuronal networks: a review. Phys Life Rev 2019;28:100–21.
[232] Panaggio MJ, Abrams DM. Chimera states: coexistence of coherence and incoherence in networks of coupled oscillators. Nonlinearity 2015;28(3):R67.
[233] Kundu S, Ghosh D. Higher-order interactions promote chimera states. Phys Rev E 2022;105(4):L042202.
[234] Ji X, Li X. Chimera-inspired dynamics: when higher-order interactions are expressed differently. Phys Rev E 2024;110(4):044204.
[235] Li X, Ghosh D, Lei Y. Chimera states in coupled pendulum with higher-order interaction. Chaos Solit Fract 2023;170:113325.
[236] Holme P, Saramäki J. Temporal networks. Phys Rep 2012;519(3):97–125.
[237] Li A, Cornelius SP, Liu Y-Y, Wang L, Barabási A-L. The fundamental advantages of temporal networks. Science 2017;358(6366):1042–6.
[238] Ghosh D, Frasca M, Rizzo A, Majhi S, Rakshit S, Alfaro-Bittner K, et al. The synchronized dynamics of time-varying networks. Phys Rep 2022;949:1–63.
[239] Guo Y, Lin W, Chen G. Stability of switched systems on randomly switching durations with random interaction matrices. IEEE Trans Automat Contr 2017;63(1):21–36.
[240] Guo Y, Lin W, Ho D WC. Discrete-time systems with random switches: from systems stability to networks synchronization. Chaos Interdiscip J Nonlinear Science 2016;26(3).
[241] Zhou S, Guo Y, Liu M, Lai Y-C, Lin W. Random temporal connections promote network synchroniz. Phys Rev E 2019;100(3):032302.
[242] Majhi S, Rakshit S, Ghosh D. Oscillation suppression and chimera states in time-varying networks. Chaos Interdiscip J Nonlinear Sci 2022;32(4):042101.
[243] Li A, Zhou L, Su Q, Cornelius SP, Liu Y-Y, Wang L, et al. Evolution of cooperation on temporal networks. Nat Commun 2020;11(1):2259.
[244] Meng Y, McAvoy A, Li A. Promoting collective cooperation through temporal interactions. Proc Natl Acad Sci 2025;122(26):e2509575122.
[245] Fisher DN, Pinter-Wollman N. Using multilayer network analysis to explore the temporal dynamics of collective behavior. Curr Zool 2021;67(1):71–80.
[246] Iacopini I, Karsai M, Barrat A. The temporal dynamics of group interactions in higher-order social networks. Nat Commun 2024;15(1):7391.
[247] Xu Y, Wang J, Xia C, Wang Z. Higher-order temporal interactions promote the cooperation in the multiplayer snowdrift game. Sci China Inf Sci 2023;66(12):222208.
[248] Anwar MS, Ghosh D. Neuronal synchronization in time-varying higher-order networks. Chaos Interdiscip J Nonl Sci 2023;33(7):073111.
[249] Sherman A. Anti-phase, asymmetric and aperiodic oscillations in excitable cells-i. coupled bursters. Bull Math Biol 1994;56(5):811–35.
[250] Anwar MS, Ghosh D. Synchronization in temporal simplicial complexes. SIAM J Appl Dyn Syst 2023;22(3):2054–81.
[251] Majhi S, Ghosh S, Pal PK, Pal S, Pal TK, Ghosh D, et al. Patterns of neuronal synchrony in higher-order networks. Phys Life Rev 2025;52:144–70.
[252] Couzin ID, Krause J. Self-organization and collective behavior in vertebrates. Adv Study Behav 2003;32(1):10–1016.
[253] Elgeti J, Winkler RG, Gompper G. Physics of microswimmers-single particle motion and collective behavior: a review. Rep Prog Phys 2015;78(5):056601.
[254] Artime O, Grassia M, De Domenico M, Gleeson JP, Makse HA, Mangioni G, et al. Robustness and resilience of complex networks. Nat Rev Phys 2024;6(2):114–31.
[255] Komareji M, Bouffanais R. Resilience and controllability of dynamic collective behaviors. PLoS ONE 2013;8(12):e82578.
[256] Xu W, Pan L, Liu X. Breakdown in interdependent directed networks under targeted attacks. Europhys Lett 2021;133(6):68004.
[257] Scarciglia A, Bonanno C, Valenza G. Physiological noise: a comprehensive review on informative randomness in neural systems. Phys Life Rev 2025;53:281–93.
[258] Tsimring LS. Noise in biology. Rep Prog Phys 2014;77(2):026601.
[259] Cucker F, Mordecki E. Flocking in noisy environments. J de Mathématiques Pures et Appliquées 2008;89(3):278–96.
[260] Sun Y, Lin W. A positive role of multiplicative noise on the emergence of flocking in a stochastic cucker-smale system. Chaos Interdiscip J Nonlinear Sci 2015;25(8):083118.
[261] Kolpas A, Moehlis J, Kevrekidis IG. Coarse-grained analysis of stochasticity-induced switching between collective motion states. Proc Natl Acad Sci 2007;104(14):5931–5.
[262] Erdmann U, Ebeling W, Mikhailov AS. Noise-induced transition from translational to rotational motion of swarms. Phys Rev E-Stat Nonlinear Soft Matter Phys 2005;71(5):051904.
[263] Chen G. Small noise may diversify collective motion in vicsek model. IEEE Trans Automat Contr 2016;62(2):636–51.
[264] Huang J, Shao Z-G. Collective motion of self-trapping chiral active particles induced by a noisy geometric environment. Phys Rev E 2025;111(5):055403.
[265] Galbraith M, Bocci F, Onuchic JN. Stochastic fluctuations promote ordered pattern formation of cells in the notch-delta signaling pathway. PLoS Comput Biol 2022;18(7):e1010306.
[266] Li S, Batra R, Brown D, Chang H-D, Ranganathan N, Hoberman C, et al. Particle robotics based on statistical mechanics of loosely coupled components. Nature 2019;567(7748):361–5.
[267] Sun Y, Li W, Zhao D. Convergence time and speed of multi-agent systems in noisy environments. Chaos Interdiscip J Nonlinear Sci 2012;22(4):043126.
[268] Li T, Wu F, Zhang J-F. Multi-agent consensus with relative-state-dependent measurement noises. IEEE Trans Automat Contr 2014;59(9):2463–8.
[269] Sun Y, Li W, Shi H, Zhao D, Azaele S. Finite-time and fixed-time consensus of multiagent networks with pinning control and noise perturbation. SIAM J Appl Math 2019;79(1):111–30.
[270] Dai H, Sun Y, Li W, Zhao D. Multiplicative measurement noise can facilitate consensus of multiagent networks. Phys Rev E 2019;100(2):022319.
[271] Zou W, Xiang Z, Ahn CK. Mean square leader–following consensus of second-order nonlinear multiagent systems with noises and unmodeled dynamics. IEEE Trans Syst Man Cybern Syst 2018;49(12):2478–86.
[272] Ma C-Q, Xie L. Necessary and sufficient conditions for leader-following bipartite consensus with measurement noise. IEEE Trans Syst Man Cybern Syst 2018;50(5):1976–81.
[273] Li W, Dai H, Zhao L, Zhao D, Sun Y. Noise-induced consensus of leader-following multi-agent systems. Math Comput Simul 2023;203:1–11.
[274] Li T, Zhang J-F. Consensus conditions of multi-agent systems with time-varying topologies and stochastic communication noises. IEEE Trans Automat Contr 2010;55(9):2043–57.

[275] Wang Y, Cheng L, Ren W, Hou Z-G, Tan M. Seeking consensus in networks of linear agents: communication noises and markovian switching topologies. IEEE Trans Automat Contr 2014;60(5):1374–9.
[276] Du Y, Wang Y, Zuo Z. Mean square bipartite consensus for multiagent systems with antagonistic information and time-varying topologies. IEEE Trans Sys Man Cybern Syst 2020;52(3):1744–54.
[277] Mikhailov AS, Zanette DH. Noise-induced breakdown of coherent collective motion in swarms. Phys Rev E 1999;60(4):4571.
[278] Zheng C, Tönjes R. Noise-induced swarming of active particles. Phys Rev E 2022;106(6):064601.
[279] Giuggioli L, McKetterick TJ, Holderied M. Delayed response and biosonar perception explain movement coordination in trawling bats. PLoS Comput Biol 2015;11(3):e1004089.
[280] Szwaykowska K, Schwartz IB, Mier-y Teran Romero L, Heckman CR, Mox D, Hsieh MA. Collective motion patterns of swarms with delay coupling: theory and experiment. Phys Rev E 2016;93(3):032307.
[281] More HL, Donelan JM. Scaling of sensorimotor delays in terrestrial mammals. Proc R Soc B 2018;285(1885):20180613.
[282] Leyman M, Ogemark F, Wehr J, Volpe G. Tuning phototactic robots with sensorial delays. Phys Rev E 2018;98(5):052606.
[283] Virágh C, Vásárhelyi G, Tarcai N, Szörényi T, Somorjai G, Nepusz T, et al. Flocking algorithm for autonomous flying robots. Bioinspir Biomimet 2014;9(2):025012.
[284] Mijalkov M, McDaniel A, Wehr J, Volpe G. Engineering sensorial delay to control phototaxis and emergent collective behaviors. Phys Rev X 2016;6(1):011008.
[285] Chen Z, Zheng Y. Persistent and responsive collective motion with adaptive time delay. Sci Adv 2024;10(14):eadk3914.
[286] Sun Y, Lin W, Erban R. Time delay can facilitate coherence in self-driven interacting-particle systems. Phys Rev E 2014;90(6):062708.
[287] Piwowarczyk R, Selin M, Ihle T, Volpe G. Influence of sensorial delay on clustering and swarming. Phys Rev E 2019;100(1):012607.
[288] Holubec V, Geiss D, Loos S AM, Kroy K, Cichos F. Finite-size scaling at the edge of disorder in a time-delay vicsek model. Phys Rev Lett 2021;127(25):258001.
[289] Liu S, Xiao R, Zhao D, Sun Y. Coordinating directional switches of multiagent systems with delayed and nonlinear interactions. Phys Rev Res 2023;5(4):043304.
[290] Pakpour F, Vicsek T. Delay-induced phase transitions in active matter. Physica A 2024;634:129453.
[291] Wang X, Chen P-C, Kroy K, Holubec V, Cichos F. Spontaneous vortex formation by microswimmers with retarded attractions. Nat Commun 2023;14(1):56.
[292] Chen P-C, Kroy K, Cichos F, Wang X, Holubec V. Active particles with delayed attractions form quaking crystallites (a). Europhys Lett 2023;142(6):67003.
[293] Blum N, Li A, O'Keeffe K, Kogan O. Swarmalators with delayed interactions. Phys Rev E 2024;109(1):014205.
[294] Wang Q, Perc M, Duan Z, Chen G. Synchronization transitions on scale-free neuronal networks due to finite information transmission delays. Phys Rev E-Stat Nonlinear Soft Matter Phys 2009;80(2):026206.
[295] Yu H, Wang J, Du J, Deng B, Wei X, Liu C. Effects of time delay on the stochastic resonance in small-world neuronal networks. Chaos Interdiscip J Nonlinear Sci 2013;23(1):013128.
[296] Liu Y, Wu J. Flocking and asymptotic velocity of the cucker–smale model with processing delay. J Math Anal Appl 2014;415(1):53–61.
[297] Pignotti C, Trélat E. Convergence to consensus of the general finite-dimensional cucker-smale model with time-varying delays.2017; arXiv preprint arXiv:170705020 .
[298] Choi Y-P, Li Z. Emergent behavior of cucker–smale flocking particles with heterogeneous time delays. Appl Math Lett 2018;86:49–56.
[299] Pignotti C, Vallejo IR. Flocking estimates for the cucker–smale model with time lag and hierarchical leadership. J Math Anal Appl 2018;464(2):1313–32.
[300] Wu C, Dong J-G. Effects of time delay on cucker–smale flocking under hierarchical leadership. IEEE Trans Automat Contr 2023;69(3):1812–17.
[301] Martinez-Corral R, Liu J, Süel GM, Garcia-Ojalvo J. Bistable emergence of oscillations in growing bacillus subtilis biofilms. Proc Natl Acad Sci 2018;115(36):E8333–E8340.
[302] Pazó D, Montbrió E. From quasiperiodic partial synchronization to collective chaos in populations of inhibitory neurons with delay. Phys Rev Lett 2016;116(23):238101.
[303] Tomka T, Iber D, Boareto M. Travelling waves in somitogenesis: collective cellular properties emerge from time-delayed juxtacrine oscillation coupling. Prog Biophys Mol Biol 2018;137:76–87.
[304] Lohmann S, Pramotton FM, Taloni A, Ferrari A, Poulikakos D, Giampietro C. Delayed jamming-induced oscillatory migration patterns of epithelial collectives under long-range confinement. Integr Biol 2024;16:zyae016.
[305] Adhikari BM, Prasad A, Dhamala M. Time-delay-induced phase-transition to synchrony in coupled bursting neurons. Chaos Interdiscip J Nonlinear Sci 2011;21(2):023116.
[306] Ma J, Qin H, Song X, Chu R. Pattern selection in neuronal network driven by electric autapses with diversity in time delays. Int J Mod Phys B 2015;29(01):1450239.
[307] Cohen R, Erez K, Ben-Avraham D, Havlin S. Breakdown of the internet under intentional attack. Phys Rev Lett 2001;86(16):3682.
[308] Flack JC, Girvan M, De Waal F BM, Krakauer DC. Policing stabilizes construction of social niches in primates. Nature 2006;439(7075):426–9.
[309] Mech LD, Boitani L. Wolves: behavior, ecology, and conservation. University of Chicago Press; 2019.
[310] Huang X, Gao J, Buldyrev SV, Havlin S, Stanley HE. Robustness of interdependent networks under targeted attack. Phys Rev E-Stat Nonlinear Soft Matter Phys 2011;83(6):065101.
[311] Dong G, Gao J, Tian L, Du R, He Y. Percolation of partially interdependent networks under targeted attack. Phys Rev E-Stat Nonlinear Soft Matter Phys 2012;85(1):016112.
[312] Dong G, Gao J, Du R, Tian L, Stanley HE, Havlin S. Robustness of network of networks under targeted attack. Phys Rev E-Stat Nonlinear Soft Matter Phys 2013;87(5):052804.
[313] Buldyrev SV, Parshani R, Paul G, Stanley HE, Havlin S. Catastrophic cascade of failures in interdependent networks. Nature 2010;464(7291):1025–8.
[314] Liu K, Zhong J, Bai G, Yang Y. A complex networks approach for reliability evaluation of swarm systems under malicious attacks. IEEE Access 2020;8:81209–19.
[315] Holling CS. Engineering resilience versus ecological resilience. Eng Ecolog Constrain 1996;31(1996):32.
[316] Gao J, Barzel B, Barabási A-L. Universal resilience patterns in complex networks. Nature 2016;530(7590):307–12.
[317] Sun Y, Wen G, Dai H, Feng Y, Azaele S, Lin W, et al. Quantifying the resilience of coal energy supply in china toward carbon neutrality. Research 2024;7:0398.
[318] Mustafa A, Modares H, Moghadam R. Resilient synchronization of distributed multi-agent systems under attacks. Automatica 2020;115:108869.
[319] Wang P, Wen G, Huang T, Yu W, Ren Y. Observer-based consensus protocol for directed switching networks with a leader of nonzero inputs. IEEE Trans Cybern 2020;52(1):630–40.
[320] Zhao D, Wen G, Wu Z-G, Lv Y, Zhou J. Resilient consensus of multiagent systems under collusive attacks on communication links. IEEE Trans Cybern 2022;54(4):2076–85.
[321] Wen G, Wang P, Lv Y, Chen G, Zhou J. Secure consensus of multi-agent systems under denial-of-service attacks. Asian J Contr 2023;25(2):695–709.
[322] Sumpter D JT. The principles of collective animal behaviour. Philos Trans R Soc B Biolog Sci 2006;361(1465):5–22.
[323] Mallon E, Pratt S, Franks N. Individual and collective decision-making during nest site selection by the ant leptothorax albipennis. Behav Ecol Sociobiol 2001;50:352–9.
[324] Pratt SC, Mallon EB, Sumpter DJ, Franks NR. Quorum sensing, recruitment, and collective decision-making during colony emigration by the ant leptothorax albipennis. Behav Ecol Sociobiol 2002;52:117–27.
[325] Biro D, Sumpter D JT, Meade J, Guilford T. From compromise to leadership in pigeon homing. Curr Biol 2006;16(21):2123–8.
[326] Vásárhelyi G, Virágh C, Somorjai G, Nepusz T, Eiben AE, Vicsek T. Optimized flocking of autonomous drones in confined environments. Sci Rob 2018;3(20):eaat3536.
[327] Couzin ID, Krause J, Franks NR, Levin SA. Effective leadership and decision-making in animal groups on the move. Nature 2005;433(7025):513–16.
[328] Arganda S, Pérez-Escudero A, de Polavieja GG. A common rule for decision making in animal collectives across species. Proc Natl Acad Sci 2012;109(50):20508–13.
[329] Sridhar VH, Li L, Gorbonos D, Nagy M, Schell BR, Sorochkin T, et al. The geometry of decision-making in individuals and collectives. Proc Natl Acad Sci 2021;118(50):e2102157118.

[330] Couzin ID. Collective cognition in animal groups. Trends Cogn Sci 2009;13(1):36–43.
[331] Krause J, Ruxton GD, Krause S. Swarm intelligence in animals and humans. Trends Ecol Evol 2010;25(1):28–34.
[332] Reid CR, Latty T. Collective behaviour and swarm intelligence in slime moulds. FEMS Microbiol Rev 2016;40(6):798–806.
[333] Seeley TD, Visscher PK. Group decision making in nest-site selection by honey bees. Apidologie 2004;35(2):101–16.
[334] Seeley TD. Honeybee democracy. Princeton University Press; 2011.
[335] Ward A JW, Sumpter D JT, Couzin ID, Hart P JB, Krause J. Quorum decision-making facilitates information transfer in fish shoals. Proc Natl Acad Sci 2008;105(19):6948–53.
[336] Sumpter D JT, Krause J, James R, Couzin ID, Ward A JW. Consensus decision making by fish. Curr Biol 2008;18(22):1773–7.
[337] Reid CR, MacDonald H, Mann RP, Marshall J AR, Latty T, Garnier S. Decision-making without a brain: how an amoeboid organism solves the two-armed bandit. J R Soc Interf 2016;13(119):20160030.
[338] Weitz JS, Mileyko Y, Joh RI, Voit EO. Collective decision making in bacterial viruses. Biophys J 2008;95(6):2673–80.
[339] Ross-Gillespie A, Kümmerli R. Collective decision-making in microbes. Front Microbiol 2014;5:54.
[340] Dinet C, Michelot A, Herrou J, Mignot T. Linking single-cell decisions to collective behaviours in social bacteria. Philos Trans R Soc B 2021;376(1820):20190755.
[341] Harcourt JL, Ang TZ, Sweetman G, Johnstone RA, Manica A. Social feedback and the emergence of leaders and followers. Curr Biol 2009;19(3):248–52.
[342] Stroeymeyt N, Franks NR, Giurfa M. Knowledgeable individuals lead collective decisions in ants. J Exp Biol 2011;214(18):3046–54.
[343] Gómez-Nava L, Bon R, Peruani F. Intermittent collective motion in sheep results from alternating the role of leader and follower. Nat Phys 2022;18(12):1494–501.
[344] Sridhar VH, Davidson JD, Twomey CR, Sosna M MG, Nagy M, Couzin ID. Inferring social influence in animal groups across multiple timescales. Philos Trans R Soc B 2023;378(1874):20220062.
[345] Khalil AA, Friedl P. Determinants of leader cells in collective cell migration. Integr Biol 2010;2(11–12):568–74.
[346] Haeger A, Wolf K, Zegers MM, Friedl P. Collective cell migration: guidance principles and hierarchies. Trends Cell Biol 2015;25(9):556–66.
[347] Riahi R, Sun J, Wang S, Long M, Zhang DD, Wong PK. Notch1–dll4 signalling and mechanical force regulate leader cell formation during collective cell migration. Nat Commun 2015;6(1):6556.
[348] Vitorino P, Meyer T. Modular control of endothelial sheet migration. Genes Develop 2008;22(23):3268–81.
[349] Gaggioli C, Hooper S, Hidalgo-Carcedo C, Grosse R, Marshall JF, Harrington K, et al. Fibroblast-led collective invasion of carcinoma cells with differing roles for rhoGTPases in leading and following cells. Nat Cell Biol 2007;9(12):1392–400.
[350] Strandburg-Peshkin A, Farine DR, Couzin ID, Crofoot MC. Shared decision-making drives collective movement in wild baboons. Science 2015;348(6241):1358–61.
[351] Bose T, Reina A, Marshall J AR. Collective decision-making. Curr Opin Behav Sci 2017;16:30–4.
[352] Mann RP. Collective decision-making by rational agents with differing preferences. Proc Natl Acad Sci 2020;117(19):10388–96.
[353] Centola D. The spread of behavior in an online social network experiment. Science 2010;329(5996):1194–7.
[354] Bakshy E, Hofman JM, Mason WA, Watts DJ. Everyone'S an influencer: quantifying influence on twitter. In: Proceedings of the fourth ACM international conference on web eearch and data mining. 2011, p. 65–74.
[355] Bruggeman J. Consensus, cohesion and connectivity. Soc Netw 2018;52:115–19.
[356] Michelena P, Jeanson R, Deneubourg J-L, Sibbald AM. Personality and collective decision-making in foraging herbivores. Proc R Soc B Biol Sci 2010;277(1684):1093–9.
[357] O'Shea-Wheller TA, Masuda N, Sendova-Franks AB, Franks NR. Variability in individual assessment behaviour and its implications for collective decision-making. Proc R Soc B Biol Sci 2017;284(1848):20162237.
[358] Clark MA, Waples E, Radford AN, Simpson SD, Ioannou CC. Group personality, rather than acoustic noise, causes variation in group decision-making in guppy shoals. Sci Rep 2025;15(1):18801.
[359] Aplin LM, Farine DR, Mann RP, Sheldon BC. Individual-level personality influences social foraging and collective behaviour in wild birds. Proc R Soc B Biol Sci 2014;281(1789):20141016.
[360] Sueur C, Deneubourg J-L, Petit O. From social network (centralized vs. decentralized) to collective decision-making (unshared vs. shared consensus). PLoS ONE 2012;7(2):e32566.
[361] Hu C, Shu X. The evolution and optimization control of collective decision-making with opinion preferences on social networks. Chin J Phys 2025;96:603–20.
[362] Sampaio E, Sridhar VH, Francisco FA, Nagy M, Sacchi A, Strandburg-Peshkin A, et al. Multidimensional social influence drives leadership and composition-dependent success in octopus–fish hunting groups. Nat Ecol Evol 2024;8(11):2072–84.
[363] Fratellone GP, Li J-H, Sheeran LK, Wagner RS, Wang X, Sun L. Social connectivity among female tibetan macaques (macaca thibetana) increases the speed of collective movements. Primates 2019;60(3):183–9.
[364] Mason W, Watts DJ. Collaborative learning in networks. Proc Natl Acad Sci 2012;109(3):764–9.
[365] Reia SM, Fontanari JF. Effect of group organization on the performance of cooperative processes. Ecol Complex 2017;30:47–56.
[366] Leonard NE, Shen T, Nabet B, Scardovi L, Couzin ID, Levin SA. Decision versus compromise for animal groups in motion. Proc Natl Acad Sci 2012;109(1):227–32.
[367] Vicente-Page J, Pérez-Escudero A, de Polavieja GG. Dynamic choices are most accurate in small groups. Theor Ecol 2018;11:71–81.
[368] Pérez-Escudero A, Miller N, Hartnett AT, Garnier S, Couzin ID, De Polavieja GG. Estimation models describe well collective decisions among three options. Proc Natl Acad Sci 2013;110(37):E3466–E3467.
[369] Calovi DS, Litchinko A, Lecheval V, Lopez U, Pérez Escudero A, Chaté H, et al. Disentangling and modeling interactions in fish with burst-and-coast swimming reveal distinct alignment and attraction behaviors. PLoS Comput Biol 2018;14(1):e1005933.
[370] Lazer D, Friedman A. The network structure of exploration and exploitation. Adm Sci Q 2007;52(4):667–94.
[371] Reia SM, Amado AC, Fontanari JF. Agent-based models of collective intelligence. Phys Life Rev 2019;31:320–31.
[372] Centola D. The network science of collective intelligence. Trends Cogn Sci 2022;26(11):923–41.
[373] Völkl B, Fritz J. Relation between travel strategy and social organization of migrating birds with special consideration of formation flight in the northern bald ibis. Philos Trans R Soc B Biol Sci 2017;372(1727):20160235.
[374] Okasaki C, Keefer ML, Westley P AH, Berdahl AM. Collective navigation can facilitate passage through human-made barriers by homeward migrating pacific salmon. Proc R Soc B 2020;287(1937):20202137.
[375] Berdahl AM, Kao AB, Flack A, Westley P AH, Codling EA, Couzin ID, et al. Collective animal navigation and migratory culture: from theoretical models to empirical evidence. Philos Trans R Soc B Biol Sci 2018;373(1746):20170009.
[376] Sasaki T, Biro D. Cumulative culture can emerge from collective intelligence in animal groups. Nat Commun 2017;8(1):15049.
[377] Simons AM. Many wrongs: the advantage of group navigation. Trends Ecol Evol 2004;19(9):453–5.
[378] Liechti F, Ehrich D, Bruderer B. Flight behaviour of white storks ciconia ciconia on their migration over southern israel. ARDEA-WAGENINGEN- 1996;84:3–14.
[379] Rabøl J, Noer H. Spring migration in the skylark (alauda arvensis) in denmark: influence of environmental factors on the flocksize and correlation between flocksize and migratory direction. Vogelwarte 1973;27(1):50–65.
[380] Dell'Ariccia G, Dell'Omo G, Wolfer DP, Lipp H-P. Flock flying improves pigeons' homing: GPS track analysis of individual flyers versus small groups. Anim Behav 2008;76(4):1165–72.
[381] Seeley TD, Visscher PK, Passino KM. Group decision making in honey bee swarms: when 10,000 bees go house hunting, how do they cooperatively choose their new nesting site? Am Sci 2006;94(3):220–9.
[382] Sirota-Madi A, Olender T, Helman Y, Ingham C, Brainis I, Roth D, et al. Genome sequence of the pattern forming paenibacillus vortex bacterium reveals potential for thriving in complex environments. BMC Genomics 2010;11:1–16.
[383] Ingham CJ, Jacob EB. Swarming and complex pattern formation in paenibacillus vortex studied by imaging and tracking cells. BMC Microbiol 2008;8:1–16.
[384] Shklarsh A, Finkelshtein A, Ariel G, Kalisman O, Ingham C, Ben-Jacob E. Collective navigation of cargo-carrying swarms. Interf Focus 2012;2(6):786–98.

[385] Olcay E, Schuhmann F, Lohmann B. Collective navigation of a multi-robot system in an unknown environment. Rob Auton Syst 2020;132:103604.
[386] Wang F, Huang J, Low KH, Hu T. Collective navigation of aerial vehicle swarms: a flocking inspired approach. IEEE Trans Intell Veh 2023;9(1):1040–53.
[387] Brambilla M, Ferrante E, Birattari M, Dorigo M. Swarm robotics: a review from the swarm engineering perspective. Swarm Intell 2013;7:1–41.
[388] Şahin E. Swarm robotics: from sources of inspiration to domains of application. In: International workshop on swarm robotics. Springer; 2004, p. 10–20.
[389] Schranz M, Di Caro GA, Schmickl T, Elmenreich W, Arvin F, Şekercioğlu A, et al. Swarm intelligence and cyber-physical systems: concepts, challenges and future trends. Swarm Evol Comput 2021;60:100762.
[390] Lauder GV. Fish locomotion: recent advances and new directions. Ann Rev Mar Sci 2015;7(1):521–45.
[391] Jiang L, Giuggioli L, Perna A, Escobedo R, Lecheval V, Sire C, et al. Identifying influential neighbors in animal flocking. PLoS Comput Biol 2017;13(11):e1005822.
[392] Berlinger F, Gauci M, Nagpal R. Implicit coordination for 3d underwater collective behaviors in a fish-inspired robot swarm. Sci Rob 2021;6(50):eabd8668.
[393] Ligman M, Lund J, Fürth M. A comprehensive review of hydrodynamic studies on fish schooling. Bioinspir Biomimet 2023;19(1):011002.
[394] Liao JC, Beal DN, Lauder GV, Triantafyllou MS. The kármán gait: novel body kinematics of rainbow trout swimming in a vortex street. J Exp Biol 2003;206(6):1059–73.
[395] Thandiackal R, Lauder G. In-line swimming dynamics revealed by fish interacting with a robotic mechanism. Elife 2023;12:e81392.
[396] Becker AD, Masoud H, Newbolt JW, Shelley M, Ristroph L. Hydrodynamic schooling of flapping swimmers. Nat Commun 2015;6(1):8514.
[397] Verma S, Novati G, Koumoutsakos P. Efficient collective swimming by harnessing vortices through deep reinforcement learning. Proc Natl Acad Sci 2018;115(23):5849–54.
[398] Marras S, Killen SS, Lindström J, McKenzie DJ, Steffensen JF, Domenici P. Fish swimming in schools save energy regardless of their spatial position. Behav Ecol Sociobiol 2015;69(2):219–26.
[399] Chung S-J, Paranjape AA, Dames P, Shen S, Kumar V. A survey on aerial swarm robotics. IEEE Trans Rob 2018;34(4):837–55.
[400] Weimerskirch H, Martin J, Clerquin Y, Alexandre P, Jiraskova S. Energy saving in flight formation. Nature 2001;413(6857):697–8.
[401] Hauert S, Leven S, Varga M, Ruini F, Cangelosi A, Zufferey J-C, et al. Reynolds flocking in reality with fixed-wing robots: communication range vs. maximum turning rate. In: 2011 IEEE/RSJ International conference on intelligent robots and systems. IEEE; 2011, p. 5015–20.
[402] Vásárhelyi G, Virágh C, Somorjai G, Tarcai N, Szörényi T, Nepusz T, et al. Outdoor flocking and formation flight with autonomous aerial robots. In: 2014 IEEE/RSJ International conference on intelligent robots and systems. IEEE; 2014, p. 3866–73.
[403] Saska M. Mav-swarms: unmanned aerial vehicles stabilized along a given path using onboard relative localization. In: 2015 International conference on unmanned aircraft systems (ICUAS). IEEE; 2015, p. 894–903.
[404] Zhang H-T, Chen Z, Vicsek T, Feng G, Sun L, Su R, et al. Route-dependent switch between hierarchical and egalitarian strategies in pigeon flocks. Sci Rep 2014;4(1):5805.
[405] Chen D, Vicsek T, Liu X, Zhou T, Zhang H-T. Switching hierarchical leadership mechanism in homing flight of pigeon flocks. Europhys Lett 2016;114(6):60008.
[406] Xie L, Zhang X. Dynamic leadership mechanism in homing pigeon flocks. Biomimetics 2024;9(2):88.
[407] Qiu H, Duan H. A multi-objective pigeon-inspired optimization approach to UAV distributed flocking among obstacles. Inf Sci 2020;509:515–29.
[408] Li S, Fang X. A modified adaptive formation of UAV swarm by pigeon flock behavior within local visual field. Aerosp Sci Technol 2021;114:106736.
[409] Zhang Z, Yuan Y, Duan H. Finite-time formation control for clustered UAVs with obstacle avoidance inspired by pigeon hierarchical behavior. Drones (2504-446X) 2025;9(4).
[410] Fan R, Wang J, Han W, Xu B. Uav swarm control based on hybrid bionic swarm intelligence. Guid Navig Contr 2023;3(02):2350008.
[411] Shen Y, Deng Y. Pigeon-inspired optimisation algorithm with hierarchical topology and receding horizon control for multi-UAV formation. Int J Bio-Insp Comput 2021;18(4):239–49.
[412] Zhang X, Xie L. Collision-avoiding flocking of fixed-wing UAV swarm using dynamic interaction mechanism inspired by pigeons. Physica A 2025;681:131071.
[413] Brask JB, Ellis S, Croft DP. Animal social networks: an introduction for complex systems scientists. J Complex Netw 2021;9(2):cnab001.
[414] Pais D, Leonard NE. Adaptive network dynamics and evolution of leadership in collective migration. Physica D 2014;267:81–93.
[415] Lihoreau M, Charleston MA, Senior AM, Clissold FJ, Raubenheimer D, Simpson SJ, et al. Collective foraging in spatially complex nutritional environments. Philos Trans R Soc B Biol Sci 2017;372(1727):20160238.
[416] Herbert-Read JE, Rosén E, Szorkovszky A, Ioannou CC, Rogell B, Perna A, et al. How predation shapes the social interaction rules of shoaling fish. Proc R Soc B Biol Sci 2017;284(1861):20171126.
[417] Ding J, Tarokh V, Yang Y. Model selection techniques: an overview. IEEE Signal Process Mag 2018;35(6):16–34.
[418] Johnson JB, Omland KS. Model selection in ecology and evolution. Trends Ecol Evol 2004;19(2):101–8.
[419] Stoica P, Selen Y. Model-order selection: a review of information criterion rules. IEEE Signal Process Mag 2004;21(4):36–47.
[420] Greenland S. Modeling and variable selection in epidemiologic analysis. Am J Public Health 1989;79(3):340–9.
[421] Emamjomeh A, Saboori Robat E, Zahiri J, Solouki M, Khosravi P. Gene co-expression network reconstruction: a review on computational methods for inferring functional information from plant-based expression data. Plant Biotechnol Rep 2017;11(2):71–86.
[422] Shojaie A, Fox EB. Granger causality: a review and recent advances. Annu Rev Stat Appl 2022;9(1):289–319.
[423] Bellomo N, Dolfin M, Liao J. Life and self-organization on the way to artificial intelligence for collective dynamics. Phys Life Rev 2024;51:1–8.
[424] Heras F JH, Romero-Ferrero F, Hinz RC, de Polavieja GG. Deep attention networks reveal the rules of collective motion in zebrafish. PLoS Comput Biol 2019;15(9):e1007354.
[425] LaChance J, Suh K, Clausen J, Cohen DJ. Learning the rules of collective cell migration using deep attention networks. PLoS Comput Biol 2022;18(4):e1009293.
[426] Ehlman SM, Scherer U, Bierbach D, Francisco FA, Laskowski KL, Krause J, et al. Leveraging big data to uncover the eco-evolutionary factors shaping behavioural development. Proc R Soc B 2023;290(1992):20222115.
[427] Chen L, Lee CF, Toner J. Moving, reproducing, and dying beyond flatland: malthusian flocks in dimensions d > 2. Phys Rev Lett 2020;125(9):098003.
[428] Toner J. Birth, death, and horizontal flight: malthusian flocks with an easy plane in three dimensions. Phys Rev E 2024;110(6):064604.
[429] Duan H, Huo M, Fan Y. From animal collective behaviors to swarm robotic cooperation. Natl Sci Rev 2023;10(5):nwad040.
[430] Pan M, Yang Y, Qin X, Li G, Xi N, Long M, et al. Applying the intrinsic principle of cell collectives to program robot swarms. Cell Rep Phys Sci 2024;5(8):102122.
[431] Han Z, Fink O, Kammer DS. Collective relational inference for learning heterogeneous interactions. Nat Commun 2024;15(1):3191.
[432] Zhang J, Qu Q, Chen X. Understanding collective behavior in biological systems through potential field mechanisms. Sci Rep 2025;15(1):3709.
[433] Albert R, Jeong H, Barabási A-L. Error and attack tolerance of complex networks. Nature 2000;406(6794):378–82.
[434] Kitano H. Biological robustness. Nat Rev Genet 2004;5(11):826–37.
[435] Barabási A-L. Network science. Philos Trans R Soc A Math Phys Eng Sci 2013;371(1987):20120375.
[436] Farine DR, Aplin LM, Sheldon BC, Hoppitt W. Interspecific social networks promote information transmission in wild songbirds. Proc R Soc B Biol Sci 2015;282(1803):20142804.
[437] Farine DR, Garroway CJ, Sheldon BC. Social network analysis of mixed-species flocks: exploring the structure and evolution of interspecific social behaviour. Anim Behav 2012;84(5):1271–7.
[438] Farine DR, Aplin LM, Garroway CJ, Mann RP, Sheldon BC. Collective decision making and social interaction rules in mixed-species flocks of songbirds. Anim Behav 2014;95:173–82.
[439] Goodale E, Sridhar H, Sieving KE, Bangal P, Colorado Z GJ, Farine DR, et al. Mixed company: a framework for understanding the composition and organization of mixed-species animal groups. Biol Rev 2020;95(4):889–910.
[440] Wei B, Tian E, Gu Z, Zhai J, Liang D. Quasi-consensus control for stochastic multiagent systems: when energy harvesting constraints meet multimodal FDI attacks. IEEE Trans Cybern 2023;54(3):1755–67.
[441] Sun Y, Yang H, Yin X, Wen G, Yang C. Time and energy costs for flocking of cucker–smale system under denial-of-service attacks. IEEE Trans Cybern 2025;56(1):537–46.